Spring 5-2000

Fundamental Capillary Electrophoresis: An Evaluation of Electrokinetic Sampling

Cindy Ann Mleziva Blake
Seton Hall University

Fundamental Capillary Electrophoresis:
An Evaluation of Electrokinetic Sampling

by

Cindy Ann Mleziva Blake

Dissertation submitted to the Department of Chemistry of Seton Hall

University in partial fulfillment of the requirements for the degree of
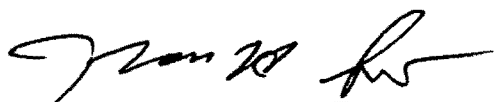
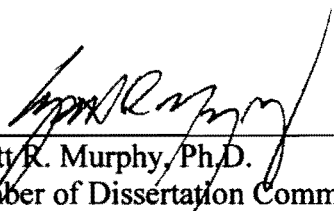DOCTOR OF PHILOSOPHY

in

Chemistry

May 2000

South Orange, New Jersey

We certify that we have read this thesis and that in our opinion it is adequate in scientific scope and quality as a dissertation for the degree of Doctor of Philosophy.

APPROVED:
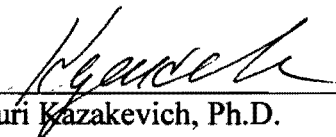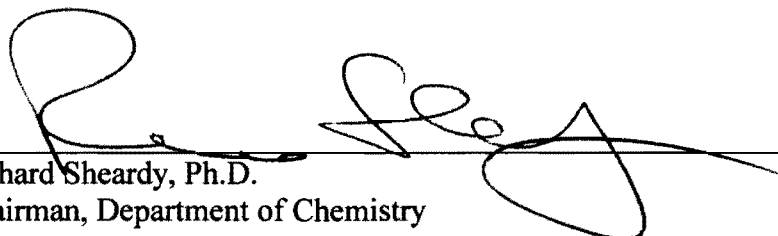

_____

Nicholas H. Snow, Ph.D.
Research Director

_____

Wyatt R. Murphy, Ph.D.
Member of Dissertation Committee

_____

Yuri Kazakevich, Ph.D.
Member of Dissertation Committee

_____

Richard Sheardy, Ph.D.
Chairman, Department of Chemistry

Abstract

Fundamental Capillary Electrophoresis:

An Evaluation of Electrokinetic Sampling

Capillary electrophoresis has become a powerful separation technique in fields of biochemical separations, inorganic ions, and chiral separations. The technique has experienced exponential growth since the historic publication of *Zone Electrophoresis in Open-Tubular Glass Capillaries* by Lukacs and Jorgenson in 1981. However, the use of capillary electrophoresis as a primary research analysis tool still remains to be seen in many pharmaceutical laboratories. One of the main reasons for this is that it remains difficult to validate CE methods using the criteria of quantitation and accuracy posed by the current government regulating agencies, as developed for high performance liquid chromatography and gas chromatography methods.

This dissertation will examine the fundamental principles of capillary electrophoresis as they pertain to quantitative reproducibility of peak areas with the primary focus on effects of electrokinetic sampling conditions. Data supporting longer sampling times and higher sampling voltages contributes to reproducibility relative standard deviation values of less the 2%. Injection plug lengths elucidated from sampling criteria are also evaluated.

Two models of predicting the injection plug length under the conditions of electrokinetic injection are contrasted. The first system employs standard electrokinetic sampling equations. The second model, developed by Otsuka and Terabe, predicts a maximum length above which a 5% variation in peak width may be observed. The combination of these models lead to the derivation of another expression describing the electrokinetic injection plug length. More accurate measurements of analyte mobility are shown through the use of this equation in a fashion similar to the graphical analysis of the standard Beer's Law plot.

Five different pre-injection conditions and four different quantitation techniques are evaluated as they affect the overall separation performance of caffeine and theophylline using capillary zone electrophoresis with electrokinetic injection. When quantitation methods such as internal standardization or internal area normalization are used, pre-injection rinsing conditions are irrelevant.

With a better understanding of analyte mobility, the field of capillary electrophoresis analysis may be extended to the analysis of polymetallic complexes. Polymetallic complexes are of current interest in the literature due to their complexity and wide range of potential applicability. The first isomeric compound to be studied is $[Ru(tpy)Cl]_2(bpm)^{2+}$ (tpy = 2,2':6',2"-terpyridine) (bpm = 2,2'-bipyrimidine). These isomers, which are of the same charge to mass ratio, were separated in approximately four minutes in a fused-silica capillary column with phosphate buffer of pH 7.5 at an

applied voltage of 20 kV followed by direct UV detection. An electrophoretic

concentration step (stacking) was utilized in order to improve peak shape.

Dedication

*This dissertation is dedicated to my husband, Adam J. Blake
and my parents, James G. and Carol Ann Mleziva,
my brother, James and my sister, Tammy.*

It is also dedicated, in loving memory, to my grandmother- Helen Ann Billets.

Acknowledgements

My father once said that too often we go through life failing to recognize those who truly made a difference in the way we live our lives. We feel it in our hearts but our minds often convince us that such appreciation is best left unsaid. Unfortunately, in a moment, those words can become part of a missed opportunity. I want to take this moment and acknowledge those who made a difference in the way I think, teach, and act as a scientist, friend, and family member. For although this dissertation marks the end of the graduate school portion of my career, the valuable lessons learned in this endeavor are some of life's lessons from which I will benefit in the years to come.

To Keith Flood, Kenneth Karaisz, Rosario LoBrutto, Steve Rentz, Tom O'Brien, Thom Laughlin, and Sohita Patel; I could not have wished for a better research group. You were hard on me when I needed it and always there to help. You are some of my closest friends. I hope that at some point during our time together at Seton Hall I was able to give back at least a portion of all the guidance and support you have provided me during these past few years. Your time and encouragement made this effort possible and I thank you for it.

To Dr. Murphy, Dr. Maloy, Dr. Huchital, Dr. Kazakevich, Dr. Sowa, Dr. Orr, Dr. Rasmussen, and Dr. Snow; the word "mentor" is defined as a wise advisor, a trusted teacher and counselor. You have all been my "mentors" throughout my college career.

Your criticisms, challenges, advice, and friendships have shaped me as a scientist and teacher. Thank you for all you have done in helping me to achieve this goal.

To my parents, James G. and Carol Ann Mleziva, my brother, James, my sister, Tammy, and all of my relatives; I am very lucky. The love and support you have all provided during these past years helped to make the completion of the doctoral degree possible. I love you all very much and thank you for always being there.

Finally, to my husband, Adam J. Blake, you are my best friend. You encouraged me when I was down and celebrated with me as we accomplished what may have seemed impossible. When it comes to you, I have no words which could express all of which you have been and continue to mean to me. I love you.

Table of Contents

List of Tables

List of Figures

List of Symbols

A	area
C	concentration
D	diffusion
E	electric field strength
E_s	field strength during sampling
e	charge of electron
ε	dielectric constant
ζ	zeta potential
F	Faraday constant
$F_{voltage}$	force due to voltage
F_{drag}	force due to drag
g	gravitational constant
H	height equivalent of a theoretical plate
h	height
I	current
J_j	flux of ion j
κ	conductivity
L_d	length to detector window
L_t	total capillary length
l_{inj}	injection plug length
N	efficiency
η	viscosity
P	pressure
p	electrochemical potential
ρ	density of sample solution
Q	quantity injected electrokinetically
R	gas law constant
r_h	hydrodynamic volume

σ^2_{tot}	total variance
σ^2_{inj}	variance due to injection
σ^2_{col}	variance due to column
σ^2_{det}	variance due to detector
T	temperature
t_m	migration time
t_o	migration time of a neutral marker
t_s	sampling time
μ_{tot}	total mobility
μ_{ep}	electrophoretic mobility
μ_{eo}	electroosmotic mobility
V	voltage
V	volume
υ_{ep}	electrophoretic velocity
υ_{eo}	electroosmotic velocity
υ_{ITP}	isotachophoretic velocity
x	distance
z	charge on the species

Chapter I

Historical

Electrophoresis

One word can summarize many of the methods for separating mixtures of ionic analytes. That word is electrophoresis. Although electrophoresis has been studied since 1909 when Michaelis first observed the migration of colloids in an electric field, it has only become a subject of intense interest over the past 20 years. The primary separation mechanism behind electrophoresis is the application of an electric field providing transport and separation of compounds. The use of an electric field to generate transport eliminates the necessity of high pressure, used in most separation techniques including gas chromatography (GC) and high performance liquid chromatography (HPLC).

In order to predict the types of separations expected in electrophoresis, information about the mobility of the ionic analytes must be obtained. In 1937, Tiselius used a method involving moving boundary electrophoresis to ascertain this type of information.[1] The U-tube shown in Figure 1-1 is a device used to determine electrophobic mobility, and forms the basis for free zone electrophoresis. Voltage is applied through an external circuit (not shown) that is connected to each of the electrodes. A small quantity of sample is introduced in a narrow band as illustrated. This is called free zone electrophoresis because it can be assumed that the more mobile ions do not interfere with the less mobile ions. In other words, there is no interference due to mass transfer among analyte ions. A common problem that
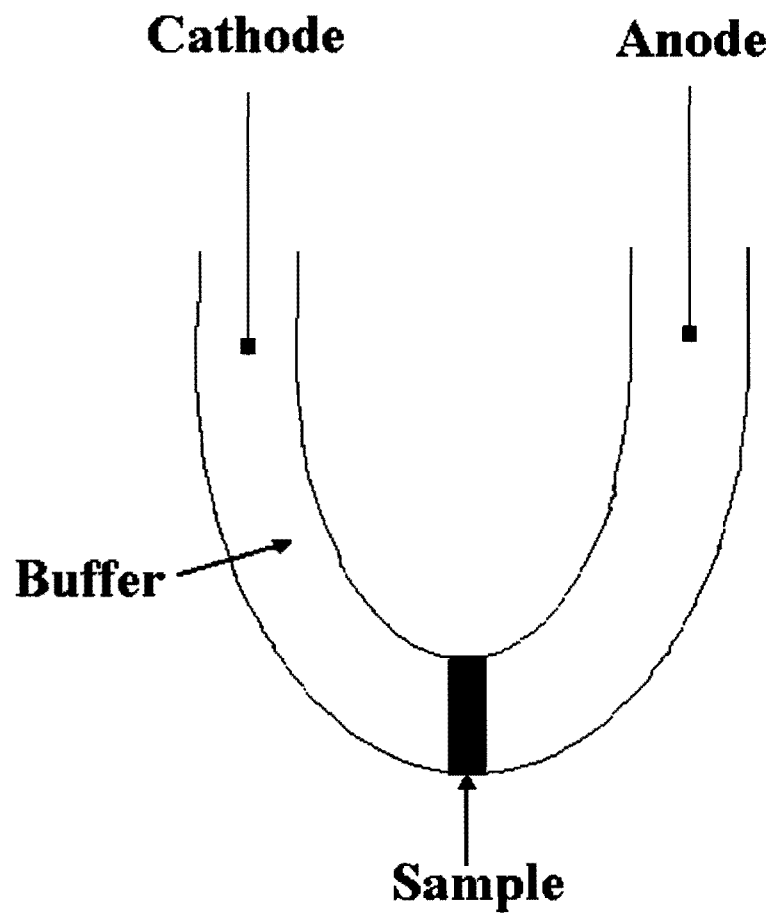
Figure 1-1: U-tube used for measuring electrophoretic mobilities.

occurs in free zone electrophoresis is joule heating that occurs when a strong electric field is applied to the U-tube filled with buffer solution. Joule heating causes a density gradient in the buffer because some areas will be warmer than others. These density gradients will increase migration rates of the analytes in a non-uniform manner.[1] Another negative effect of joule heating, convection, causes analyte bands to be unfocused and wide as opposed to being narrow and focused.[1] Although joule heating occurs to a great extent in a large U-tubes, a small capillary, currently utilized with today's technology, will not heat as much because of its size. Capillary electrophoresis will be discussed in more detail shortly.

In the 1950's, Wieland and Fisher performed the first zone electrophoresis on a planar system.[2] This led to the development of gel electrophoresis and thereby improved the analyses of starch gels, cellulose acetate, agarose, etc... The planar system is shown in Figure 1-2. In this technique, the separation is performed by placing the sample on a supporting medium such as a piece of paper or gel soaked with electrolyte. An electric field, typically up to 500 V, is then applied. Each charged substance will migrate within the carrier electrolyte toward its respective electrode. The speed of analyte migration depends upon it's net charge and frictional interaction with the supporting medium.[1,3] The carrier electrolyte, or buffer, maintains the requisite pH and provides sufficient conductivity to allow for the passage of electrical current.[3] The overall process can take up to several hours to complete, however, multiple samples can be processed within the same slab gel, in conjunction with the necessary calibration standards. Two-dimensional analysis is also possible. The relative mobility of each analyte is calculated from the distance it has moved relative to the calibration standard. In electrophoresis, differences in mobility are key to the separation
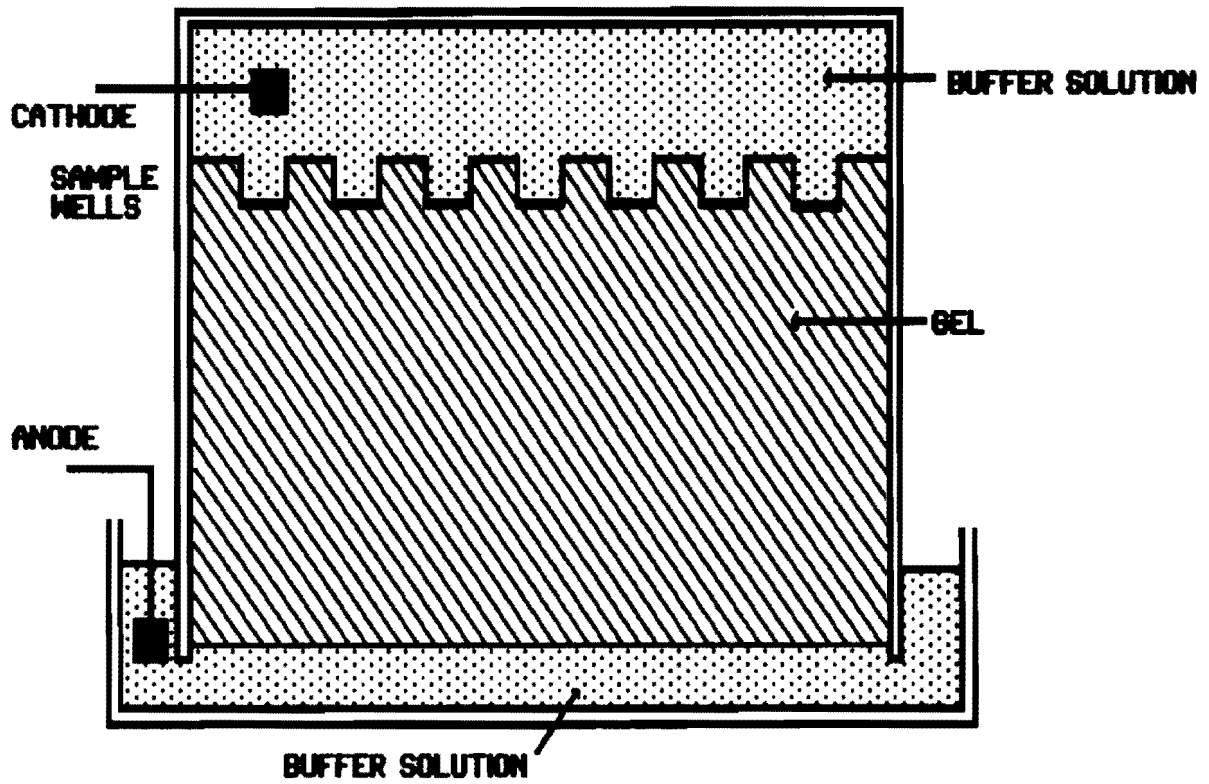
Figure 1-2: Slab-gel apparatus. (Weinberger, R. *Practical Capillary Electrophoresis*; Academic Press, Inc.: New York, 1993.)

process. In order to view the analyte bands gels are usually subjected to either a dye or the samples are tagged with radioactive label in order for the eluted bands to be seen. They are then photographed or scanned for permanent record.[2,3] Problems encountered with gel electrophoresis include the development of a solvent front that does not allow the matching of our analyte bands to the bands eluted from the calibration standard. The supporting slab gel electrophoresis media, commonly used to provide physical stabilization for the above process, assists in band matching. The media itself will function to reduce band broadening associated with diffusion and convection for both the analyte bands and the calibration standard.[4] The use of large glass plates to support the gel increases the effects of joule heating. Better resolution is obtained with smaller glass plates. As mentioned previously, convection is the result of joule heating. The high viscosity of most gels deters movement arising from joule heating and diffusion. However, it cannot stop it completely. Quantitation can be difficult.[2] In addition, mobility is not the sole contributor to the separation process. The gel network acts as a molecular sieve, slowing the necessary movement of the analyte ions.[2] The development of routine planar gel electrophoresis postponed further development of capillary electrophoresis (CE).

Hjerten developed the direct forerunner of modern CE technology in 1967.[2] Glass capillaries, rather than flat bed gels, were filled with electrolyte. In order to reduce the detrimental effects associated with joule heating, the 3 mm internal diameter glass capillary was rotated. This helped smooth the differences in viscosity throughout the column, minimizing the effects of convective gradients.[2] As methods of heat dissipation improved and smaller diameter capillaries became readily available, higher separation potentials were

implemented without column rotation. Eventually, in 1979 zone electrophoresis was performed in a capillary by Everarts using a 200 μm internal diameter teflon column.[5] This was at approximately the same time that fused silica GC capillaries were developed for gas chromatography.[6] In 1981, Jorgenson and Lukacs coined the term capillary zone electrophoresis (CZE) with their separation of dansyl amino acids using 75 μm internal diameter columns with fluorescence detection, shown in Figure 1-3.[7] The electropherogram demonstrates the separation of cations and anions. Neutral compounds co-elute in the area surrounding 12.5 minutes.

Throughout the 1980's capillary zone electrophoresis was expanded to include a family of techniques slightly different in nature but similar in principle. Gel electrophoresis and isoelectric focusing techniques were adapted to the capillary format.[8,9] In 1984, Terabe developed micellar electrokinetic capillary chromatography (MECC).[10] This involved the addition of a surfactant to the buffer above the critical micelle concentration before performing electrophoresis. The analytes partition back and forth between the micelle and solution. The addition of this pseudo-stationary phase adds interfacial mass-transfer to the system.[10] MECC is used for a broad range of charged, neutral, and small species including aromatic hydrocarbons,[11-14] corticosteroids,[15,16] metal chelates,[17-20] vitamins,[21-25] and urinary porphyrins.[26]

Advances in sensitive detectors were also achieved in the 1980's. Previous detector technology was not designed to accommodate mass limits of detection attainable in CZE. Detectors with high sensitivities are needed because of the small amounts of material that can
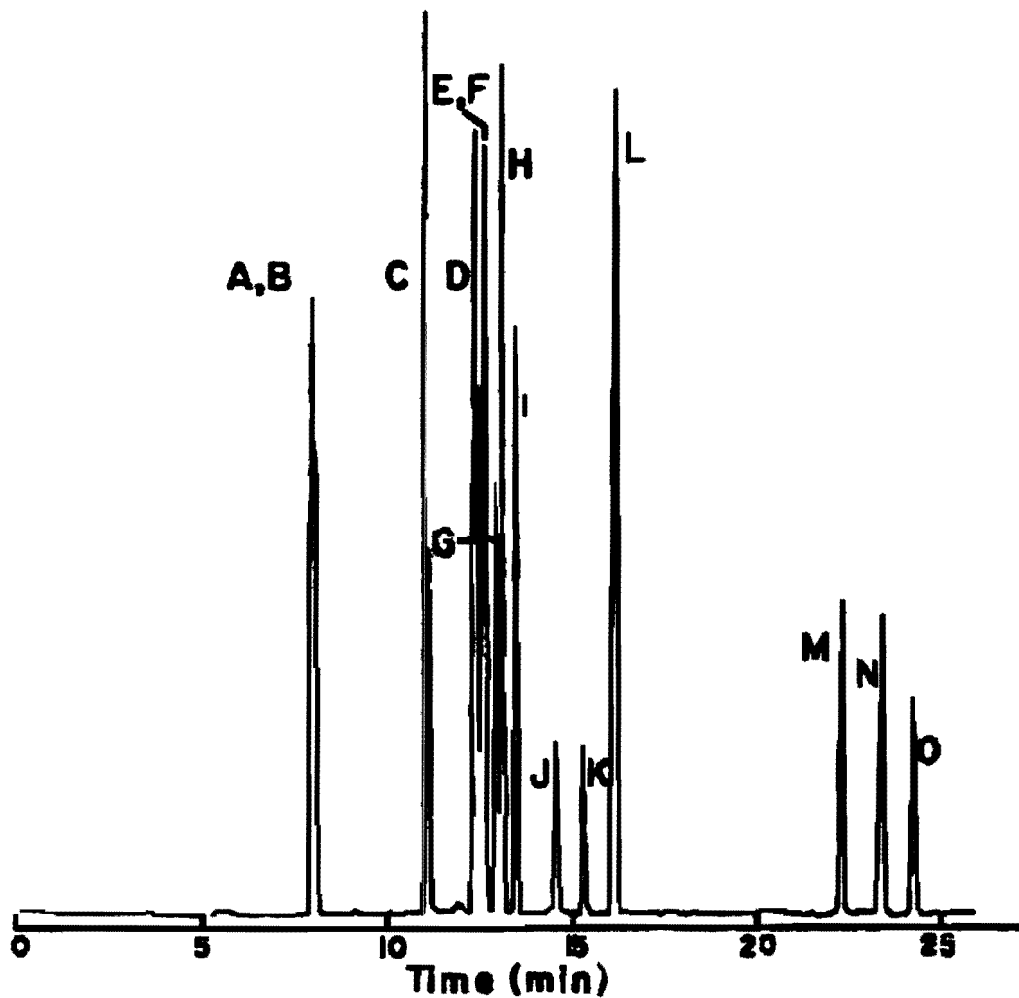
A	Unknown impurity	H	Alanine
B	Labeled lysine	I	Glycine
C	Dilabeled lysine	J and K	Unknown impurities
D	Asparagine	L	Di-labeled cysteine
E	Isoleucine	M	Glutamic acid
F	Methionine	N	Aspartic acid
G	Serine	O	Cysteic acid

Figure 1-3: Separation of dansyl amino acids. (Jorgenson, J.W. and Lukacs, K.D. *Anal. Chem.* **1981**, *53*, 1298.)

be injected into the capillary. Injection reproducibility was also an issue. Injection and detector sensitivity were two main disadvantages of CZE for these reasons. Concentrated samples help to alleviate short-comings in detector sensitivity, however, the general tendency is to dilute samples in order to assuage troublesome matrix effects.[2] Also, spectroscopic detector technology had to be modified to accommodate narrow-bore columns. Flow cells cannot be used because the narrow, separated bands attained by the CZE technique would be significantly broadened. When chromatographic techniques moved toward miniaturization, loading capacities simultaneously decreased.[2] In GC this was not a problem because sensitive detectors such as flame ionization, electron capture, and mass spectrometers were easily interfaced. Liquid separation techniques, such as μ-LC, did not share the same ease for detector adaptation. The same difficulties were expected for CZE. By 1984, fluorescence and ultraviolet (UV) detectors were physically modified to monitor CZE bands directly on-column.[2] A diagram illustrating the focusing optics employed for on-column UV detection are shown in Figure 1-4. Techniques involving laser-induced florescence,[27] mass spectrometry,[28] electrochemical detection,[29] and indirect detection[30] have also been developed. However, the most common detectors used today remain UV and fluorescence.

Capillary Zone Electrophoresis (CZE)

Capillary zone electrophoresis represents the merging of two technologies: gel electrophoresis and chromatography.[2] The combination of these two analytical tools has led to a family of capillary electrophoresis techniques, each of which involves a slightly different separation mechanism. These include capillary zone electrophoresis (CZE), capillary isoelectric focusing (CIEF), capillary gel electrophoresis (CGE), capillary isotachophoresis

PHOTODIODE

SAPPHIRE LENS

APERTURE
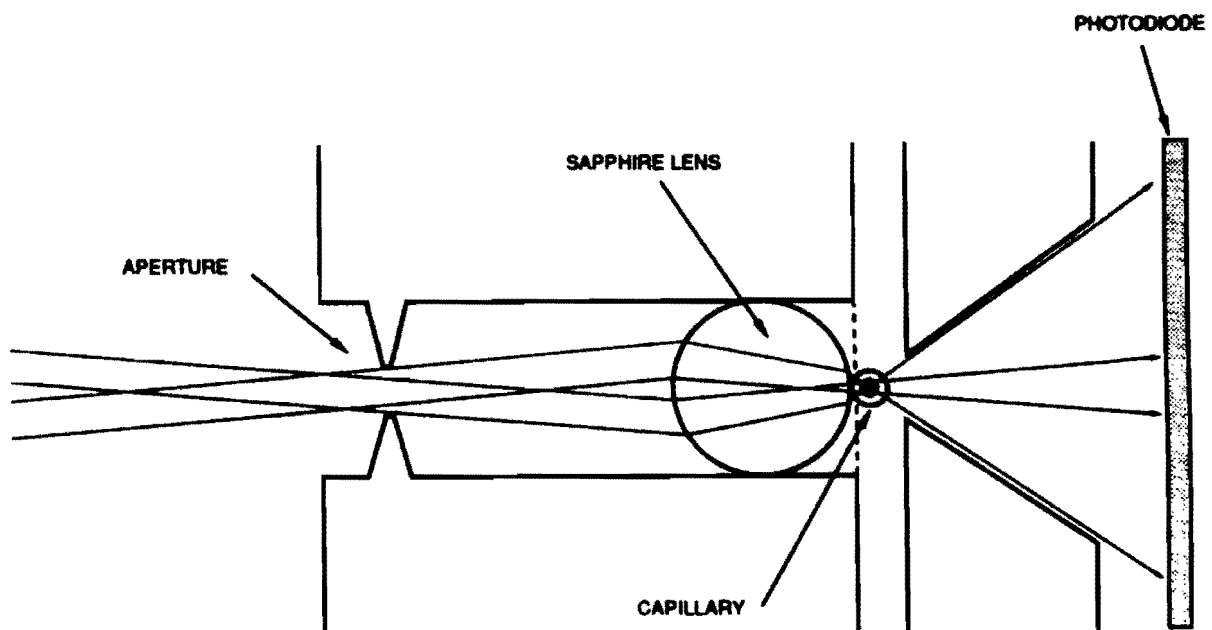
CAPILLARY

Figure 1-4: Focusing optics employed for on-column UV detection. (Weinberger, R. *Practical Capillary Electrophoresis*; Academic Press, Inc.: New York, 1993.)

(CITP), micellar electrokinetic chromatography (MECC or MEKC), and capillary electroosmotic chromatography (CEC).[31] Of these, the focus of study throughout this dissertation will be the simplest form of capillary electrophoresis, namely CZE.

In many ways, the movement of ions in CZE may be compared to the voltaic cell experiment performed in many freshman laboratories. In a voltaic cell, a spontaneous redox reaction serves as a source of electrical energy. Figure 1-5 illustrates a simple voltaic cell.[32] In this cell, zinc metal is reacted with protons.[32]

$$Zn_{(s)} + 2\,H^+_{(aq)} \quad Zn^{2+}_{(aq)} + H_{2(g)} \tag{1-1}$$
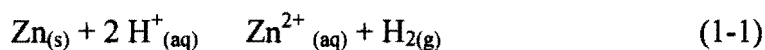
At the anode, zinc metal will be oxidized to Zn^{+2} and at the cathode, H^+ will be reduced to hydrogen gas. Because no metal is involved in the cathode half reaction, an inert electrode is used. Inert electrodes consist of an unreactive material that is capable of conducting an electrical current. Platinum wires are commonly used for this purpose, however, graphite rods and nichrome wires may also be used.[32] Electrons generated at the anode move through the external circuit towards the cathode establishing the current. A voltmeter is used to measure the voltage obtained. (Figure 1-5) In order to maintain a constant current through the external circuit, ions must be allowed to move through the aqueous solutions in the cell in order to establish electrical neutrality. A salt bridge serves to complete the circuit, permitting the ion transport. Within the salt bridge, there is a solution of ions which do not participate in the redox reactions. It consists of an inverted U-tube filled with solution and plugged with
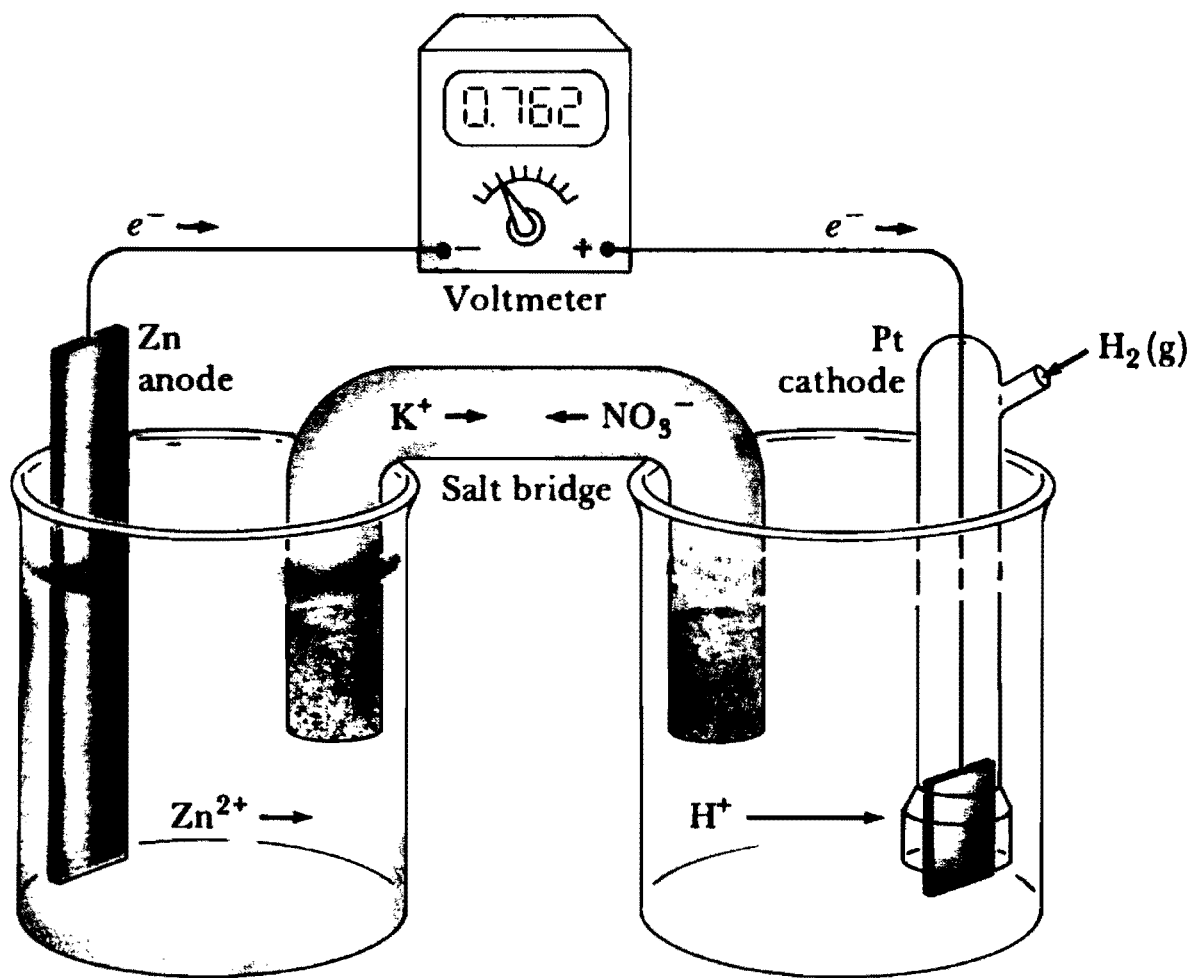
Figure 1-5: Typical voltaic cell setup. (Masterson, W.L. and Hurley, C.N. *Chemistry Principles and Reactions*; Saunders Publishing Company, Inc.: New York, 1989.)

cotton on both ends.[32] In order to maintain electrical neutrality, cations will move toward the cathode and anions will move toward the anode through the salt bridge. This will compensate for the surplus of Zn^{+2} ions at the anode and the resulting deficit of H^+ ions created at the cathode.[32] The movement of ions through the salt bridge is required if electrical neutrality is going to be maintained.

Similarly, the movement of ions through a salt bridge becomes the focus of study in CZE. However, it is more commonly referred to as the capillary and the ends are no longer plugged with cotton. It functions a little more like an electrolytic cell where ions are forced to move through the column while energy is pumped into the system.[32] Platinum electrodes exist at both the anode and cathode ends of a CZE system. When a positive potential is applied, ions are siphoned from the anode buffer reservoir, moved through the capillary, and deposited in the cathode buffer reservoir. The ionization of water maintains electrical neutrality.[2] When separating ions in solutions, proper pH control is essential. The electrolysis of water does not support preserving a constant pH on both sides of the CZE system. Therefore, buffers, or background electrolytes, assist the separation with minimal pH variations influencing the mobility of the analyte ions. A typical CZE system is illustrated in Figure 1-6. A high voltage power supply capable of ±30 kV provides current movement through the external circuit. The capillary provides the mechanical support of the carrier electrolyte. Detection is shown directly on-line, close to the detector side buffer reservoir. As in all electrophoresis techniques, separation of charged molecules will be achieved provided each of the analytes experience different velocities (or mobilities) under the influence of the electrical field.
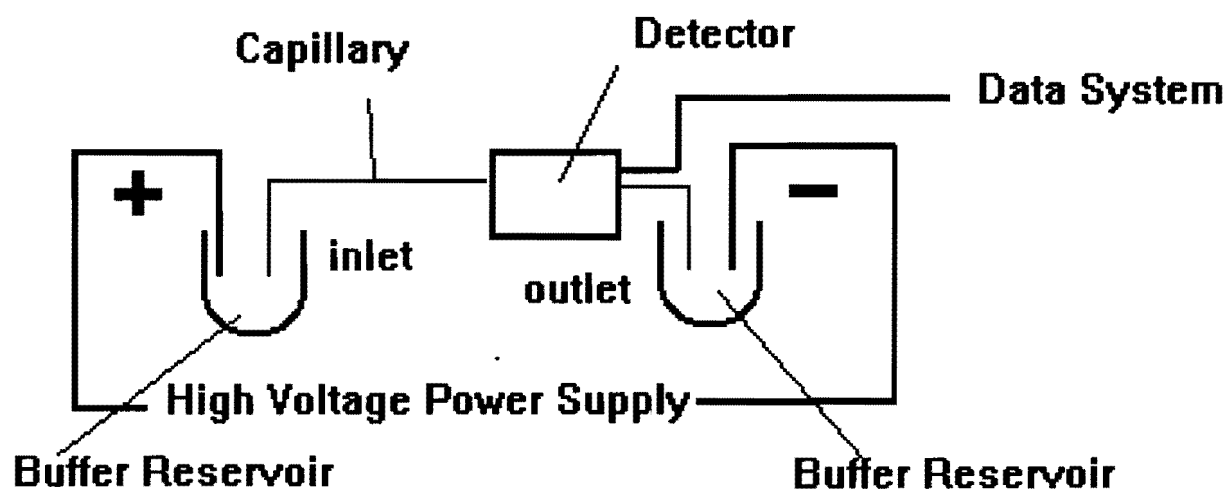
Figure 1-6: Block diagram of CZE instrument.

Ion Transport in Solution

Since separations in CZE are primarily based upon differences in ion mobility through an electrolytic solution, it is important to have an understanding of why ion transport is occurring. Bockris and Reddy note two aspects of ion motion in electrolyte solutions.[4] First there is the individual aspect, concerning the behavior of ions as individuals. These movements are essentially random in direction and speed.[4] Group aspects occur when groups of charged atoms or molecules move in preferred directions producing a flux of ions.[4] Ion flux is merely the rate of ion transport. There are three ways to produce ion flux in solution: diffusion, migration, and hydrodynamic flow.[4] As mentioned previously, diffusion arises from differences in the concentration of ions in different regions of electrolyte. The resulting concentration gradient induces the flow of ions to less concentrated regions.[4] This movement is illustrated in Figure 1-7. In Figure 1-8 migration is observed when ions move toward their respective electrodes. When there are differences in electrostatic potentials at various point of electrolyte, migrational flow will occur in the direction of the field.[4] This type of behavior will form the basis of electrophoretic mobility in terms of CZE, and will be discussed in more detail later in this chapter. If differences in temperature, pressure, or density exist in different regions of bulk electrolyte, hydrodynamic flow will occur to alleviate the stress of the non-homogeneous environment. This may incorporate the movement of the solution as a whole or in parts. Convection will occur if parts of the solution move relative to other parts.[4]

The consideration of the mass transfer effects of diffusion and migration are important to method development in CZE.[2] Conditions fostering convective motion are usually avoided.
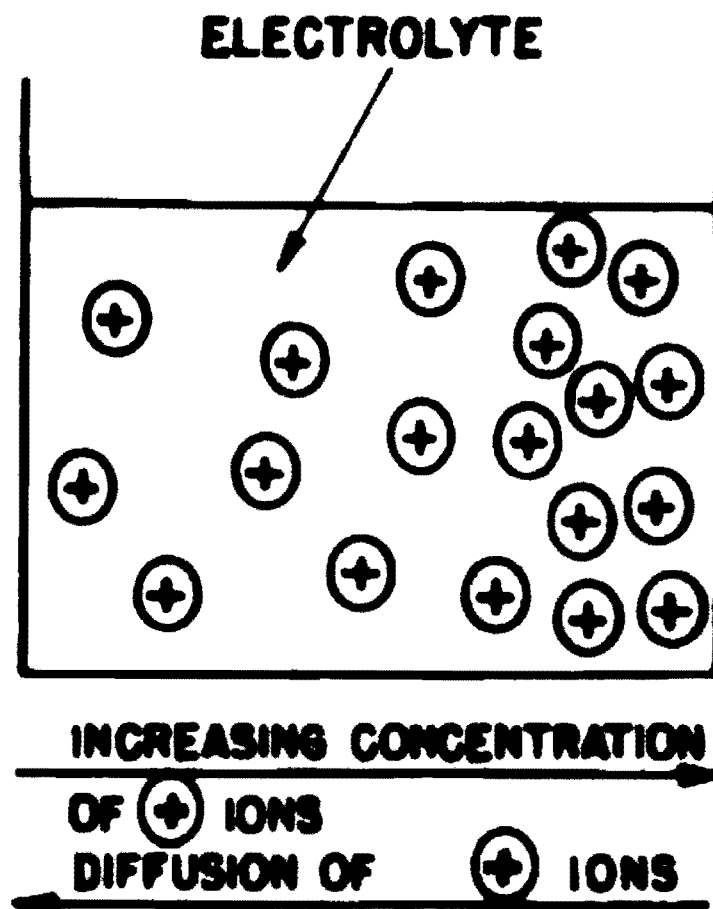
Figure 1-7: The diffusion of positive ions resulting from a concentration gradient of these ions in an electrolytic solution. The directions of increasing ionic concentration and of ionic diffusion are shown below the diagram. (Bockris, J. O'M. and Reddy, A.K.N. *Modern Electrochemistry · 1*; Plenum Publishing Corporation: New York, 1970.)
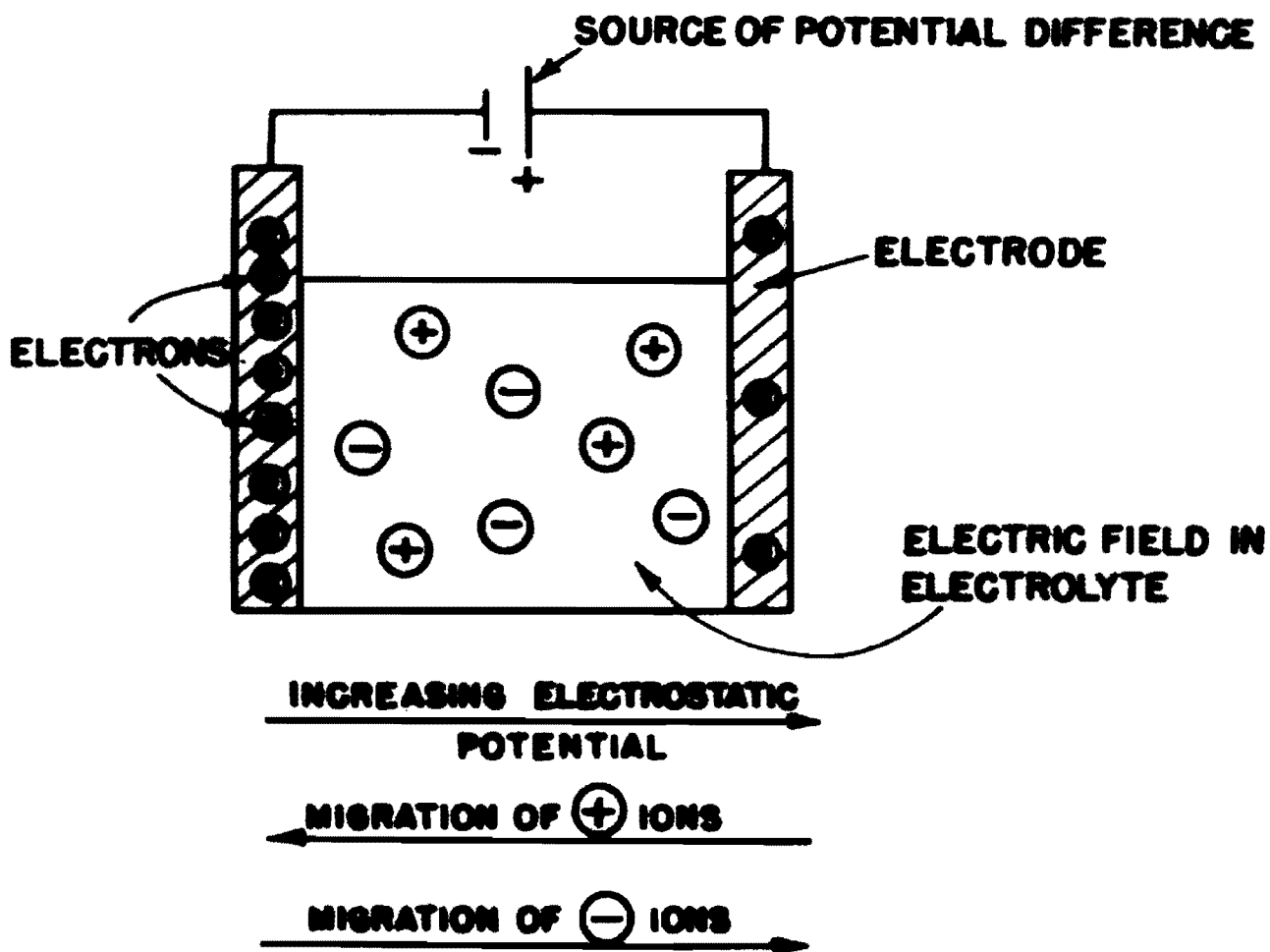
Figure 1-8: The migration of ions resulting from a gradient of electrostatic potential in an electrolyte. The directions of increasing electrostatic potentials and of ionic migration are shown below the diagram. (Bockris, J. O'M. and Reddy, A.K.N. *Modern Electrochemistry · 1*; Plenum Publishing Corporation: New York, 1970.)

This includes problems arising from joule heating. The construction of Ohm's law plots assists in the avoidance of these experimental conditions.[2] In an Ohm's law plot, shown in Figure 1-9, current is plotted against voltage. Deviation from linearity mark regions at which joule heating is influencing the experimental controls.

To quote Giddings, "Separation is the art of maximizing separative transport relative to dispersive transport."[1] Perhaps if Giddings was speaking directly about the separation power of CZE he would clarify by stating, "It is the art of differentiating migration behavior while minimizing the effects of diffusion." Differences in analyte mobility arising from the migration of ions will achieve separation in CZE. Diffusive properties of analytes in solution contribute to a broadening of the zones in which the analytes migrate. Both processes combine in the derivation of the mass transfer equation as it applies to ion movement in CZE.

Referring to Figure 1-10 and using the equations derived by Bard and Faulkner,[33] the flux (J) experienced by ion j will be proportional to the gradient p_j where p is representative of differences in electrochemical potential.[33]

$$J_j \propto \nabla p_j \qquad (1\text{-}2)$$

The constant of proportionality is $- (C_j D_j / RT)$ where C is the concentration of j, D is j's diffusion coefficient, R is the gas law constant, and T is the temperature in Kelvin. This factor is negative because flux generally opposes the direction of increasing electrochemical potential.[33]
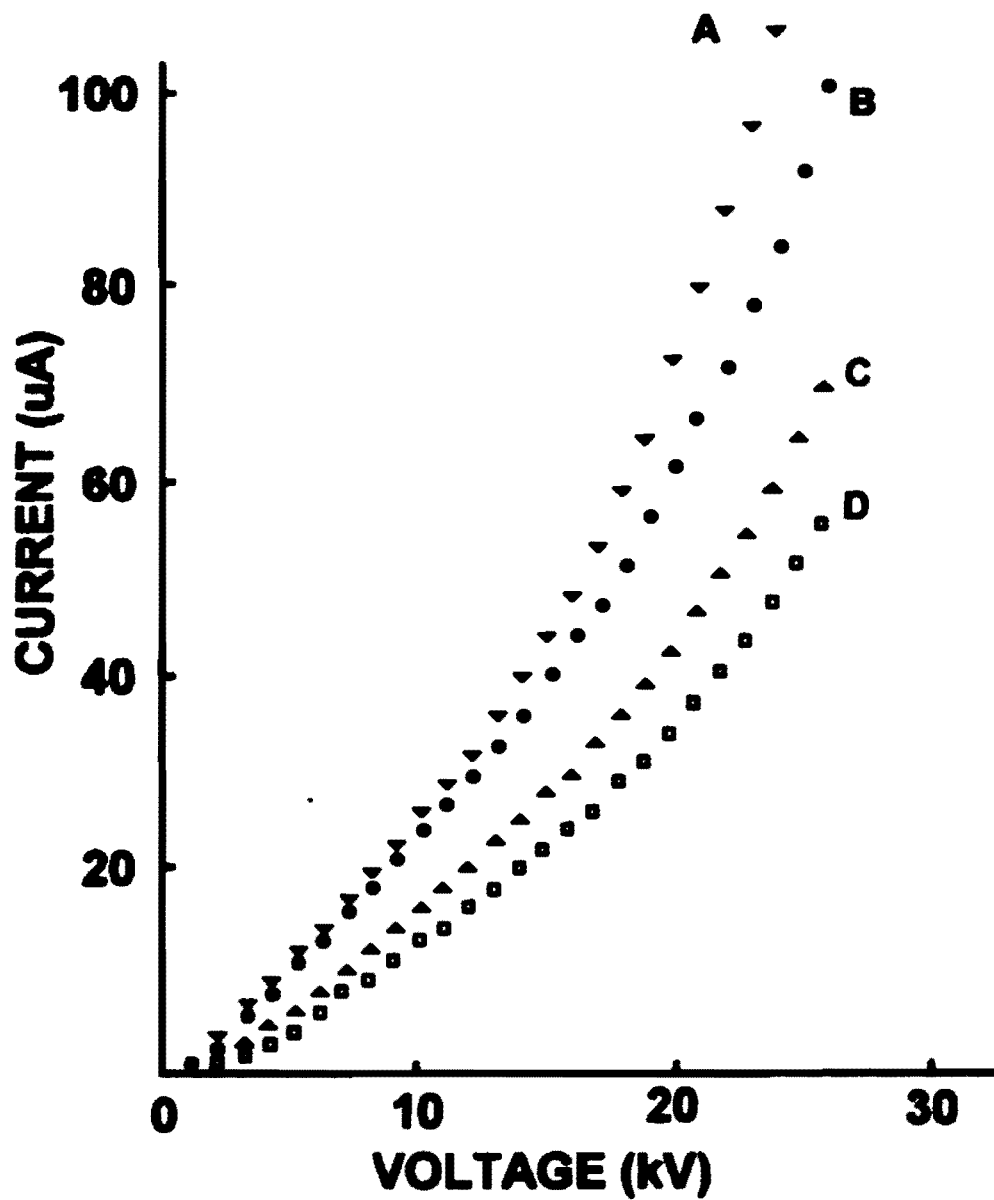
Figure 1-9: Example of an Ohm's Law plot. (Weinberger, R. *Practical Capillary Electrophoresis*; Academic Press, Inc.: New York, 1993.)
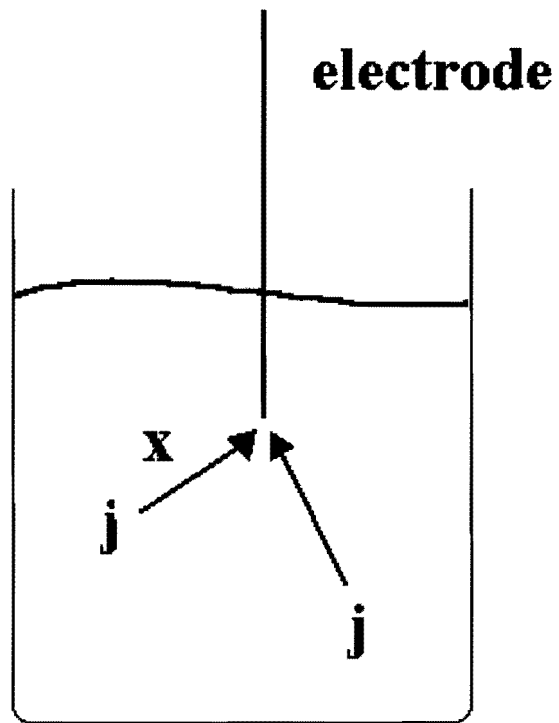
Figure 1-10: Illustration of ion "j" movement towards electrode in an electrolyte solution.

$$J_j = -(C_jD_j / RT) \nabla p_j \qquad\qquad (1\text{-}3)$$

Assuming one-dimensional linear analysis, the flux due to linear mass transfer becomes[33]

$$J_j = -(C_jD_j / RT)(\partial p_j / \partial x) \qquad\qquad (1\text{-}4)$$

where x is the distance between ion j and the electrode. If convection causes solution movement, there is another term added to the above expression, C_jv_x. The symbol "v" is the velocity of the bulk solution. This term should be insignificant in capillary electrophoresis because, as mentioned previously, factors causing convection are usually avoided. Substituting the Nernst-Plank equations by assuming the activity of ion j is equal to its concentration, the following expression is obtained.[33]

$$Jj(x) = -D_j \frac{\partial C_j(x)}{\partial x} - \frac{z_jFD_jC_j}{RT}\frac{\partial p(x)}{\partial x} \qquad\qquad (1\text{-}5)$$

This is regarded as the general form of the mass transfer expression as it pertains to CZE. The first term comprises the effects of diffusion and the second term relates transfer mechanisms associated with ion migration. For further information regarding the development of the above relationship, refer to reference 33.

The Language of Electrophoresis

When discussing CZE, the mechanisms of ion movement are related in terms that are

much simpler than the mathematical derivations described above. Essentially there are two types of flow that must be considered while performing CZE: electrophoretic and electroosmotic flow.[2] As mentioned earlier, flow occurs because the ions are moving towards the appropriate electrodes. The types of buffer solutions used to aid in this transportation are very dependent on the application, but the two important factors are that the buffer will provide transfer without joule heating and that the sample will be soluble in it.[2]

Inside the capillary, the ions will experience forces due to voltage (Equation 1-6) and viscous drag. (Equation 1-7)[2]

$$F_{voltage} = zeE \qquad\qquad (1\text{-}6)$$

The force due to the voltage, $F_{voltage}$, is equal to the product of the charge of the ion (z), charge of an electron (e), and the strength of the electric field (E). As the ion accelerates within the electric field, it is retarded by a viscous drag and reaches only a limiting drift velocity (electrophoretic velocity), v_{el}.[34] The force due to viscous drag equals the following:[2,34]

$$F_{drag} = 6\pi\eta r_h v_{el} \qquad\qquad (1\text{-}7)$$

where η is the viscosity of the buffer, r_h is the hydrodynamic radius, and v_{el} is the electrophoretic velocity of the ion. It follows from Equations 1-6 and 1-7 that when electrophoretic velocity is established:[1,2,34-36]

$$6\pi\eta r_h v_{el} = zeE \qquad\qquad (1\text{-}8)$$

which may be rearranged to:

$$v_{el} = \frac{zeE}{6\pi\eta r_h} \qquad\qquad (1\text{-}9)$$

where charge and hydrodynamic radius are variable. Selectivity is based on the ratio of the charge to the hydrodynamic radius.[1,2,36] Therefore small cations will elute first, followed by larger cations. Neutral molecules will elute together. Finally, large anions will sequentially fall into place followed by small anions.[37] A clear illustration of this elution adapted from Heiger is presented in Figure 1-11.[37]

Electroosmotic flow constitutes the bulk flow within the capillary.[2] It can cause both advantages and disadvantages to separation and occurs because the silica capillary can be made into a charged surface upon which there will be electrostatic interactions with charged particles. This charged surface is generally referred to as the electrical double layer. According to Weinberger and as illustrated in Figure 1-12, cations are attracted as counter ions to the negatively charged column wall.[1,2] The adsorbed layer is tightly bound and immobile even when there is an applied electrical field. A rigid Stern layer and the diffuse Gouy-Chapman layer define the electrical double-layer.[2] When there is an electric field component parallel to the capillary wall, that field will pull these counter ions along the surface, dragging the solution with it.[1] Flow is induced. Removing the charged surface
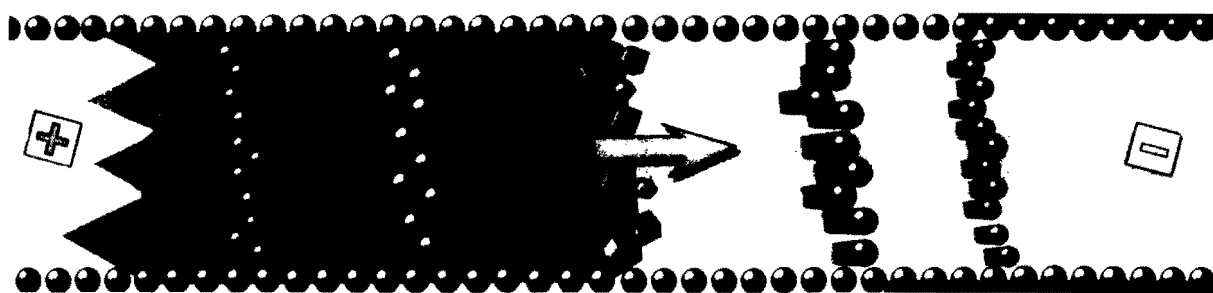
Figure 1-11: Separation of ions based on charge to hydrodynamic radius ratio. Charges on walls of capillary contribute to the formation of electroosmotic flow. (Heiger, D. *High Performance Capillary Electrophoresis, 2ⁿᵈ ed.*; Hewlett-Packard Company: France, 1992.)
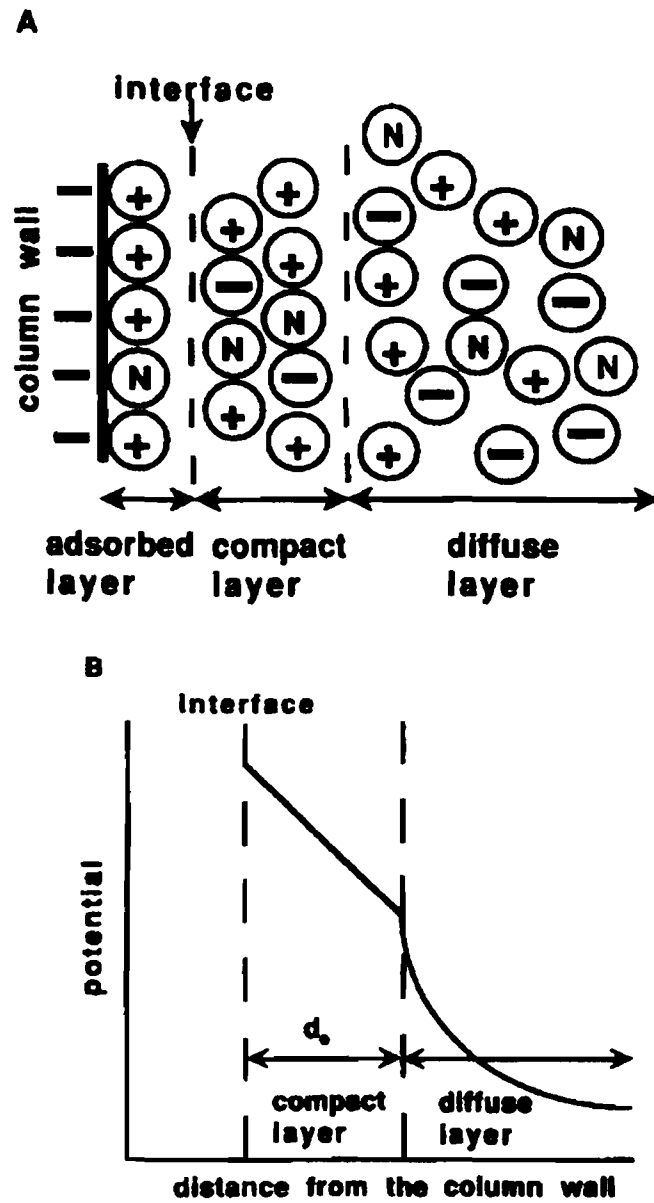
Figure 1-12: Representation of the electrical double layer versus the capillary wall. (Weinberger, R. *Practical Capillary Electrophoresis*; Academic Press, Inc.: New York, 1993.)

would minimize this type of flow. Under the influence of positive separation potentials and when electrophoretic and electroosmotic flow are in the same direction, overall transport of most species will be towards the cathode.[2] This allows both anions and cations to be detected, as shown in Figure 1-3. This will occur if the electroosmotic flow component outruns the electrophoretic component of an anionic compound. The overall movement generated within the bulk solution is dependant upon buffer concentration, pH, and the addition of organic modifiers. All of these play a role in modifying the variables composing the electroosmotic flow (v_{eo}) as defined by the Smoluchoski equation.[2,34]

$$v_{eo} = \frac{\varepsilon \xi E}{\eta} \qquad (1\text{-}10)$$

where ε is the dielectric constant, ξ is the zeta potential of the liquid-solid interface, E is the field strength, and η is the viscosity of the buffer.

Electroosmotic flow also flattens our flow profile. In pressure driven systems, such as HPLC, the frictional forces of the mobile phase interacting at the walls result in a parabolic flow profile.[2] This is illustrated in Figure 1-13a. In CE, electroosmotic flow permits flatter flow profiles and therefore, higher transport efficiencies (Figure 1-13b).[2] Efficiency may be calculated using the following equation:[35]

$$N = 5.54 \, (t_m / (A/h))^2 \qquad (1\text{-}11)$$

Where t_m is the migration time of either the neutral marker or ion, A is the peak area, and h is

(a) Parabolic Flow

(b) Electroosmotic Flow
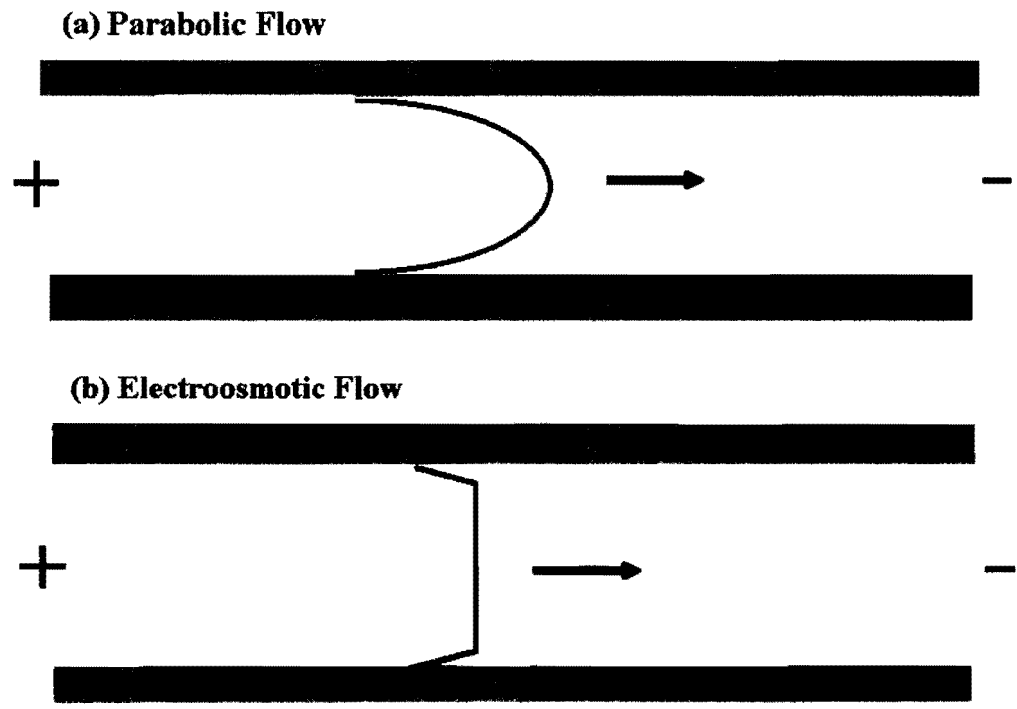
Figure 1-13: **(a)** Parabolic flow profile due to hydrodynamic flow. **(b)** Flow profile with addition of electroosmotic flow.

the peak height.

Evaluation of Total Mobility (μ_{tot})

The total mobility of an analyte (μ_{tot}), sometimes referred to as the apparent mobility, is the combination of electrophoretic mobility, μ_{el}, and electroosmotic flow, μ_{eo}.[2]

$$\mu_{tot} = \mu_{el} + \mu_{eo} \qquad (1-12)$$

Experimentally, the total mobility may be calculated using the following equation: [2]

$$\mu_{tot} = \frac{(L_d / t_m)}{(V / L_t)} \qquad (1-13)$$

where L_d is the length to the detector window, t_m is the migration time, V is the separation voltage, and L_t is the total length of the capillary. In the above expression, the numerator is the total velocity ($v_{ep} + v_{eo}$) and the denominator is the field strength employed during the separation process. All analytes in solution will be affected by the electroosmotic flow. Therefore, in order to obtain separation, proper control of the parameters governing electrophoretic mobility is essential. The electrophoretic mobility is commonly found by combining Equations 1-12 and 1-13 above to obtain the following expression:[38-42]

$$\mu_{ep} = \frac{L_d L_t}{V} (1/t_m - 1/t_o) \qquad (1-14)$$

In this equation t_0 is the migration time of a neutral marker, such as thiourea or acetone. It is used to measure the extent of electroosmotic flow. As described earlier in Equation 1-9, differences in the charge to hydrodynamic radius ratio will correlate directly to the separation of ions in solution because of the differences in the calculated μ_{ep}. Therefore, the role of buffer pH is critical in the selection of separation parameters. Typically, electrophoretic mobility plots are constructed as a tool in the method development process.[2,38] This is simply a map of analyte electrophoretic mobility as a function of pH. An example of an electrophoretic mobility plot is shown in Figure 1-14.[2] Ideally, the pH is chosen where ions are experiencing different mobilities and are not experiencing any type of equilibria associated with their pKa values. For instance, if one were trying to separate glutamate and acetate, a pH of 7.5 would be satisfactory. In accordance with the theory presented above, neutral molecules will exhibit no electrophoretic mobility and will serve only to measure the movement of the electroosmotic forces associated with bulk solution transfer. Glycine illustrates this behavior at pH's of 5.5 or less.

Performing the CZE separation

When a separation is performed using CZE, common preparations include conditioning the new capillary for 15 minutes with 1 N NaOH, 15 minutes with de-ionized H_2O, and 15 minutes with 0.1 N NaOH.[2,34] The base conditioning procedure is essential to make sure that the surface of the capillary is fully charged.[2] Finally, the run buffer is circulated through the column and the capillary is ready for use. A typical separation sequence consists of two pre-sampling steps. A base wash is necessary when solutes or sample matrix components bind to
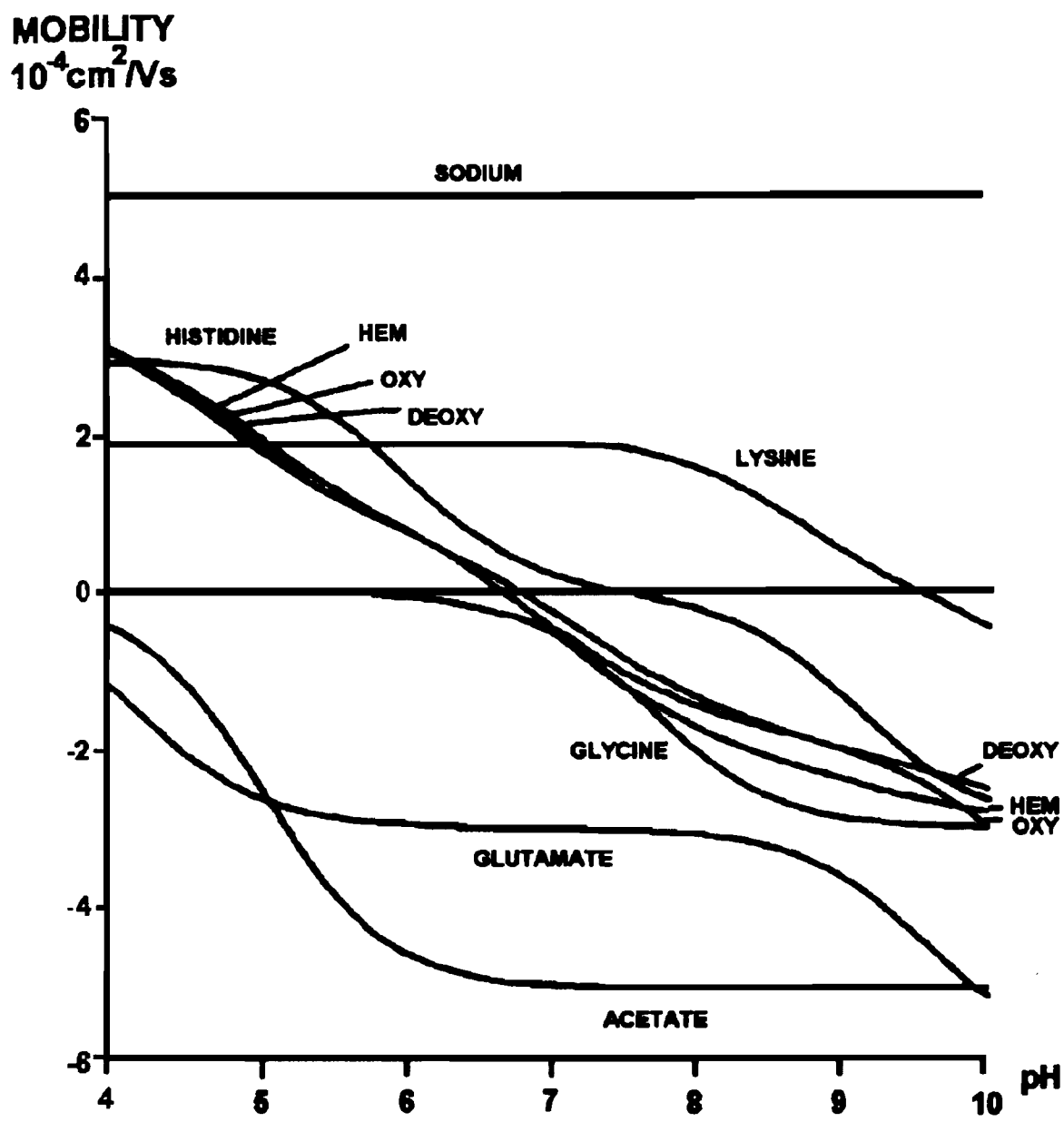
Figure 1-14: Example of an electrophoretic mobility plot. (Weinberger, R. *Practical Capillary Electrophoresis*; Academic Press, Inc.: New York, 1993.)

the capillary wall. The capillary is first washed with 0.1 N NaOH. The separation buffer is then cycled through the column. Injection and timed separation cycles follow immediately. Using a strong base such as sodium hydroxide ionizes free silanol groups and cleaves any epoxide linkages within the capillary wall.[2] On occasions where analytes adhere to the capillary wall, a strong base wash step will help in their removal prior to subsequent separations, thus rejuvenating capillary performance. Performance is regained because each time 0.1N NaOH is passed through the column there is a redistribution of the zeta potential along the capillary wall. Sometimes, however, alterations in the electrical double layer distribution are difficult to restore to the exact original conditions.

Disadvantages Associated with CZE

As discussed previously, two difficulties associated with CZE are getting the analytes onto the capillaries and detecting them once they are there. Modern detectors have been developed to accommodate the narrow capillary columns.[2] Injection, however, has been an area of concern due to the lack of reproducibility obtained using CZE.[43] Even with the availability of commercial instrumentation in 1988, the difficulties attributed to irreproducible migration times and peak areas has made it difficult to validate CZE methods.[43,44] Injection mechanisms and their influence on the separation parameters pertaining to reproducibility is the focus of study in this dissertation.

Chapter II

Introduction

Problems Encountered with Current Injection Mechanisms

Although capillary zone electrophoresis techniques have experienced rapid growth in terms of commercialism and application over the past 20 years, CZE still remains in the background of separation methods in research and quality control laboratories. One of the most common difficulties in CZE is the struggle to validate analytical methods using similar methodology to gas and liquid chromatography.[43,45] Recently, several efforts have focused on developing more representative validation procedures for CZE methods.[44,45] These new procedures combine the validation protocols of gel electrophoresis and chromatographic methods. Altria, *et.al.* outline these validation procedures, which include the necessity of evaluating capillary pre-injection rinsing techniques, capillary variation, reagent source, electrolyte stability, long-term injection precision, operator training, and additional robustness parameters.[45] In CZE, injection is believed to be one of the primary sources of ambiguity in the completion of these tasks.[43,44,46] The error may be attributed to the physical properties of the injection process itself.[47] When an injection is performed there is a physical disruption of the separation capillary. The capillary-electrode assembly must be moved to the sampling container and then moved back to the buffer solution.[47] This leads to spontaneous injection[48] and other difficulties such as analyte loss resulting from ohmic heating.[49] This movement of the column is rarely seen in any other separation technique. In

chromatography, most of the time the sample is dispensed in a narrow band in the column

inlet where the inlet itself is a separate entity of the system. In capillary electrophoresis, part

of the column is the inlet.[47]

Giddings describes all processes contributing to the variance of a system as additive.[1]

$$\sigma^2_{tot} = \sigma^2_{inj} + \sigma^2_{col} + \sigma^2_{det} \qquad (2\text{-}1)$$

σ^2_{col} = variance generated in the column

σ^2_{inj} and σ^2_{det} = extra-column variances due to injection and

detection respectively

By observing σ^2_{inj}, the injection portion of the system can be evaluated as it affects injection

plug length and peak area reproducibility. The contribution to variance from a plug injection

is related in the following equation:[2,50]

$$\sigma^2_{inj} = l_{inj}^2 / 12 \qquad (2\text{-}2)$$

where l_{inj} is the length of an injection plug. There are two common methods of injection in

CZE: hydrodynamic and electrokinetic.[2]

Hydrodynamic Injection

Hydrodynamic injection has proven to be the more accepted of these two forms in the literature.[43,44,51,52] Prior to the onset of commercial CZE systems, hydrodynamic injection was performed using home-made systems by moving the capillary physically from the sample-side buffer reservoir and into the sample solution at an elevated level.[2,34] An illustration of this movement is shown in Figure 2-1. The differences in height lead to siphoning of the sample. The capillary was held in the elevated sample vial for a short period of time and then returned to the sample-side buffer reservoir where the separation voltage was applied.[2] The volume of sample injected per unit time may be calculated using the Poiseuille equation:[2,53]

$$V_t = \frac{\Delta P \, D^4 \, \pi}{128 \eta L_T} \qquad (2\text{-}3)$$

where ΔP was the pressure drop, D is the internal diameter of the capillary, η is the viscosity, and L_T is the total length of the capillary. The pressure drop was determined by implementing the following relationship:[2]

$$\Delta P = \rho \, g \, \Delta h \qquad (2\text{-}4)$$

where ρ is the density of the sample solution and g is the gravitational constant. The height difference between the liquid levels of the sample container and the detector-side buffer reservoir is represented by Δh.
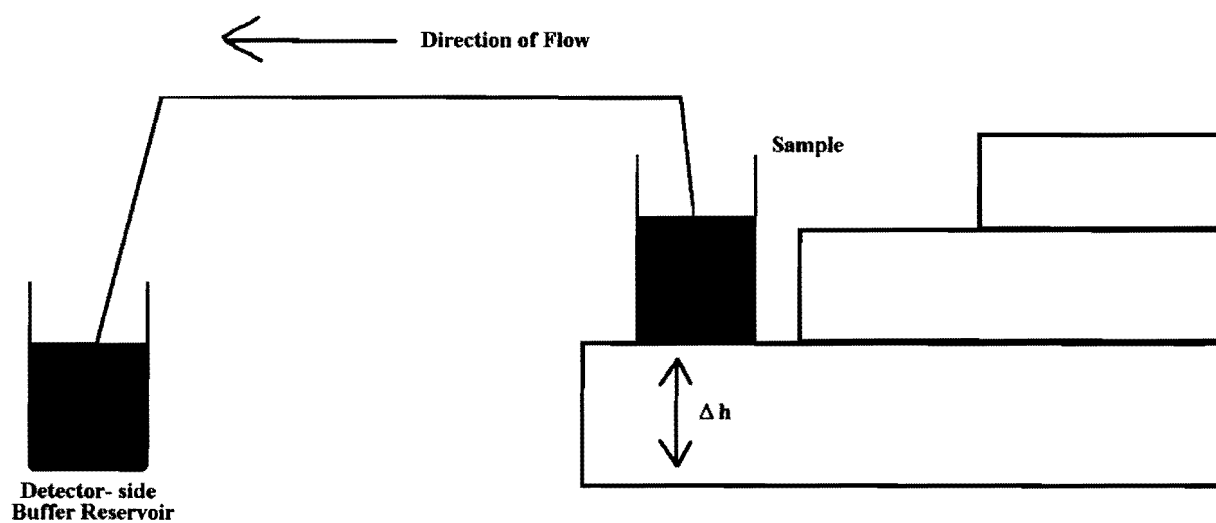
Figure 2-1: Schematic of hydrodynamic sample introduction mechanism.[34]

The arrival of commercial CZE systems in the early 1980's led to two other methods of performing hydrodynamic injection. CZE instruments were capable of applying a vacuum to the detector-side buffer reservoir or pressure to the sampling vial in order to perform the injection.[2] The latter method is preferred when the instrument is coupled to a mass spectrometer.[2]

Electrokinetic Injection

When performing an electrokinetic injection, solution is drawn into the capillary using electrophoretic and electroosmotic flow. The equation below is used to calculate the amount of material on the column (Q) when an electrokinetic injection is performed.[2]

$$Q = (\mu_{ep} + \mu_{eo})\pi r^2 E_s C t_s \qquad (2\text{-}5)$$

μ_{ep} = electrophoretic mobility E_s = field strength during sampling

μ_{eo} = electroosmotic mobility t_s = injection time

r = capillary radius C = concentration of solute

This equation corrects for sampling discrimination caused by varying degrees of electrophoretic mobility experienced by each of the solutes.[2,36] Initially, it was believed this dependence would lead to a non-uniform and biased injection plug.[47] However, recent work by Qi, *et.al.* has shown this bias to be irrelevant.[54,55] The electrokinetic injection plug bias cancels the detection bias seen in CZE techniques. The detection bias consists of

discrepancies that occur due to the different rates at which analytes pass the detector window.[54] Usually, parameters such as corrected peak area are applied in quantitation to account for the detection bias when hydrodynamic injection is performed. However, due to the cancellation, the correction is not necessary when electrokinetic injection is used.[54] CZE methods requiring electrokinetic sampling are not as popular in the literature as those implementing hydrodynamic sampling. This is excluding techniques which demand the usage of electrokinetic sampling such as capillary gel electrophoresis (CGE). Hydrodynamic forces imposed on a CGE column would siphon the gel out of the capillary.

Other Injection Methods

Other injection methods have also developed for CZE in order to allow better control of the amounts of sample entering the column. Tsuda, *et. al.* implemented rotary-type split injectors for CZE.[56,57] They were very similar in design and function to the rheodyne injectors commonly employed in HPLC systems. As illustrated in Figure 2-2, the sample is placed within the rotary valve and eluted through a delivery tube via an LC pump. At the interface between the delivery tube and capillary column, sample is drawn into the capillary using electrokinetic injection.[56,57] Dual-barrel micro injectors have also been developed by Wallingford and Ewing.[58] This method of injection is inherently based on the principles of microiontophoresis. It concerns the ejection of exogenous substances into specific regions of a biological system.[58] Micropipettes are typically less the 1 μm o.d. A micropipette is illustrated in Figure 2-3. Usually, the micropipette is filled with sample and then current is passed though the pipette, ejecting the sample into the specified biological region.[58]
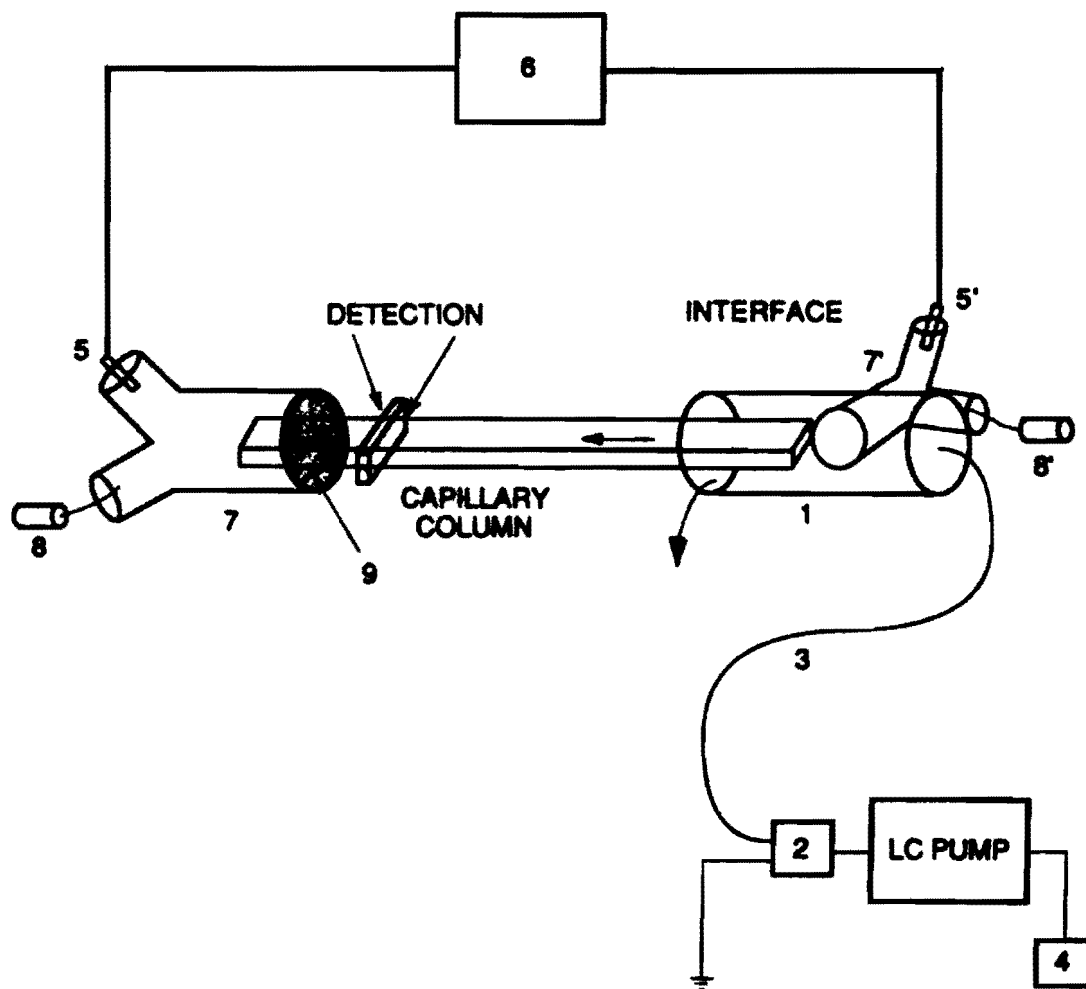
Figure 2-2: Schematic of CZE system with rotary split injection system. 1 = interface; 2 = injection valve; 3 = delivery tube of fused silica capillary; 4 = reservoir for LC pump; 5 and 5' = electrodes; 6 = high voltage power supply; 7 and 7' = reservoirs using 3-way PTFE connectors; 8 and 8' = syringes for filling reservoirs; 9 = epoxy seal. (Tsuda, T. and Zare, R.N. *J. Chromatogr.* **1991**, *559*, 103.)
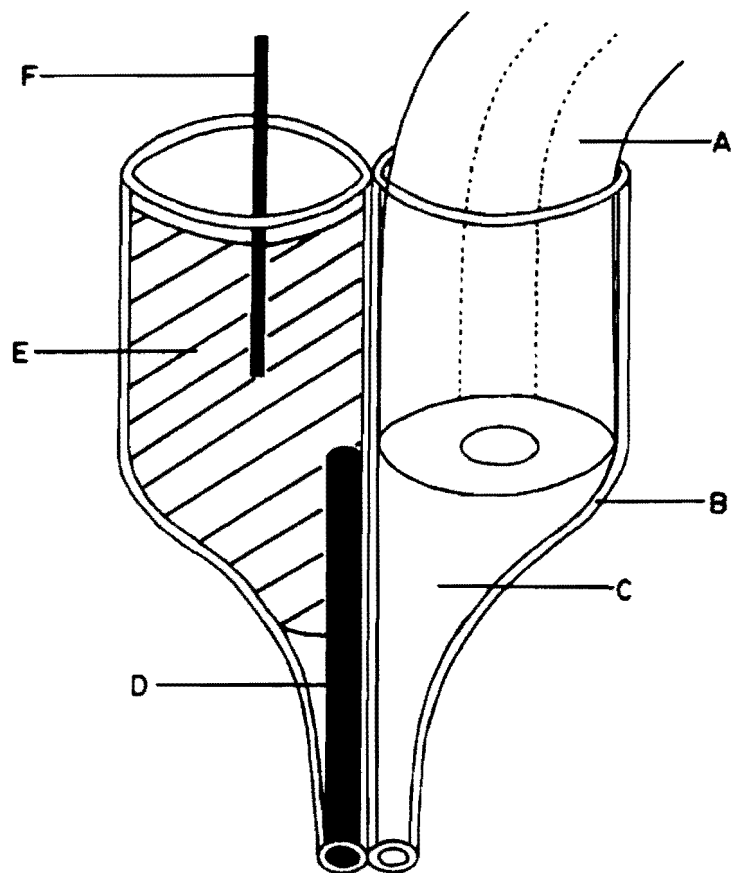
Figure 2-3: Illustration of micropipette used in microiontophoresis. A = fused silica capillary column; B = glass dual-barrel micropipette; C= buffered solution; D = carbon fiber; E = mercury; F = platinum wire. (Wallingford, R.A. and Ewing, A.G. *Anal. Chem.* **1987**, *59*, 678.)

For use in CZE, the electroosmotic flow along with iontophoretic effects can be made to cause migration of the analyte into the injector tip and then into the CZE column.[58] Sziele, et. al. also made contributions to micro injector mechanisms.[59] Their work, however, differed significantly regarding physical implementation. The injection mechanism was representative of the same technologies used in ink jet printers.[59] Linhares and Kissinger created on-column "electroosmotic syringes" illustrated in Figure 2-4. Sample was drawn into the capillary through an on-column fracture using electroosmotic flow.[60] Pu and Fang have also contributed to injection design using a similar device.[61] Other injection mechanisms include membrane interfaces,[62] microdialysis,[63,64] and microfluidic chips.[65,66] Currently, none of these injection mechanisms are employed to the same extent as the aforementioned hydrodynamic and electrokinetic injection techniques.

Improvements in Quantitative Reproducibility

Over the past 12 years, precision of quantitative parameters resulting from hydrodynamic and electrokinetic injection has been the most debated disadvantage of CZE. Even with the availability of commercial instrumentation in 1988, poor reproducibility of migration times and peak areas have been an area of extensive criticism.[44] Today, reproducibility values have been shown to be less than 1.0% relative standard deviations (RSD) in regards to migration time and peak area when internal standardization and hydrodynamic sampling are employed.[44,46,67] On-column sample enrichment techniques may also be used to enhance reproducibility. Common enrichment techniques include sample stacking, field amplified injection, and capillary isotachophoresis.[2]

39
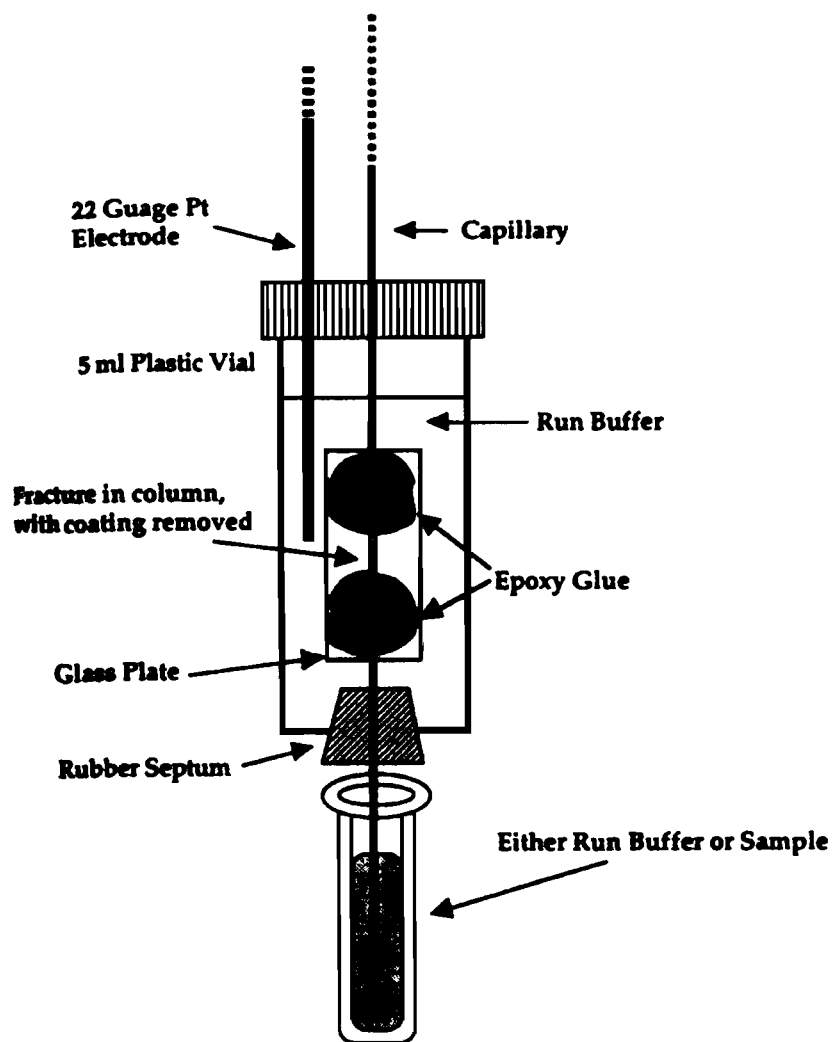
Figure 2-4: Diagram of on-column fracture injection mechanism. (Linahares, M.C. and Kissinger, P.T. *Anal. Chem.* **1991**, *63*, 2076.)

Sample Stacking

Sample stacking involves the compression of the sample plug after injection directly on the capillary.[2] The simplest way to perform this technique is by diluting the sample in a more dilute form of the run buffer. The objective is to make the ionic strength of the sample solution less than that of the run buffer.[2] After injection and when the separation potential is applied, the electric field strength experienced by the sample zone will be higher than the zones occupied by the run buffer due to the differences in conductivity.[2] This effect is illustrated in Figure 2-5. Because electrophoretic velocity is directly proportional to the imposed field strength, the analytes in the sample zone will be moving at elevated velocities until they reach the low field boundary.[2] At that point, the velocity of the ions in the front of the zone will abruptly drop because of the lower field strength.[2] Meanwhile, the ions in the middle and rear of the zones are still moving forward. The overall effect is a compression of the sample plug (stacking). This works for cations (Figure 2-5) and anions.[2] Sample stacking has been implemented in a number of applications using hydrodynamic and/or electrokinetic injection for the separation of phenylthiohydantonin (PHT)-amino acids,[68,69] peptides,[70] and the analysis of DNA adducts,[71] to name a few. Large-volume stacking has also been accomplished in the separation of arsenious acids with the addition of polarity switching.[72] Polarity switching helps to alleviate the differences in electroosmotic flow between the sample matrix and run buffer.[72]
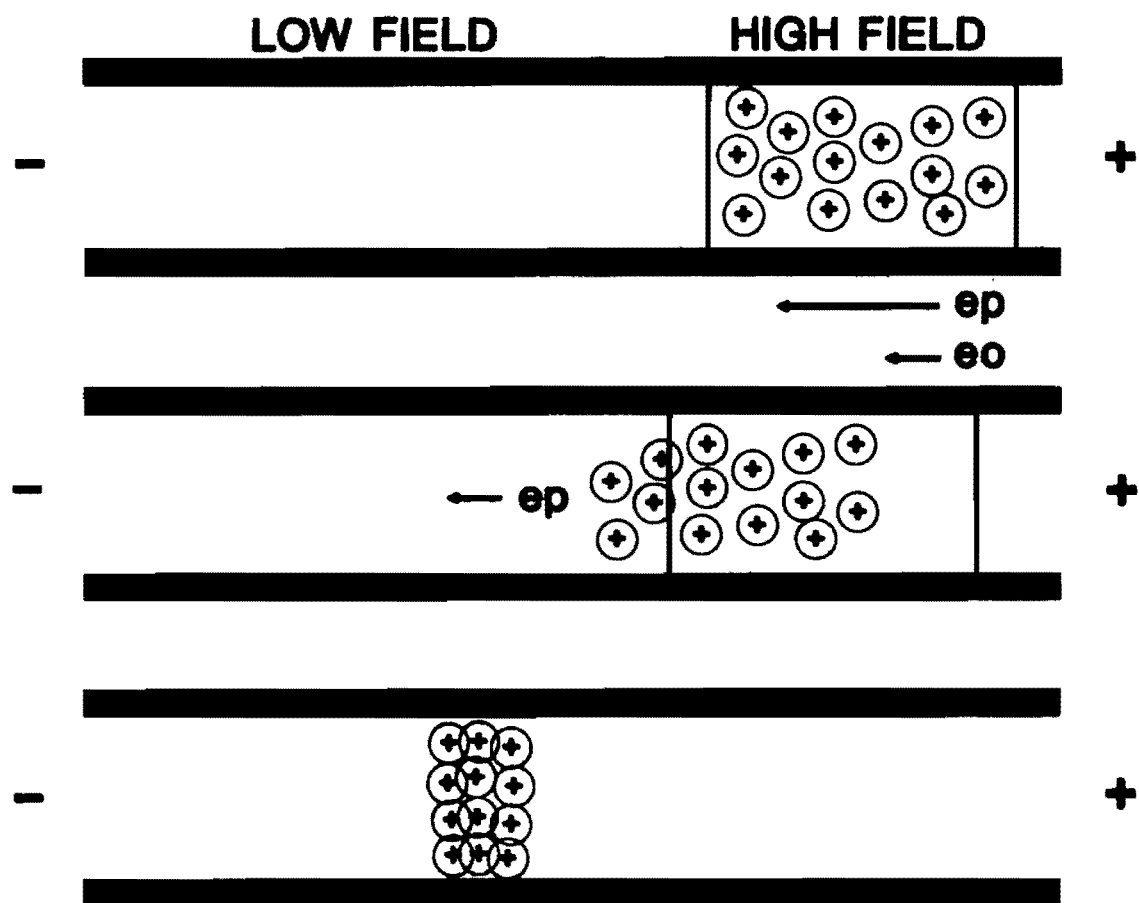
Figure 2-5: On-column sample zone compression for positively charged ions. (Weinberger, R. *Practical Capillary Electrophoresis*; Academic Press, Inc.: New York, 1993.)

Field Amplified Injection

Field amplified injection, or electrokinetic stacking, is exactly the same in principle to the stacking mechanism described above.[2,73] The only difference is that prior to injection of the sample, a plug of water is introduced into the capillary. This will amplify the stacking effects imposed by the various field strengths affecting the run buffer, sample, and water plug zones.[2,73] Chien and Burgi introduced this method in an application involving the separation of PTH-arginine and PTH-histidine.[73] Zhang and Thormann have shown a 1000-fold improvement in detector sensitivity using this technique.[74]

Capillary Isotachophoresis

Capillary isotachophoresis (CITP) can be considered a different member of the family of capillary electrophoresis techniques.[75-81] The term "isotachophoresis" mean that the analytes will move through the capillary at uniform speeds.[2] Cations and anions are separated in different forms of CITP. Hence, cationic-CITP and anionic-CITP exist.[2] In anionic-CITP the capillary is first filled with an electrolyte solution specifically chosen to have mobility higher than the terminating electrolyte and each of the analytes.[2] The detect-side buffer reservoir is filled with the same solution. The terminating electrolyte is chosen to have mobility less than any of the analytes. Sample is introduced between the two zones. Ohm's Law dictates:[2]

$$I \propto E_L \kappa_L + E_S \kappa_S + E_T \kappa_T \qquad (2\text{-}6)$$

where I is the current, κ is the conductivity associated with the leader (L), sample (S), and terminator (T), and E is the field strength for each zone. The column conditions at the beginning of the run are shown in Figure 2-6. Upon electrophoresis, the samples will separate and the field strengths over the sample zones will change. This process of zone separation will continue until the system reaches and equilibrium state.[2] At this point, zones will all move at the same speed and have well-defined boundaries.[2] This is shown in the bottom half of Figure 2-6. The isotachophoresis velocity (υ_{ITP}) may now be defined as follows:[2]

$$\upsilon_{ITP} = E_L\mu_L = E_S\mu_S = E_T\mu_T \tag{2-7}$$

where μ is the mobility of each zone. Diffusion effects are limited using this slightly different form of electrophoresis, which is why it is a good on-column enrichment technique.[2] If analytes migrate into other zones, field strength differences will force them to re-focus.[2] Low concentrations of analyte will generate high field strengths. This permits correction for any zonal concentration variations. Substantial trace enrichment is possible with this technique.[2] However, since it is different from regular CZE, no further details will be presented.

Research Objectives

The goal of our research was to evaluate the effects of injection as it influences migration time and peak area reproducibility. Much work has already been completed in this area with
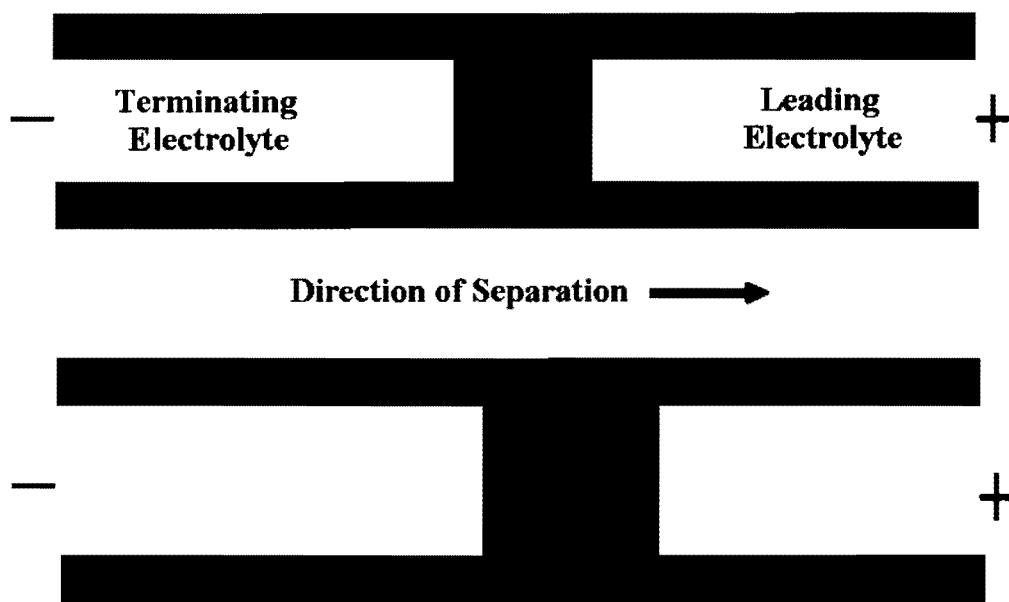
Figure 2-6: Zone separation and concentration using CITP. (Weinberger, R. *Practical Capillary Electrophoresis*; Academic Press, Inc.: New York, 1993.)

regard to hydrodynamic sampling;[43,45,46,82] the most common injection technique implemented in analytical method development and validation processes. This thesis will evaluate the aforementioned variables in an effort to define the limits of another common sampling mechanism, electrokinetic injection. These limits are evaluated in comparison to mathematical models previously developed for the prediction of such extremities.[50] With the advent of graphical mobility analysis, analyte mobility is assessed as it effects analyte migration time precision and proper consideration of buffering systems. The influences of pre-injection conditions are also evaluated. Finally, we will apply our newfound knowledge in the separation of bimetallic isomers. It is our hope that the work presented here regarding the fundamental aspects of electrokinetic injection will provide further motivation for the use of CZE in an ever-increasing number of validated methods for industrial and pharmaceutical analysis.

Chapter III

Defining the Limits of Electrokinetic Injection

SUMMARY

In this chapter, the reproducibility of electrokinetic injection is evaluated as it applies to injection plug lengths and peak areas for a standard mixture of caffeine and theophylline using capillary zone electrophoresis (CZE). The injection plug length is calculated using the standard equations associated with electrokinetic injection in an attempt to define the upper limit of electrokinetic sampling. Otsuka and Terabe have proposed a method of calculating the maximum injection plug length that can be introduced to the capillary before a 5% variance in peak width can be perceived.[50] Therefore, the maximum injection plug length is also calculated for each set of conditions using the equations defined in their model. Longer sampling times and higher sampling voltages (field strengths) result in better reproducibility values. Mobility considerations are the main source of difference between the two mathematical methods evaluated in this study. As a result of this work, a new method of mobility analysis has been developed. Graphical mobility analysis (GMA) offers a new and unique method for determining the total mobility values of each analyte with greater precision.

INTRODUCTION

Since its inception, precision of quantitative parameters in capillary zone electrophoresis (CZE) has been the most debated disadvantage of the technique. Even with the availability of commercial instrumentation in 1988, poor reproducibility of migration times and peak areas have been an area of extensive criticism.[44] In 1988, values for such parameters were approximately within 5% relative standard deviations (RSD) of the mean for the sample population.[83] Five years later, in 1993, these values improved to an acceptable level of 1-2%.[45,84-86] In much of industry, the term "acceptable" may be defined as peak area RSD values of less than 2%.[45] As the approaching millennium grew near, reproducibility values have been shown to be less than 1.0% RSD in regards to migration time and peak area when internal standardization and hydrodynamic sampling are employed.[44-46]

In CZE injection is believed to be one of the primary contributors to error[43,44,46] and internal standardization helps to alleviate the problems it may cause.[43,51,82,84] This may be attributed to the physical processes of the injection itself.[47] As noted by Evans, when an injection is performed there is a physical disruption of the separation capillary. The capillary must be moved to the sampling container and then moved back to the buffer solution.[47] This commonly leads to spontaneous injection[48] and other difficulties such as analyte loss resulting from ohmic heating.[49] This movement of the column is rarely seen in any other separation technique. In most chromatographic techniques the sample is dispensed in a narrow band in the column inlet where the inlet itself is a separate entity of the system. In CZE, the inlet is part of the column.[47] The use of an internal standard for the quantitation of

migration time and peak area compensates for this.[47] Electrokinetic injection has been

reported to have RSD values ranging from 1-2% using internal standardization.[44]

Despite the improvements over the years, CZE still remains in the background as HPLC

and GC exist as the forerunners of validated methods utilized in industrial applications.

Altria, *et.al.* have made significant advances in analyzing the parameters of analytical

method validation as they pertain to capillary electrophoresis techniques.[44,45] They suggest

the need for some of the procedures monitored in regular gel electrophoresis laboratories to

become part of the CZE method validation protocol. Too often, the instrumental parameters

of capillary electrophoresis are validated under the same guidelines as chromatography,

causing problems. Since CZE was developed from a combination of chromatographic and

electrophoretic techniques, the addition of such validation parameters as electrolyte stability,

operator training, and capillary variation, among others, is legitimate and recommended.[43-45]

At the 1989 HPCE conference it was stated that there are only three problems with

capillary electrophoresis: injection, separation, and detection.[2] Giddings describes all

processes contributing to the variance of a system as additive.[1]

$$\sigma^2_{tot} = \sigma^2_{inj} + \sigma^2_{col} + \sigma^2_{det} \qquad \qquad (3\text{-}1)$$

σ^2_{col} = variance generated in the column

σ^2_{inj} and σ^2_{det} = extra-column variances due to injection and detection

By observing σ^2_{inj}, the injection portion of the system can be evaluated as it affects injection plug length and peak area reproducibility. In CZE, the length of the injection plug (l_{inj}) relates directly to the variance associated with the injection process through the following equation:[2,50]

$$\sigma^2_{inj} = l_{inj}^2 / 12 \qquad\qquad (3\text{-}2)$$

Hydrodynamic injection generates reproducible injection plug lengths and is therefore the most common injection method used in industry today.[43-45] However, hydrodynamic injection is not the method of choice in all forms of capillary electrophoresis. In areas such as capillary gel electrophoresis, hydrodynamic injection would siphon the gel out of the capillary.[2] Capillary gel electrophoresis requires the use of electrokinetic sampling. When an electrokinetic injection is performed, the size of the injection plug varies for each analyte under each set of sampling conditions such as applied sampling voltages and times. This occurs because the electrokinetic technique is inherently dependent on the electrophoretic mobility of each different sample component. Initially, it was believed this dependence would lead to a non-uniform and biased injection plug.[47] However, recent work by Qi, et.al. has shown this bias to be irrelevant.[54,55] The electrokinetic injection plug bias cancels the detection bias seen in CZE techniques. The detection bias consists of variabilites that occur due to the rate at which analytes pass the detector window.[54] Usually, parameters such as corrected peak area are implemented in quantitation to account for the detection bias when hydrodynamic injection is performed. However, due to the cancellation, the correction is not necessary when electrokinetic injection is implemented.[54]

Electrokinetic Injection

The equation below is used to calculate the amount of material on the column (Q) when an electrokinetic injection is performed.[2]

$$Q = (\mu_{ep} + \mu_{eo})\pi r^2 E_s C t_s \qquad (3\text{-}3)$$

μ_{ep} = electrophoretic mobility E_s = field strength during sampling

μ_{eo} = electroosmotic mobility t_s = injection time

r = capillary radius C = concentration of solute

This equation corrects for sampling discrimination caused by varying degrees of electrophoretic mobility experienced by each of the solutes.[2,36] Assuming minimal solute-wall effects, the injected volume, V_{inj}, of each solute can be calculated from the original analyte concentration.

$$C = Q/V_{inj} \qquad (3\text{-}4)$$

The injection plug length (l_{inj}) can now be determined using the following equation.

$$l_{inj} = V_{inj}/\pi r^2 \qquad (3\text{-}5)$$

With the length of the injection plug determined, variables such as sampling field strength

(E_s) and sampling time (t_s) can be studied and an attempt can be made to elucidate an ideal set of sampling conditions that will permit low %RSD values.

Predicting the Maximum Injection Plug Length (Otsuka/Terabe Model)

In 1989, Otsuka and Terabe proposed a mathematical model that predicts the maximum injection plug length allowed in CZE.[2,50] Their model assumes that efficiency and resolution are not significantly impaired by a 5% variation in peak width. From Equation 3-1, extra-column band broadening is attributed to the injection volume of the sample solutions and the cell volume of the detector. According to Ostuka and Terabe, σ^2_{tot} for the system must meet the following requirements to maintain levels below 5%.[2,50]

$$\sigma^2_{tot} \leq (1.050\sigma_{col})^2 = 1.103\sigma^2_{col} \qquad (3\text{-}6)$$

This model assumes $\sigma^2_{col} = HL$ where H and L are plate height and column length, respectively. In order to calculate the plate height, it is first necessary to calculate the efficiency exhibited by each of the analytes in solution. Efficiency (N) may be calculated as follows:[35]

$$N = 5.54 \ (t_m \ / \ (A/h))^2 \qquad (3\text{-}7)$$

Plate height (H) will equal the efficiency divided by the effective column length.[35] With these variables calculated, the model continues to state that if σ^2_{ext} is kept smaller than 10.3%

HL, a maximum variation of 5% in peak width values would be observed.[2,50] Using

Equation 3-2 and the following model assumptions:

$$\sigma^2_{ext} = \sigma^2_{inj} + \sigma^2_{det} \tag{3-8}$$

$$\sigma^2_{inj} = \sigma^2_{det} \tag{3-9}$$

the injection length required to keep the peak width variation below 5% can be predicted using the following equation:[50]

$$l_{inj} \leq 0.786(HL)^{1/2} \tag{3-10}$$

Equation 3-10 can be used to identify the conditions above which analyte resolution and column efficiency is expected to be compromised. These conditions may be thought of as a theoretical limit.

Goals of Chapter

In this chapter, the injection plug length arising from electrokinetic injection is evaluated as it affects linearity and precision of peak areas and injection plug lengths for a standard mixture of caffeine and theophylline using CZE.[34] Because this is only a two-component system, results are presented using external standardization to allow the quantitation of both the neutral marker (caffeine) and theophylline. The main goal is to determine the sets of

electrokinetic sampling conditions that optimize reproducibility of injection plug length and peak area. This will be completed using the standard electrokinetic sampling Equations 3-3 to 3-5. The second goal of this chapter is to evaluate the experimental lengths of the injection plugs as they compare to the predicted values based on the Otsuka/ Terabe model. (Equation 3-10)

EXPERIMENTAL SECTION

Chemicals. Standard samples of caffeine and theophylline, whose structures are shown in Figure 3-1, were obtained from Aldrich Chemical Co. (Milwaukee, WI) and used without further purification. Sodium hydroxide was purchased from Aldrich. Sodium phosphate monobasic and sodium phosphate dibasic were received from Fisher Scientific (Fair Lawn, NJ) and prepared at concentrations of 0.01 M each using de-ionized water. The pH 7.5 buffer solution was prepared by mixing monobasic and dibasic phosphate solutions until the proper pH was measured. This was followed by vacuum filtration using a 0.45 μm disk filter. Caffeine and theophylline were prepared at concentrations of 0.2 mg/mL and 0.1 mg/mL. Both compounds were diluted with the buffer solution.

Instrumentation. An ABI 270A CE instrument (PerkinElmer, Norwalk, CT) was used. This system was upgraded to the software level of an ABI 270A-HT model to allow controlled sampling at various voltages. Sampling voltages and times are shown in Table 3-1. A PerkinElmer fused silica capillary was used (72 cm x 50 μm i.d.) for the separation.

Caffeine (Neutral)

pKa = 8.8
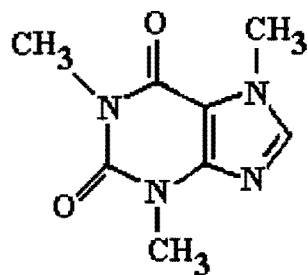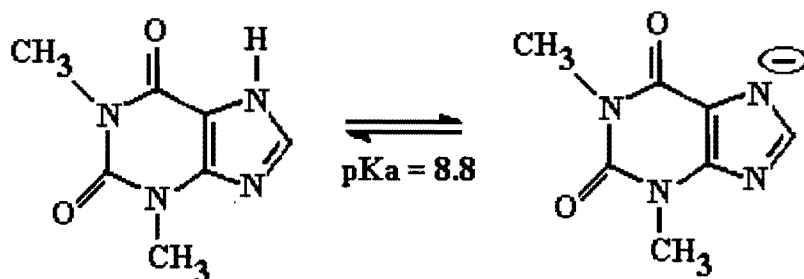
Theophylline

Figure 3-1: Caffeine and theophylline. The two molecules differ in placement of a methyl group on the seventh position nitrogen.

Table 3-1: Electrokinetic Sampling Voltages and Times

Voltage (kV)	Time (seconds)
1	1
3	3
5	5
7	7
9	9
11	

*5 Replicate Injections

The length to the detection window was 50 cm. The Dionex SP4270 integrator (San Jose, CA) provided the data output.

Electrophoretic Conditions. The method used in this study is similar to a method found in the literature used to evaluate system suitability.[34] A new capillary was cleaned using the following hydrodynamic wash routine at 20 psi: 15 minutes 1.0 N NaOH, 15 minutes de-ionized water, 15 minutes 0.1 N NaOH, 15 minutes run buffer. Samples were run consecutively. Overall column temperature was held at 30°C. The following steps were taken to complete the separation. The column was flushed for 2 minutes with the buffer. Sampling was completed at the conditions described in Table 3-1. Finally, separation was performed at 30 kV with a run time of 5 minutes. The ultraviolet adsorption detector was set to 220 nm.

RESULTS AND DISCUSSION

A typical electropherogram illustrating the separation of caffeine and theophylline is depicted in Figure 3-2. Caffeine and theophylline are baseline resolved with migration times of 2.52 minutes and 2.60 minutes, respectively. Before electrokinetic injection reproducibility can be accurately measured, the theoretical assumption of minimal solute-wall interactions (Equation 3-4) must be proven. A linear response of peak area versus sampling time at each of the sampling voltages is expected if the sample is not adhering to the capillary wall. These lines should likewise intercept the y-axis at the origin.[34] If an unknown amount of analyte is consistently lost, there will be a non-zero intercept. The
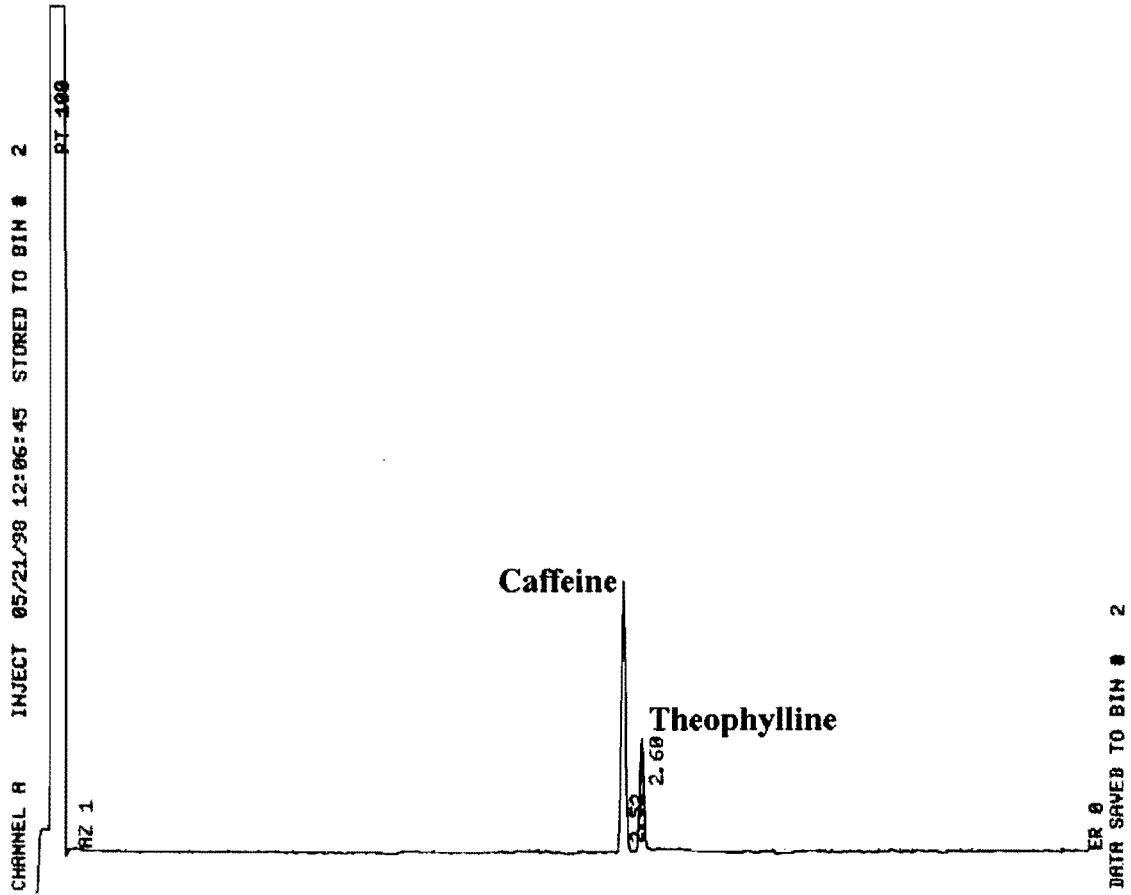
Figure 3-2: Typical separation of caffeine and theophylline. Injection was performed at 5 kV, 5 seconds.

linearity results are shown in Figures 3-3 and 3-4 for caffeine and theophylline, respectively.

Each of these graphs shows the peak area response as a function of sampling time for each of

the sampling voltages listed in Table 3-1. Correlation coefficients are at least 0.99 with the

exception of the 1 kV data. It is assumed that the reason why the 1 kV data is only showing a

correlation coefficient of approximately 0.90 for both caffeine and theophylline is primarily

due to the extremely low operating current. The voltage is simply not high enough to pull the

ions toward the electrode in a steady stream and a reproducible fashion each time. Also, each

of the lines demonstrate an intercept of approximately zero. The y-axis intercepts for

caffeine range from 518 μV·sec to 3,958 μV·sec and theophylline range from 42 μV·sec to

2,776 μV·sec. Although these values may appear large it is important to realize that this is

less than 1% of the displayed y-axis scale. Therefore, the assumption of minimum solute-

wall interactions is justified.

Figures 3-5 and 3-6 display variation of injection plug length with sampling conditions.

The injection plug length is calculated using Equations 3-3 to 3-5 and is plotted against the

sampling time for each of the sampling voltages listed in Table 3-1. As sampling time is

increased for each voltage, the linear responses of injection plug lengths are maintained

throughout the defined experimental range.

Figures 3-7 and 3-8 show the effect of the sampling conditions on peak area quantitative

reproducibility for caffeine and theophylline. The %RSD values calculated for each set of

the five replicate analyses are depicted graphically as a function of sampling time for each

sampling voltage as outlined in Table 3-1. The 1 kV and 3 kV data are random and no visual

59
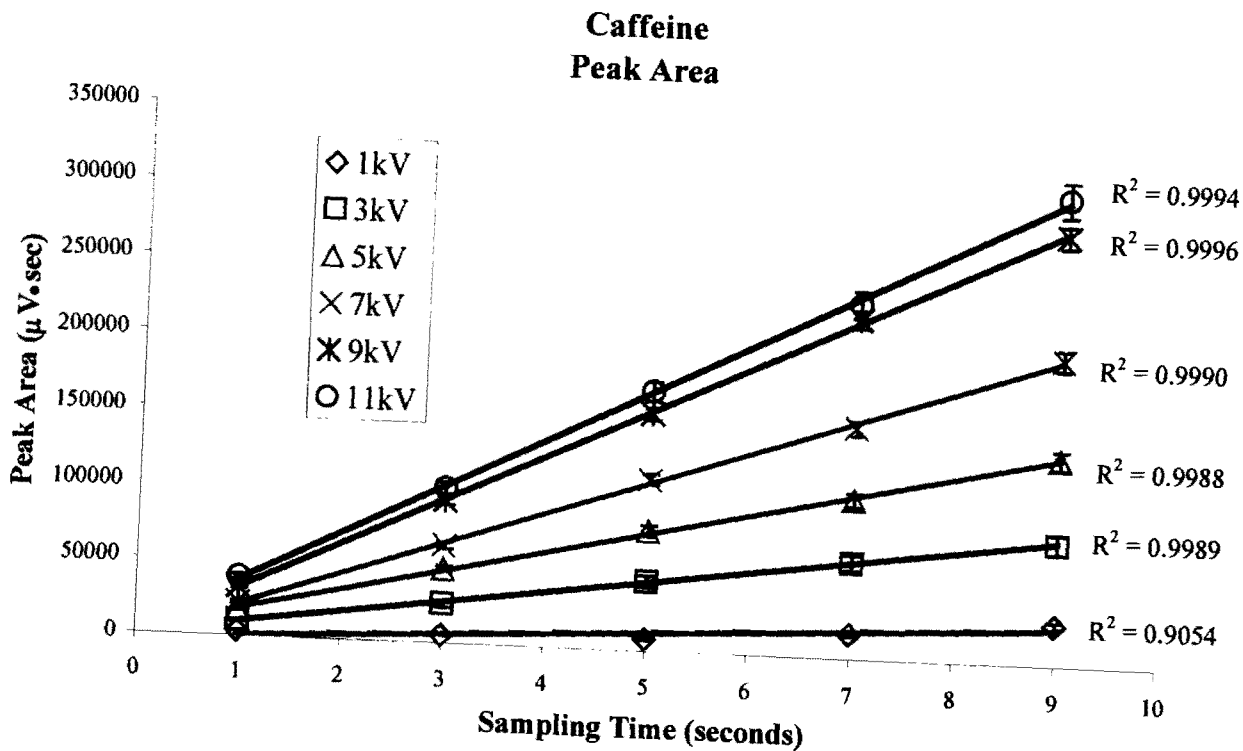
Figure 3-3: Caffeine peak area linearity

Theophylline Peak Area
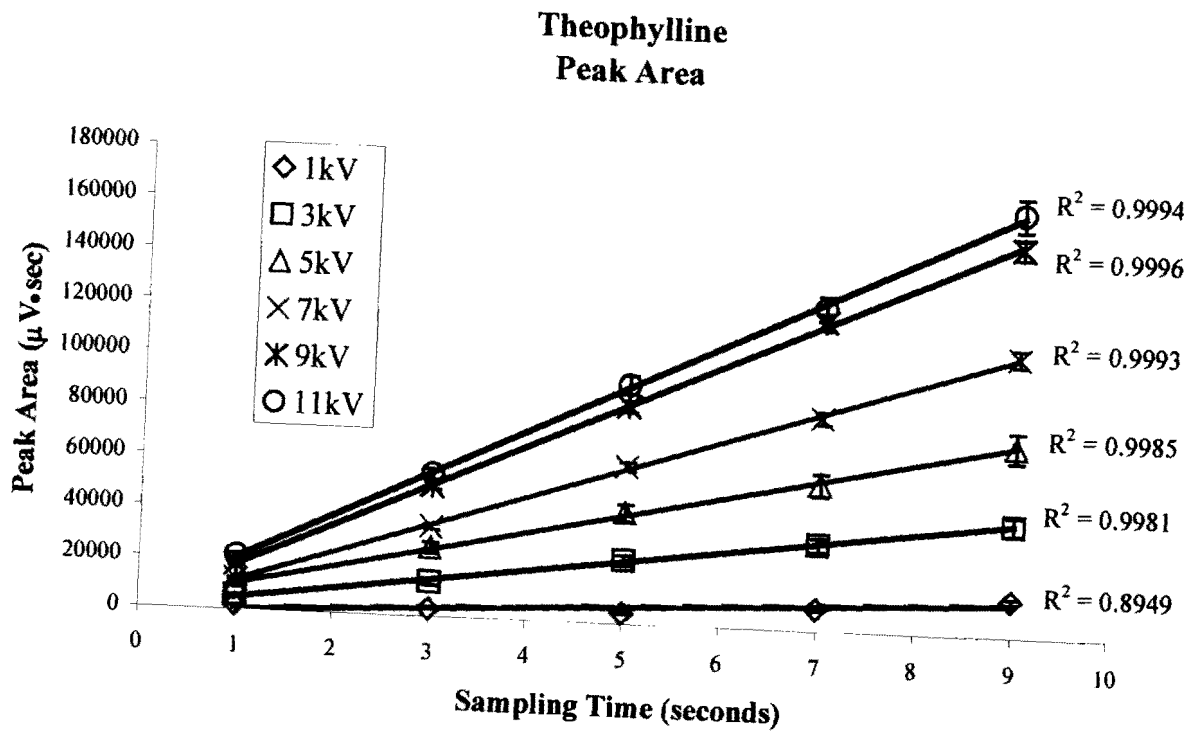
Figure 3-4: Theophylline peak area linearity
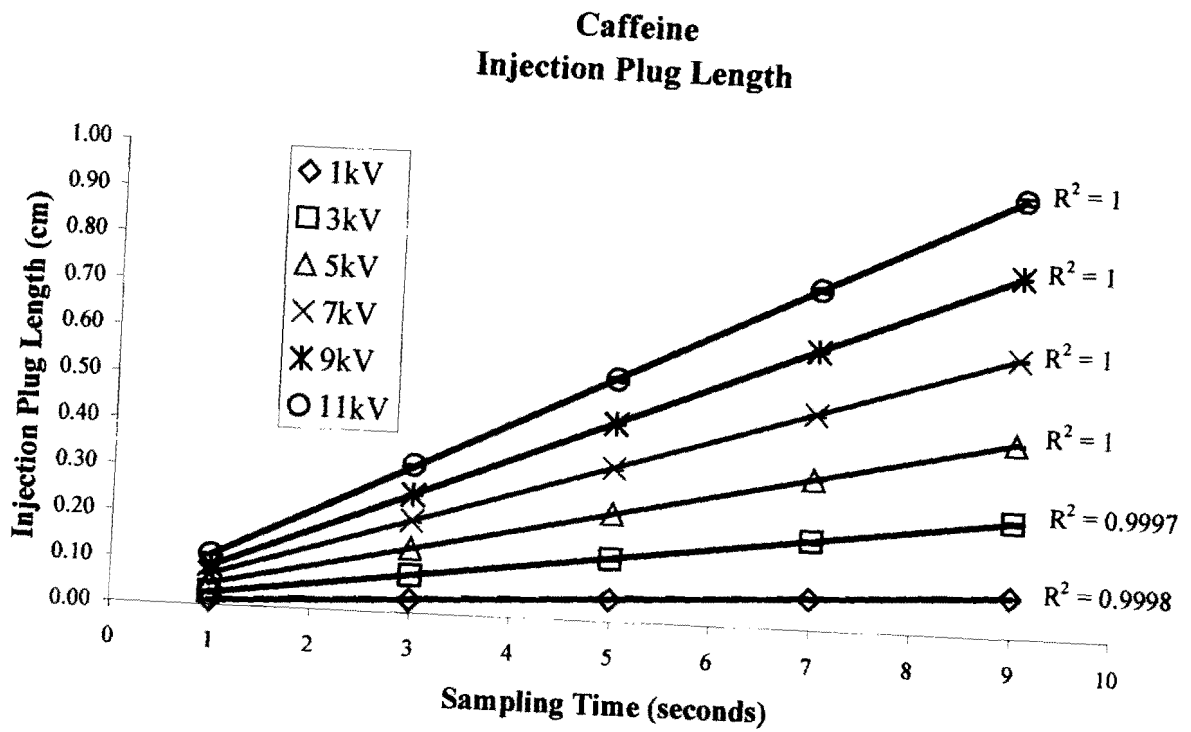
Figure 3-5: Injection plug length linearity for caffeine
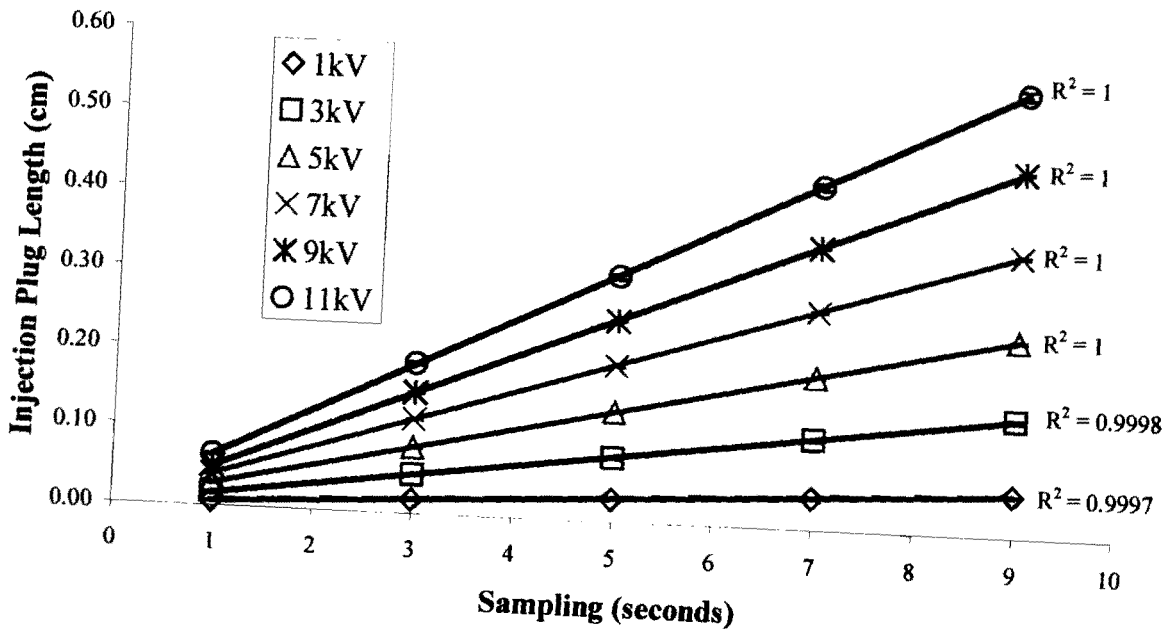
Figure 3-6: Injection plug length linearity for theophylline.
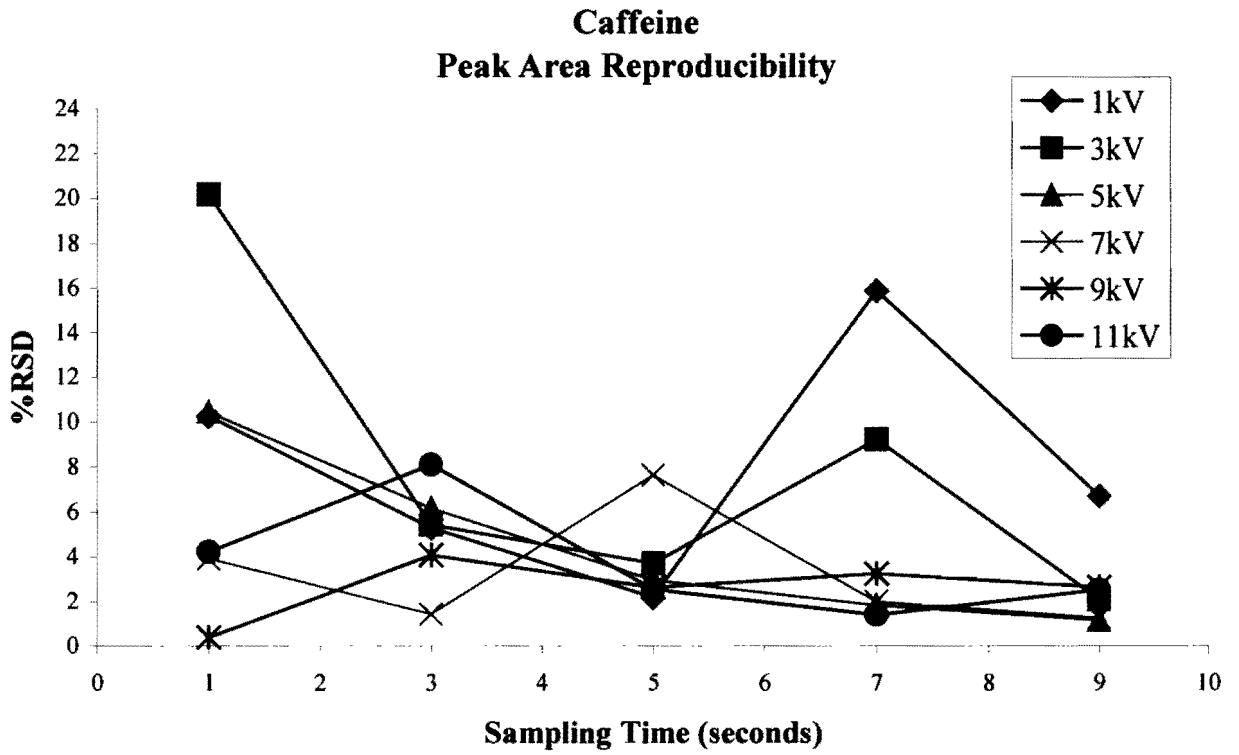
Figure 3-7: Peak area reproducibility of caffeine.
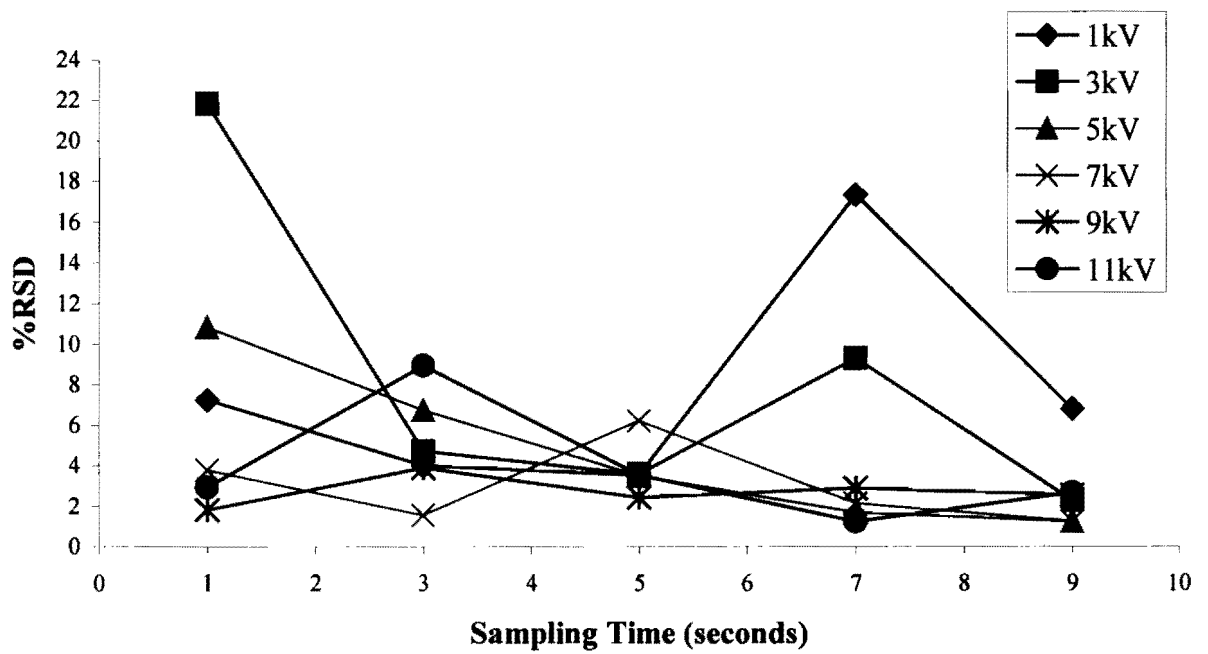
Figure 3-8: Peak area reproducibility for theophylline.

trend can be identified. As mentioned previously, low operating currents interfere with the

ability to maintain a steady flow to and within the capillary. This is also true of the shorter

sampling times. At the 1-second sampling time, the %RSD values have a broad range.

Overall, the 5-11 kV data generally trend towards better reproducibility values at longer

sampling times. This statement is made excluding the unexplainable deviation occurring at

the 7 kV, 5-second data point. The use of longer sampling times contributing to better

precision is of no surprise based on previous work that involved hydrodynamic injection.[46]

Reproducibility was improved when pressure was applied for longer times.

Contrary to the general trend concluded above, at the extreme high end of the sampling

conditions imposed in this study there was an increase in the relative standard deviation

values beginning at 9 kV, 7-seconds and 11 kV, 9-seconds in Figure 3-7. This is attributed

to sample depletion of the diffuse layer surrounding the capillary inlet-solution interface as

shown in Figure 3-9. This is interpreted as being due to a concentration gradient in this

region.[33,87] The effect is also illustrated in Figure 3-8 for theophylline. Small increases are

noticeable at the same voltage and sampling time values discussed above. Therefore,

although it has been previously stated that longer sampling times and higher sampling

voltages lead to better quantitative reproducibility, the deviation at the extreme ends indicate

a possible set of maximum electrokinetic sampling conditions at which the conclusion loses

its validity.

Trends observed in the injection plug length reproducibility data are similar to those

above regarding peak area. Figures 3-10 and 3-11 show the reproducibility of injection plug
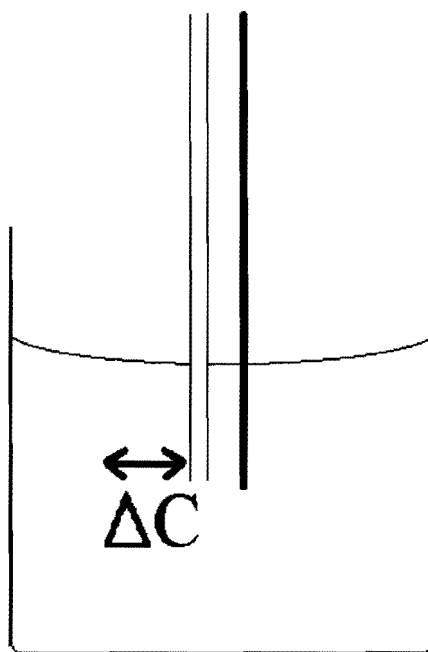
Figure 3-9: Concentration gradient occurring in the diffuse region surrounding the capillary-electrode assembly.
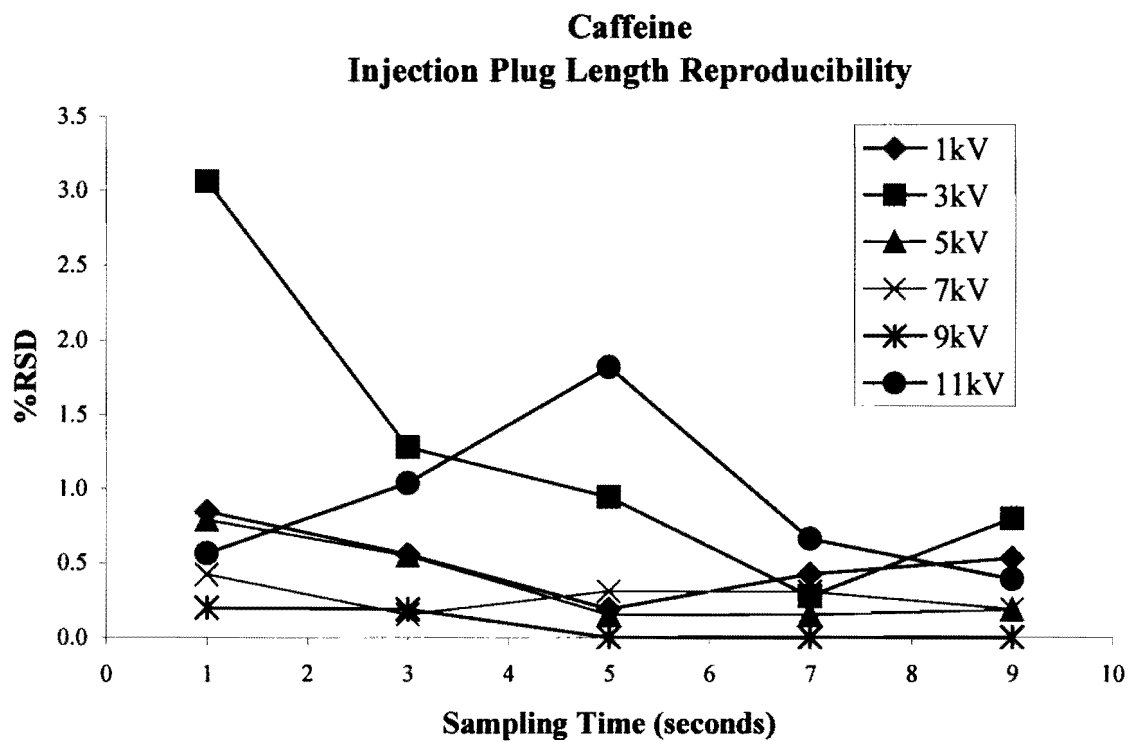
Figure 3-10: Injection plug length reproducibility for caffeine.

**Theophylline
Injection Plug Length Reproducibility**
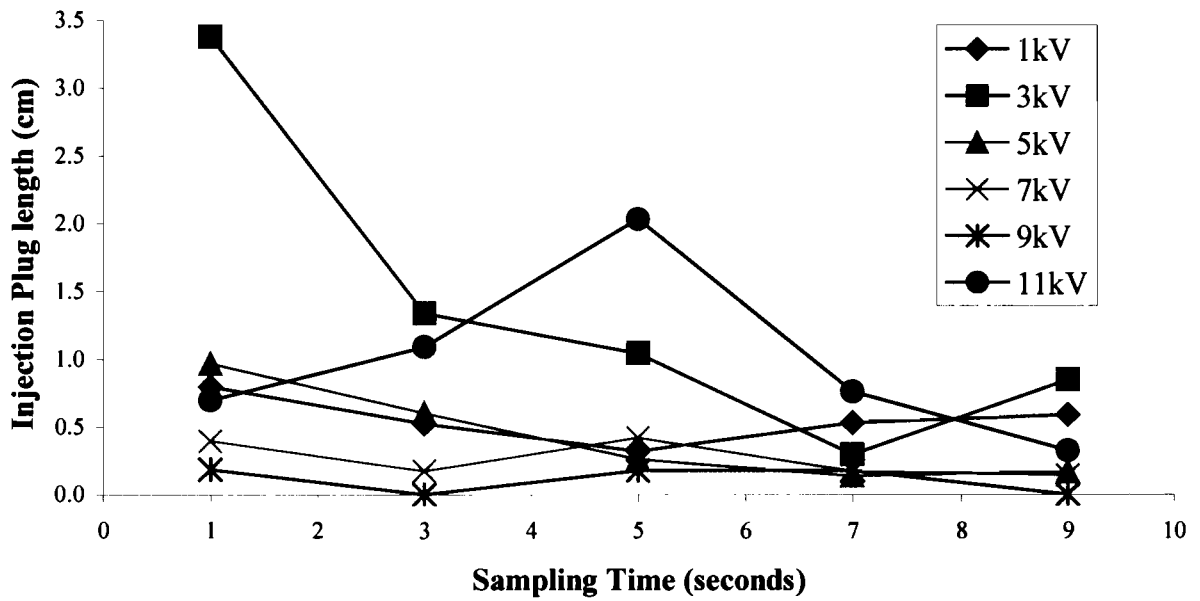
Figure 3-11: Injection plug length reproducibility for theophylline.

lengths for caffeine and theophylline, respectively. The %RSD values determined for each set of 5 replicate analyses is plotted as a function of sampling time for each sampling voltage as outlined in Table 3-1. In general, longer sampling times and higher voltages lead to better reproducibility of the injection plug lengths. However, the 11 kV data for both caffeine and theophylline appeared slightly erratic. Actual numerical values for the reproducibility of caffeine and theophylline regarding peak area and injection plug length for each set of electrokinetic injection conditions defined in the scope of this study is given in Tables 3-2 and 3-3.

Figures 3-12 through 3-14 show a compromise in the use of higher sampling voltages and times. This compromise is the expected loss of column efficiency and resolution.[2] Efficiency is a function of diffusion and mass transfer, both discussed in the previous chapter. Figures 3-12 and 3-13 illustrate the losses of column efficiency as a function of sampling time for each of the sampling voltages for caffeine and theophylline, respectively. The longer the sampling time is, the longer the time available for the analytes to migrate within the capillary during injection. This decreases the total amount of column left for the separation to occur. Therefore, it is natural that the decreasing efficiency trends are observed as we increase sampling voltages and times. However, this is not without exception. Once again, the 1 kV data has resulted in an unexpected trend. Reasons for this behavior have already been discussed (p. 59).

In Figure 3-14, the identical trend is found regarding resolution. Resolution is a parameter that categorizes overlap of two specified component zones.[1] Mathematically, it is

Table 3-2: Numerical reproducibility values for caffeine regarding peak area and injection plug length.

Caffeine
Peak Area Reproducibility

	1	3	5	7	9	seconds
1kV	10.247	5.257	2.169	15.858	6.674	
3kV	20.179	5.422	3.672	9.202	2.067	
5kV	10.448	6.148	2.943	1.799	1.122	
7kV	3.907	1.416	7.630	1.979	1.244	
9kV	0.396	4.074	2.616	3.217	2.621	
11kV	4.207	8.103	2.524	1.387	2.496	

Caffeine
Injection Plug Length Reproducibility

	1	3	5	7	9	seconds
1kV	0.847	0.555	0.187	0.422	0.532	
3kV	3.062	1.279	0.943	0.275	0.799	
5kV	0.789	0.546	0.150	0.149	0.183	
7kV	0.421	0.153	0.306	0.305	0.187	
9kV	0.197	0.187	0.000	0.000	0.000	
11kV	0.565	1.038	1.820	0.663	0.391	

Table 3-3: Numerical reproducibility values for theophylline regarding peak area and injection plug length.

Theophylline
Peak Area Reproducibility

	1	3	5	7	9	seconds
1kV	7.228	3.972	3.506	17.322	6.801	
3kV	21.827	4.685	3.566	9.280	2.242	
5kV	10.813	6.724	3.471	1.673	1.233	
7kV	3.772	1.534	6.214	2.127	1.253	
9kV	1.794	3.864	2.404	2.854	2.511	
11kV	2.923	8.933	3.531	1.233	2.659	

Theophylline
Injection Plug Length Reproducibility

	1	3	5	7	9	seconds
1kV	0.798	0.523	0.323	0.534	0.593	
3kV	3.381	1.339	1.043	0.297	0.849	
5kV	0.969	0.602	0.264	0.141	0.172	
7kV	0.396	0.176	0.421	0.176	0.144	
9kV	0.186	0.000	0.177	0.177	0.000	
11kV	0.699	1.090	2.034	0.763	0.324	

**Caffeine
Efficiency**

Figure 3-12 plot: N (plate number) vs Sampling Time (seconds)

Legend:
◇ 1kV   □ 3kV
△ 5kV   ✕ 7kV
✳ 9kV   ○ 11kV

$R^2 = 0.9767$
$R^2 = 0.7713$
$R^2 = 0.9887$
$R^2 = 0.9938$
$R^2 = 0.9835$
$R^2 = 0.9580$
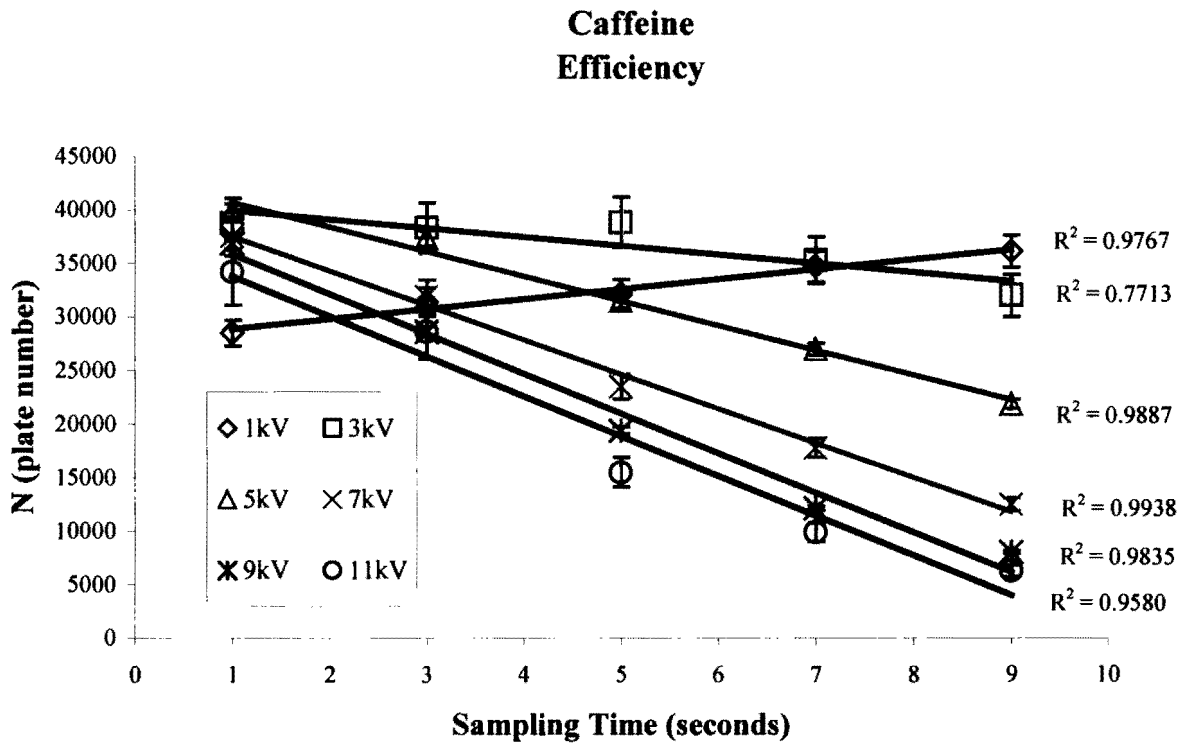
Figure 3-12: This graph illustrates the loss in column efficiency for caffeine as increasing sampling voltage and sampling times are applied. The 1 kV data does not support this trend.

Theophylline Efficiency

$R^2 = 0.8917$

$R^2 = 0.9183$

$R^2 = 0.9982$

$R^2 = 0.9931$

$R^2 = 0.9839$

$R^2 = 0.9563$

◇ 1kV □ 3kV

△ 5kV ✕ 7kV

✖ 9kV ○ 11kV

N (plate number)

Sampling Time (seconds)
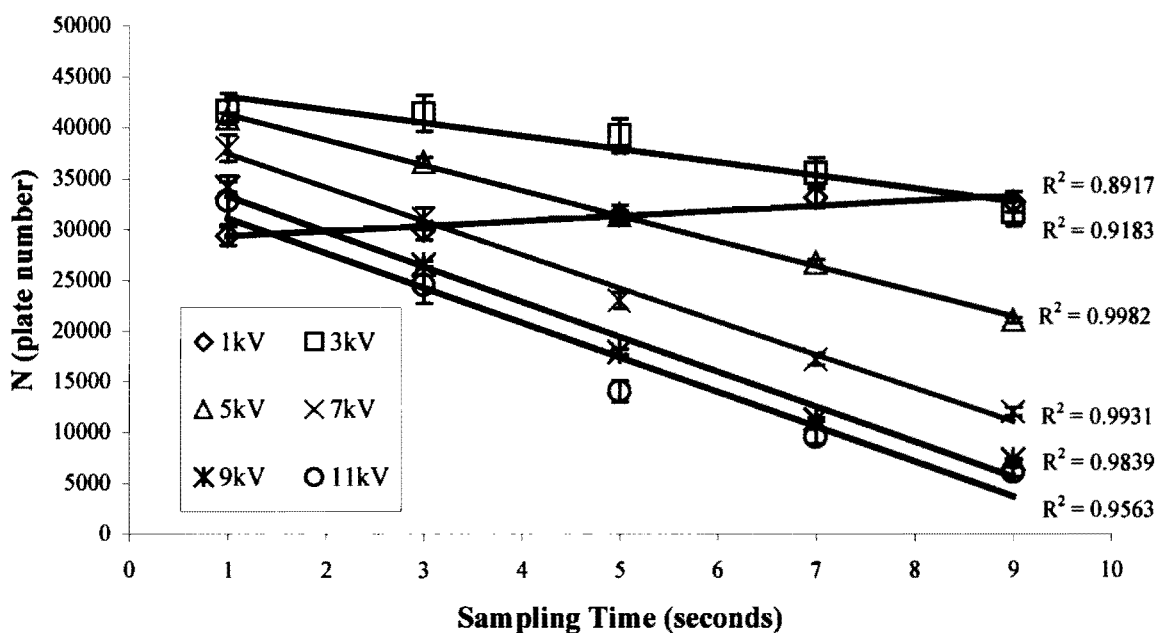
Figure 3-13: This graph illustrates the loss in column efficiency for theophylline as increasing sampling voltage and sampling times are applied. The 1 kV data does not support this trend.

**Resolution
Caffeine and Theophylline**
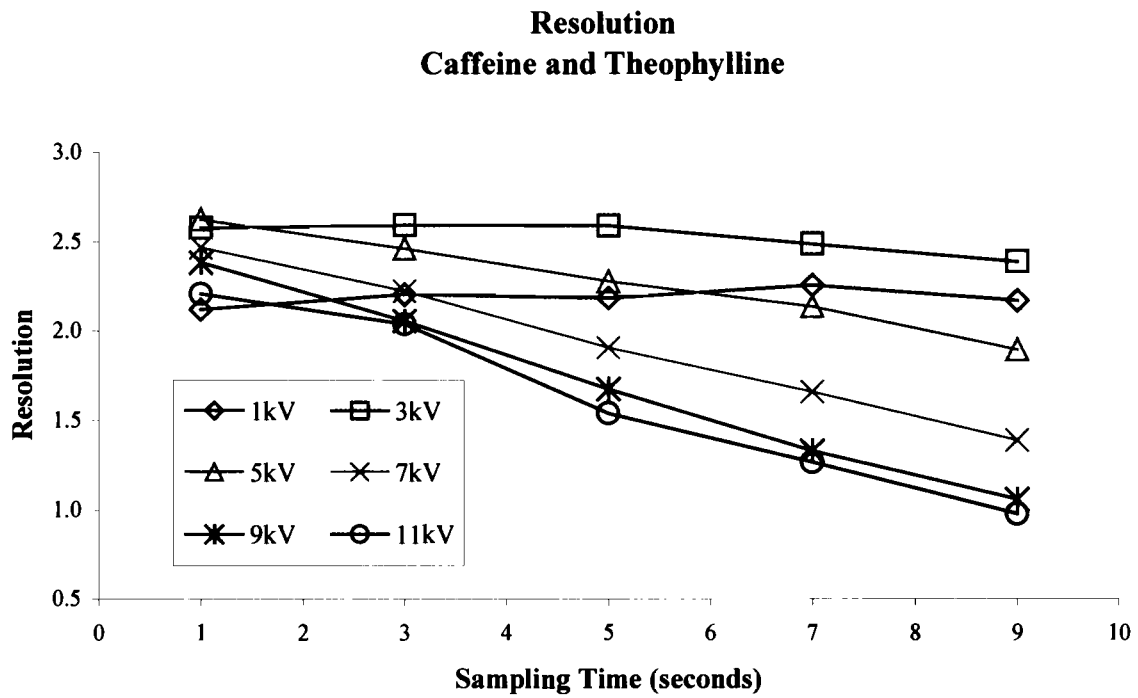
Figure 3-14: Resolution of caffeine and theophylline also declines as more of the column is utilized for the injection plug.

defined by the following equation:[35]

$$R_s = \frac{t_{m(2)} - t_{m(1)}}{0.5\ (W_{b(1)} + W_{b(2)})} \qquad (3\text{-}11)$$

The average resolution of caffeine and theophylline is reported in Table 3-4 for each sample set defined in Table 3-1. These values were depicted graphically in Figure 3-14 as a function of sampling time for each sampling voltage described previously.

The above data regarding quantitative reproducibility supports the usage of longer sampling times and higher sampling voltages. However, we have also seen that concentration gradients form within the sampling vial when the extreme right-hand values are approached (Figures 3-7 and 3-8). This lends itself to the idea that there must be an upper limit to our sampling conditions. Otsuka and Terabe proposed a mathematical model that may be used to define the maximum injection plug length permissible for each of the analytes in question.[50] Figures 3-15 through 3-20 illustrates the theoretical limit and experimental results for caffeine. The solid black lines in each of these graphs are the theoretical limits imposed by the mathematical model. (Equation 3-10) The experimental values are also shown as calculated using the standard electrokinetic equations described previously (Equations 3-3 to 3-5). Figure 3-15 shows the results for the 1 kV data. Here the theoretical and experimental lines do not appear to intersect. In accordance with the model, the experimental data does not exceed the theoretical limits, therefore, we would not expect more than a 5% variation in the peak widths attained.[50] The 3-11 kV experimental data, however, does intersect the model limits. The recommendation of Otsuka and Terabe is to

Table 3-4: Average resolution of caffeine and theophylline for each sample set.

	1	3	5	7	9	seconds
1kV	2.12	2.21	2.19	2.26	2.17	
3kV	2.58	2.59	2.59	2.49	2.39	
5kV	2.62	2.46	2.28	2.14	1.89	
7kV	2.47	2.22	1.90	1.66	1.39	
9kV	2.39	2.06	1.68	1.33	1.06	
11kV	2.21	2.04	1.54	1.27	0.98	
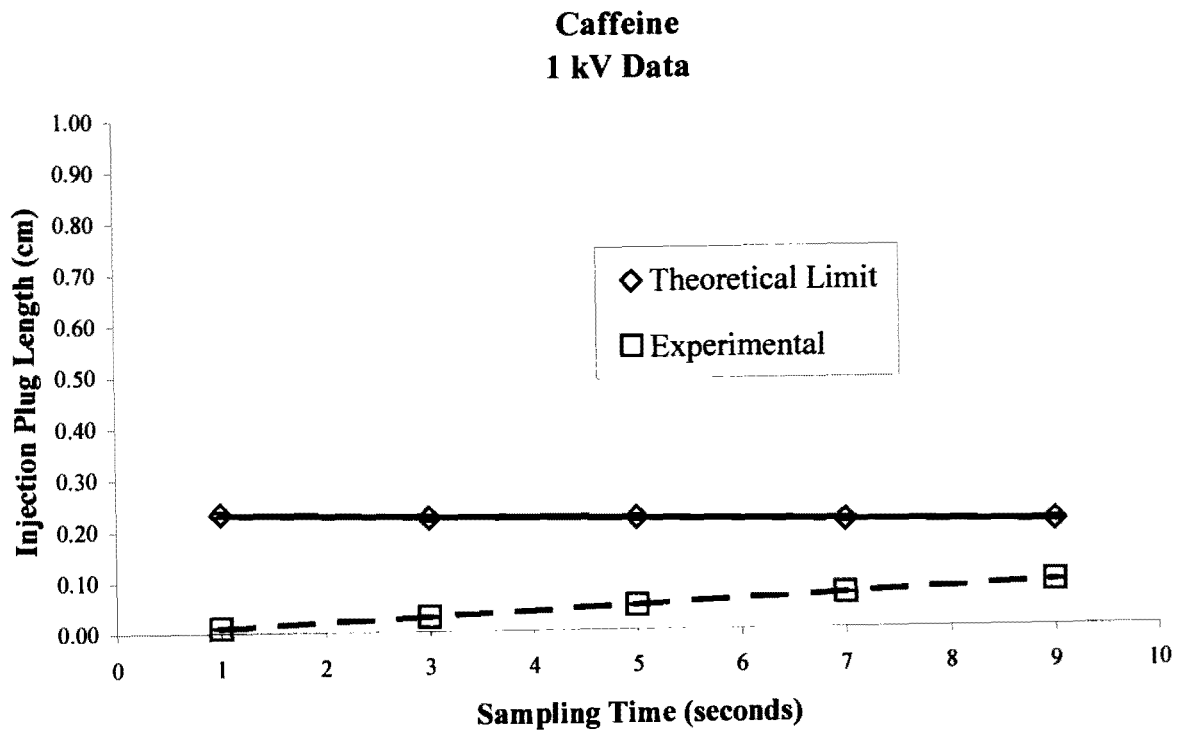
Caffeine
1 kV Data

Figure 3-15: Caffeine 1 kV data. Approximate intersection 18 kV·sec.

Caffeine
3 kV Data
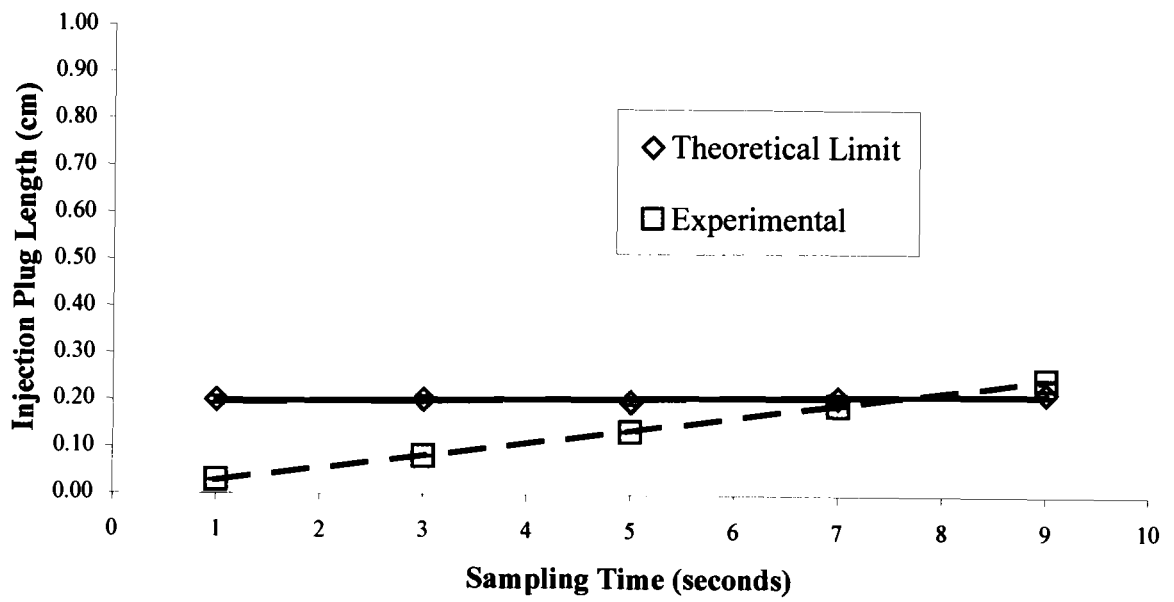
Figure 3-16: Caffeine 3 kV data. Approximate intersection is 23 kV·sec.

Caffeine
5 kV Data

◇ Theoretical Limit

△ Experimental
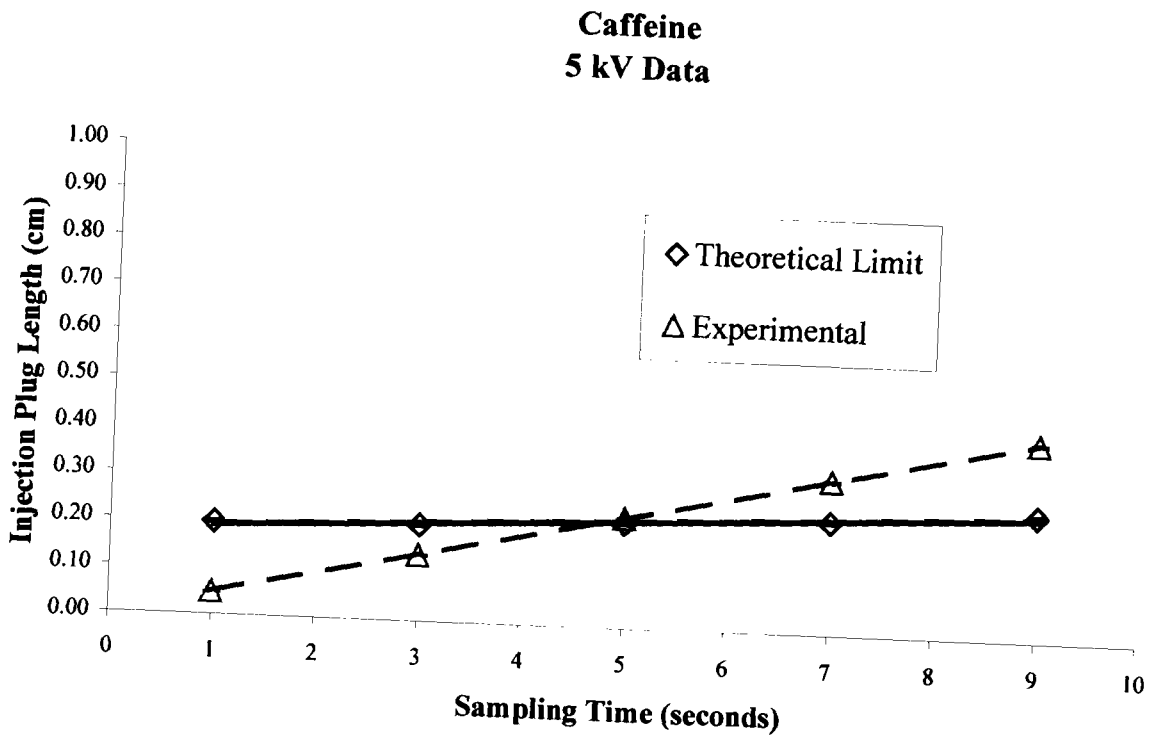
Figure 3-17: Caffeine 5 kV data. Intersection approximates 24 kV·sec.
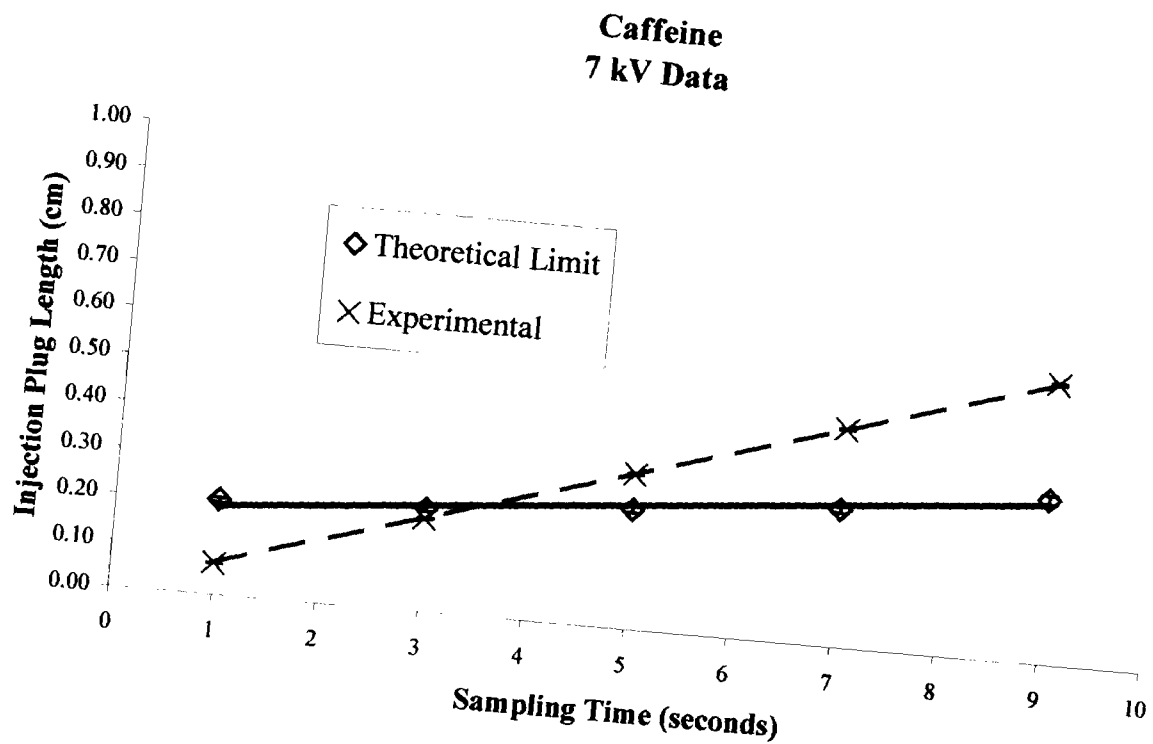
**Caffeine
7 kV Data**

Figure 3-18: Caffeine 7 kV data. Intersection approximates 25 kV·sec.
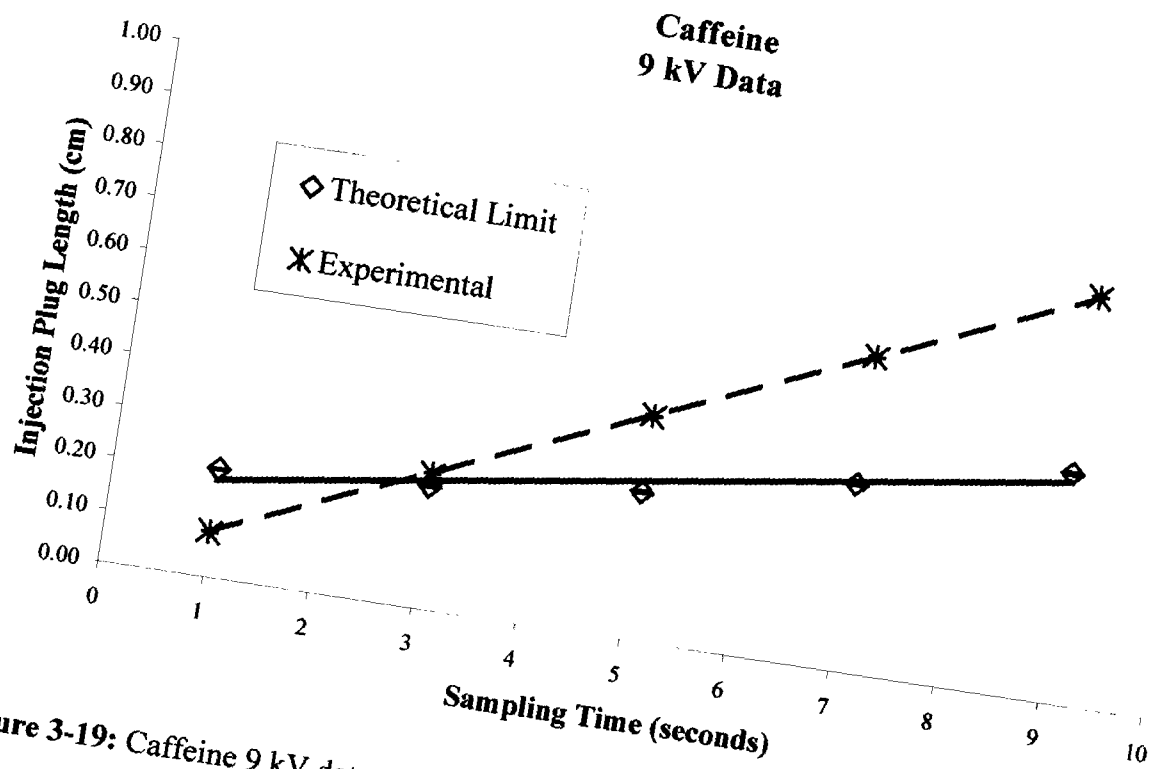
Figure 3-19: Caffeine 9 kV data. Intersection approximates 24 kV·sec.
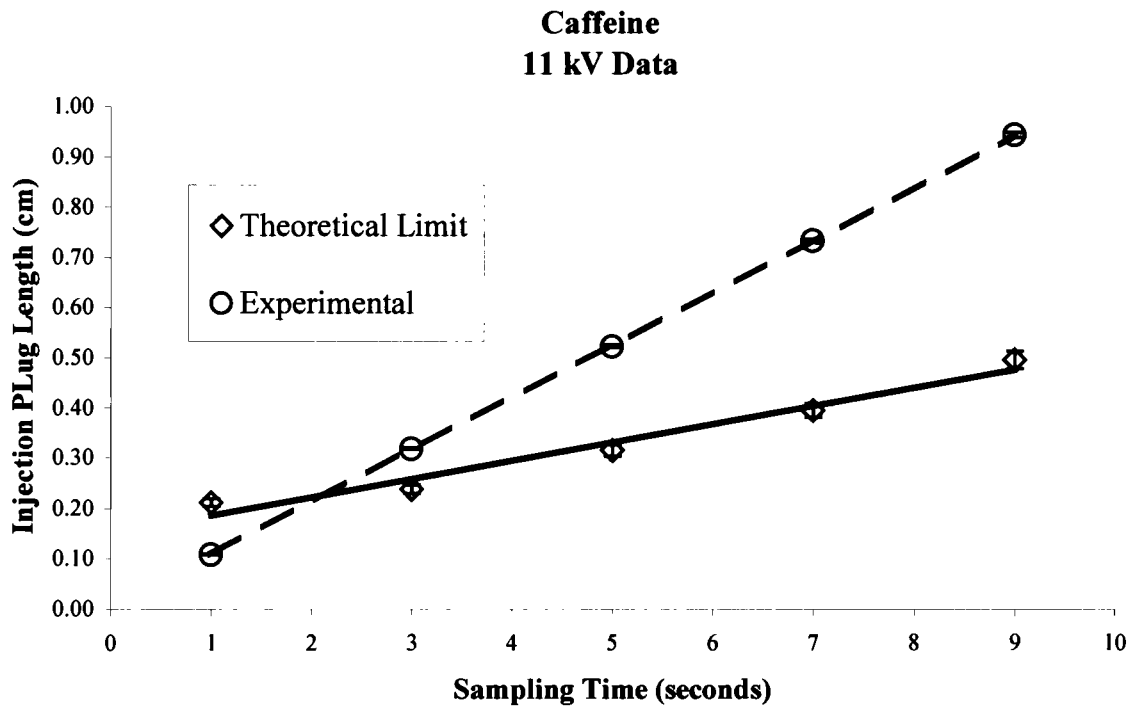
Caffeine
11 kV Data

Figure 3-20: Caffeine 11 kV data. Intersection approximates 24 kV·sec.

maintain electrokinetic sampling conditions at values less than the point of intersection.[50] For instance, in Figure 3-16, the point of intersection is at 7.5 seconds for the 3 kV data. If the sampling time at which the intersection occurs is multiplied by the sampling voltage used, the same constant intersection value for each of the 5-11 kV data sets is seen. This value is approximately 24 kV·sec for caffeine. In order to maintain the peak width variation of caffeine at a level less than 5%, sampling combinations less than 24 kV·sec should be employed. Thus for a given compound the upper limit of voltage and sampling time for effective electrokinetic injection may be defined.

Theophylline behaves in much the same way as caffeine. However, its upper limit is maintained at approximately 60 kV·sec. This is shown in Figures 3-21 through 3-26. Theophylline (0.1 mg/mL) is at half the concentration of caffeine (0.2 mg/mL) in the test solution. The point of intersection approximates 60 kV·sec and can be deduced visually in the 7 kV data set. (Figure 3-24) The difference in the upper limit values obtained for caffeine and theophylline suggests possible concentration dependence of the upper limits. Confirmation of this hypothesis will require further experimentation.

Second Experiment: Concentration

In order to evaluate concentration effects on the upper limits, the experimental design described above was repeated using different analyte concentrations. Caffeine was prepared at a concentration of 0.1 mg/mL and theophylline concentration was doubled to 0.2 mg/mL. The resulting upper limit value of electrokinetic injection for caffeine remained at 24 kV·sec.

**Theophylline
1 kV Data**
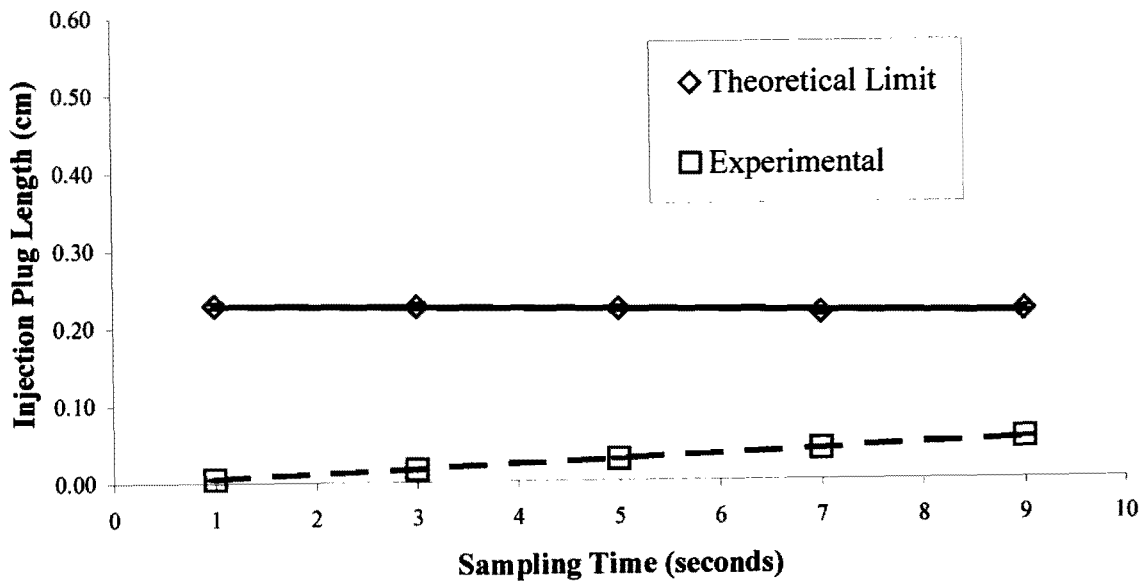
Figure 3-21: Theophylline 1 kV data. Intersection approximates 30 kV·sec.

**Theophylline
3 kV Data**
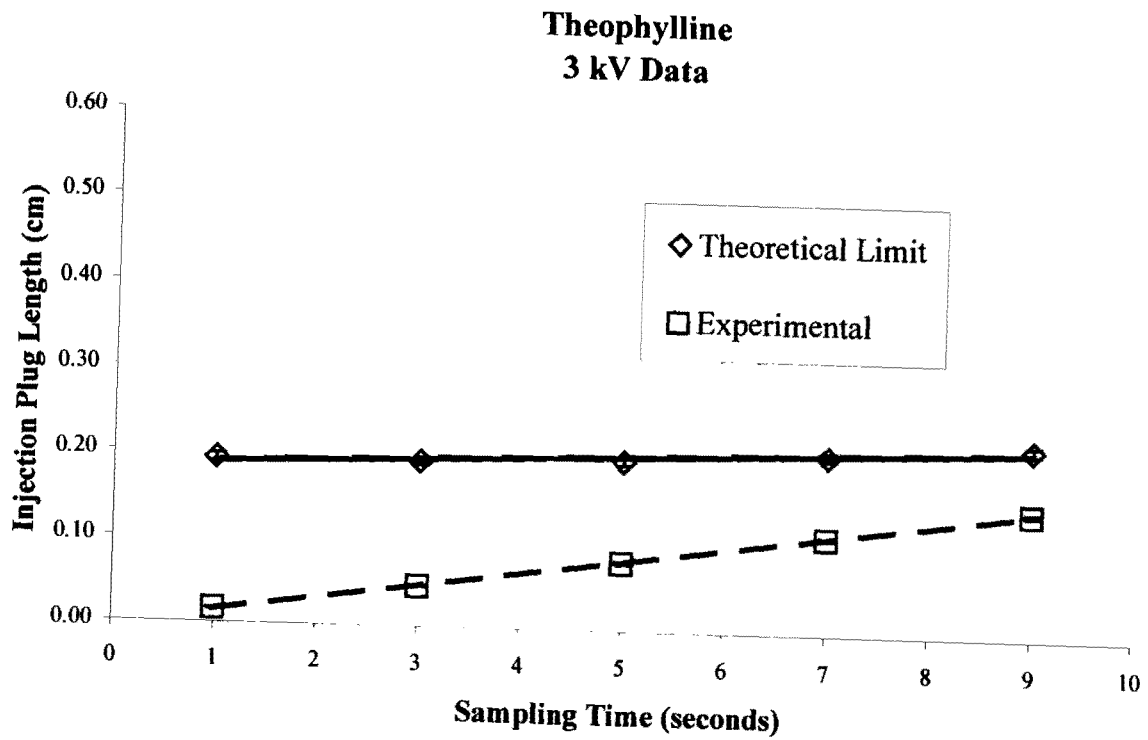
Figure 3-22: Theophylline 3 kV data. Intersection approximates 44 kV·sec.

**Theophylline
5 kV Data**
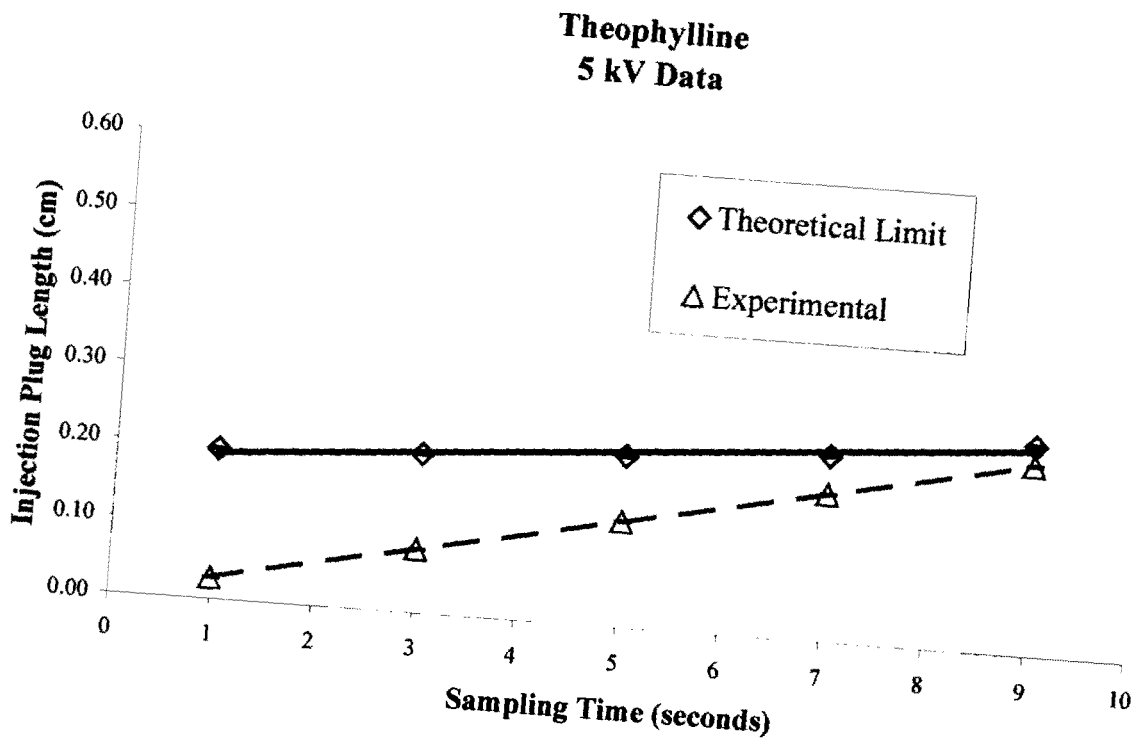
Figure 3-23: Theophylline 5 kV data. Intersection approximates 50 kV·sec.
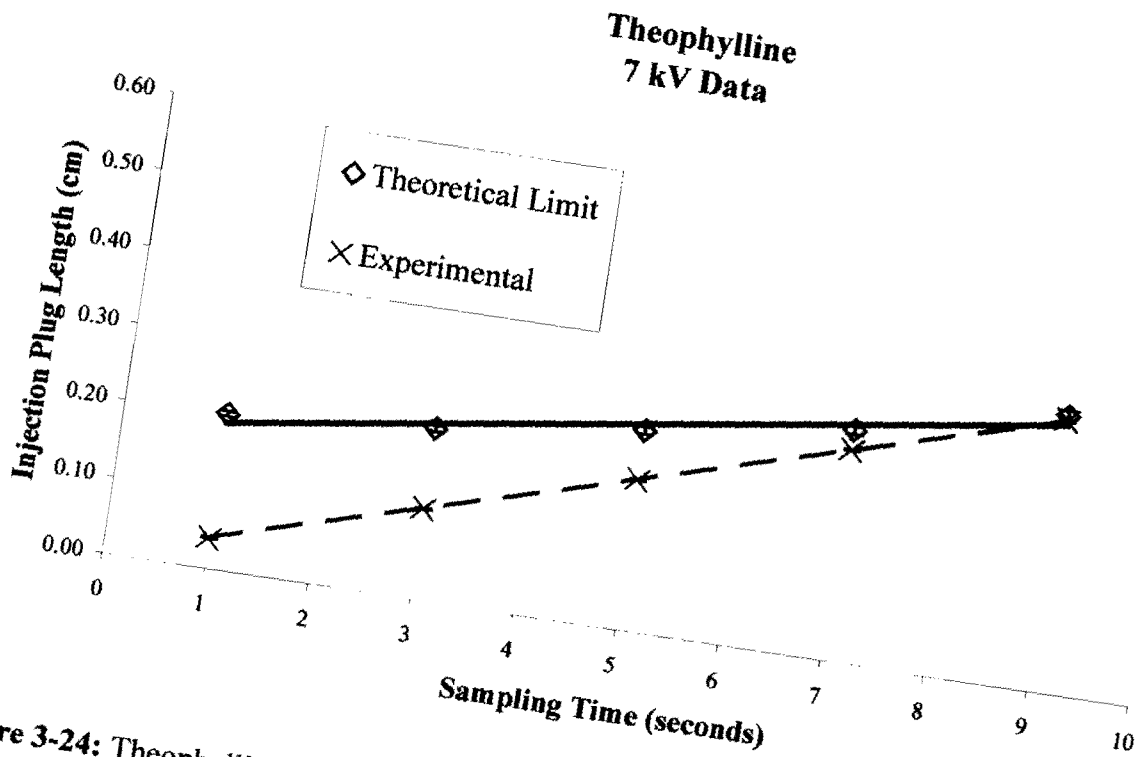
Figure 3-24: Theophylline 7 kV data. Intersection approximates 61 kV·sec.

Theophylline
9 kV Data
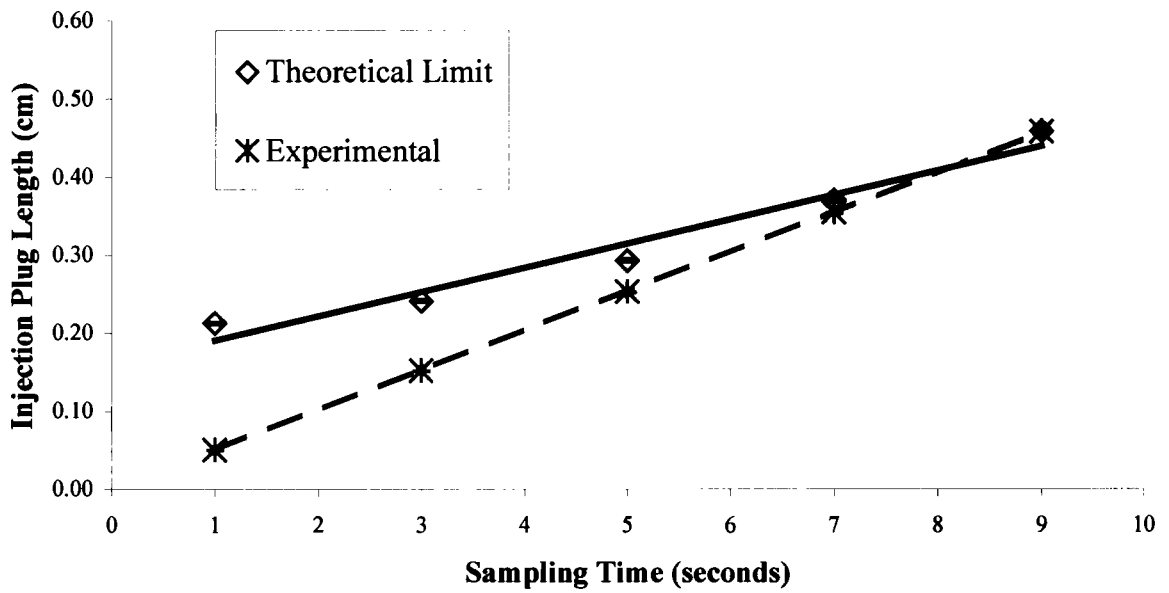
Figure 3-25: Theophylline 9 kV data. Intersection approximates 74 kV·sec.

**Theophylline
11 kV Data**
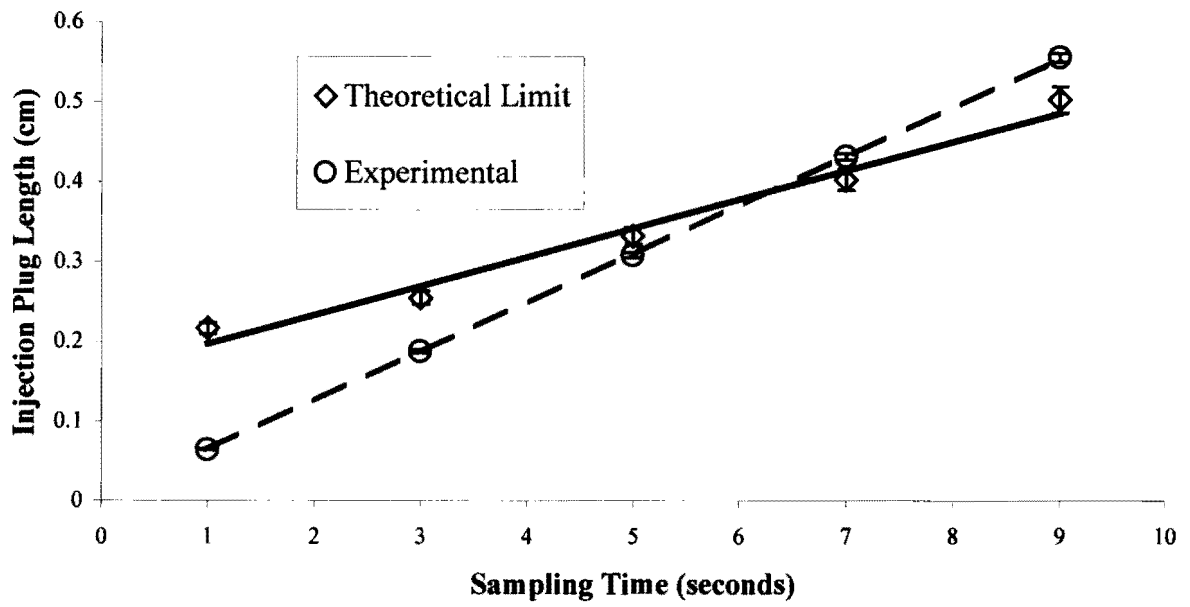
Figure 3-26: Theophylline 11 kV data. Intersection approximates 69 kV·sec.

Theophylline, on the other hand, switched from 60 kV·sec to 10 kV·sec. Table 3-5 lists the points of intersection for both caffeine and theophylline for the two sets. For the graphs where no intersection could be located visually, the equations of the experimental and theoretical lines were set equal to solve for the corresponding sampling time at which the intersection would have occurred. Caffeine intersects at approximately the same value in both the set 1 and set 2 data series. The concentration of caffeine in set 1 was twice the concentration in set 2. On the other hand, the concentration of set 2 for theophylline was twice its concentration in set 1. The intersection for theophylline changed three-fold from set 1 to set 2 data. Because of the variability in these results, it could not be concluded that the concentration was the operating factor.

Standard Electrokinetic Equations

The next step was to re-examine the starting equations. (Equations 2-4) Starting with the assumption noted in Equation 3-4 and Equation 3-5, the following is obtained through substitution.

$$l_{inj} = (Q/C) / \pi r^2 \tag{3-12}$$

Since Q, the quantity injected, is defined by Equation 3-3; it may be substituted into Equation 3-12. Most of the factors will cancel including the concentration. Therefore, it is evident that concentration does not play a defining role in calculating the length of the injection plug.

Table 3-5: Point of intersection for caffeine and theophylline in two-day study. Averages represent the values upon which the intersection remained relatively constant. The letter "X" represents data statistically removed from the table.[88,89]

Data set	Caffeine Set 1 0.258 mg/mL (kV·sec)	Theophylline Set 1 0.155 mg/mL (kV·sec)	Caffeine Set 2 0.113 mg/mL (kV·sec)	Theophylline Set 2 0.258 mg/mL (kV·sec)
1kV	18	X	25	10
3kV	23	44	26	12
5kV	24	50	28	11
7kV	25	61	28	11
9kV	24	74	28	9
11kV	24	69	27	9
Average→	24 ± 0.70	60 ± 13	27 ± 0.90	10 ± 1.3

The length of the injection plug is defined by the equation below:[90]

$$l_{inj} = \mu_{tot}E_s t_s \tag{3-13}$$

Equation 3-13 shows that the differences in the values of the intersection of the theoretical and experimental lines in Table 3-5 are due to analyte mobility. Analyte mobility depends on the operating pH. Caffeine is a neutral marker and therefore, will only move due the forces governing electroosmotic flow. The movement of theophylline, however, is due to both electroosmotic and electrophoretic flow. Since theophylline has a pKa of 8.8 and we are operating at a pH of 7.5, it is starting to experience some anionic character. (Figure 3-1) The original method called for an operating pH of 7.0. We chose to switch to a pH of 7.5 in order to obtain baseline resolution between the two components. (Figure 3-27) We believe pH variances contributed to the mobility differences observed for theophylline between the two sets of data. At pH 7.5, theophylline is 4.75% anionic.

Graphical Mobility Analysis (GMA)

Another way to illustrate the differences in theophylline's total mobility between the two experimental data sets presented may be accomplished by graphical mobility analysis (GMA). Equation 3-13 states that if the length of the injection plug were plotted against the product of the sampling field strength multiplied by the sampling time, the slope would be equal to each analyte's total mobility. Total mobility, μ_{tot}, is the sum of the electrophoretic
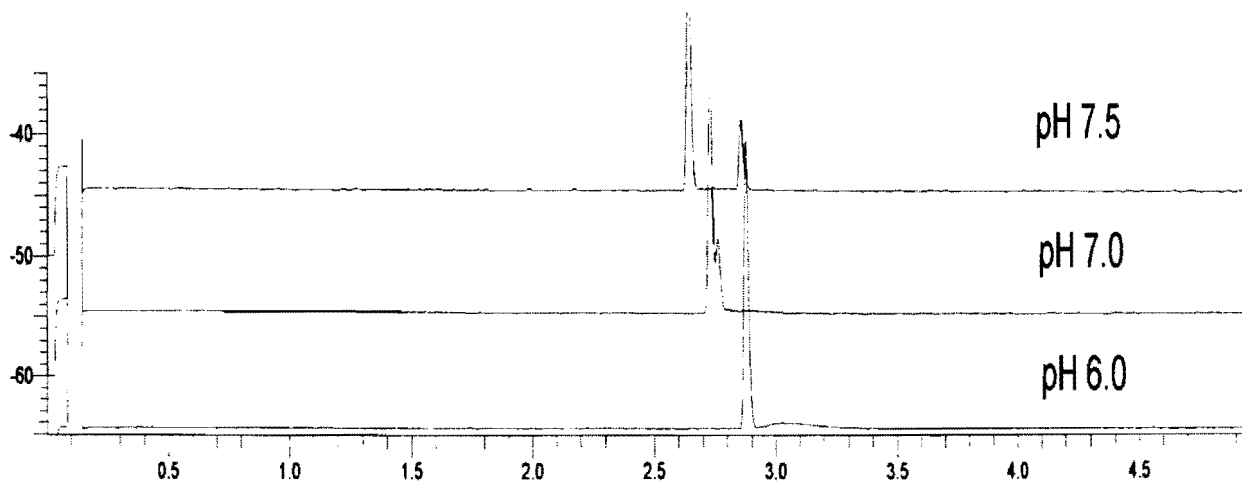
Figure 3-27: Poor resolution between caffeine and theophylline at pH 7.0 justifies need to increase run pH to 7.5.

and electroosmotic mobilities. Thus, this procedure provides a graphical method for analyzing total mobility using CZE with electrokinetic sampling.

Figures 3-28 and 3-29 display the results of the GMA for set 1 and 2 data, respectively. Overlaying these two graphs, it is once again clear that the slope (μ_{tot}) for caffeine remains rather constant when comparing the two data sets. The slope for theophylline has changed by a factor of about three. In Table 3-6, the results of the total mobility are listed as they were determined graphically. Also displayed in the table are the average total mobility values for caffeine and theophylline as tabulated from each of the 150 runs performed using Equation 3-14 below:[2]

$$\mu_{tot} = \frac{(L_d / t_m)}{(V / L_t)} \qquad (3\text{-}14)$$

where L_d and L_t are the length to the detector and total column length, respectively, and V is the separation voltage. Relative standard deviation values prove better precision when using the GMA technique as opposed to averaging the mobility values obtained from 150 analyses.

Graphical Mobility Analysis of the Otsuka/ Terabe Model

Graphical mobility analysis was performed on the theoretical limit and experimental plug lengths determined for caffeine and theophylline using the original set 1 data. (Figures 3-5 and 3-6) The average injection plug lengths for each set of electrokinetic conditions (Table 3-1) were plotted as a function of the field strength multiplied by the sampling time. Figure

95

Mobility Plots
Set 1

Injection Plug Length (cm)

◇ Caffeine
□ Theophylline

$y = 0.687x - 0.0021$
$R^2 = 0.9998$

$y = 0.405x - 0.0013$
$R^2 = 0.9997$

Sampling Field Strength • Sampling Time ((kV/cm)•sec)
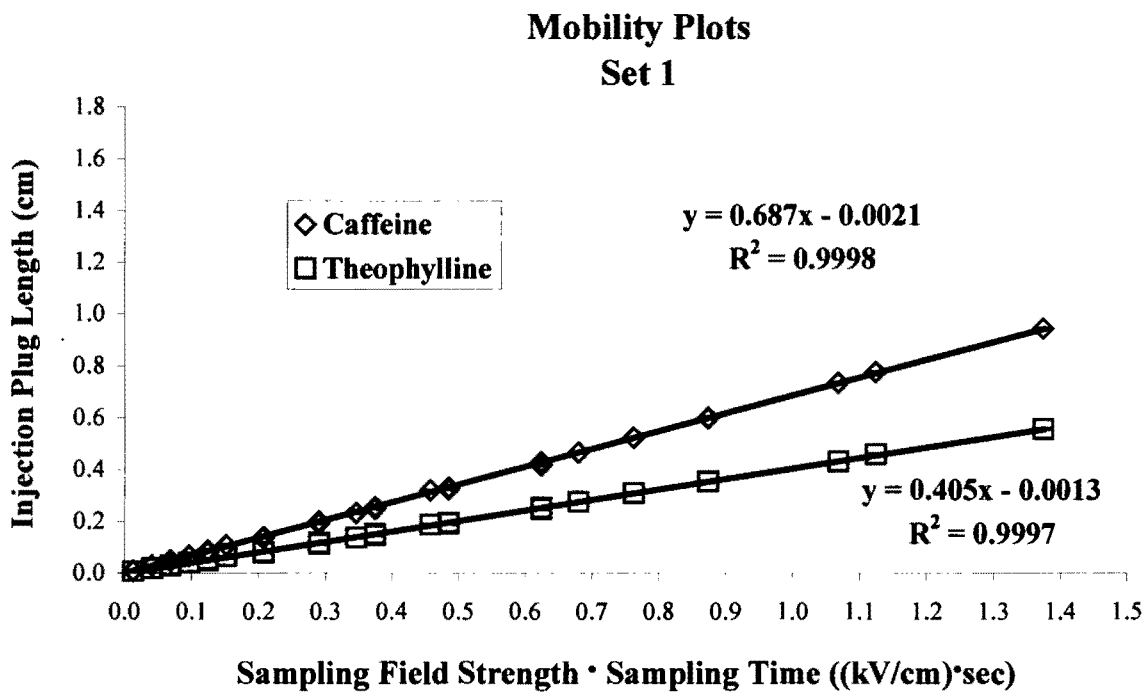
Figure 3-28: Graphical mobility analysis of caffeine and theophylline, set 1 data. Slope of line equals the total mobility (μ_{tot}).
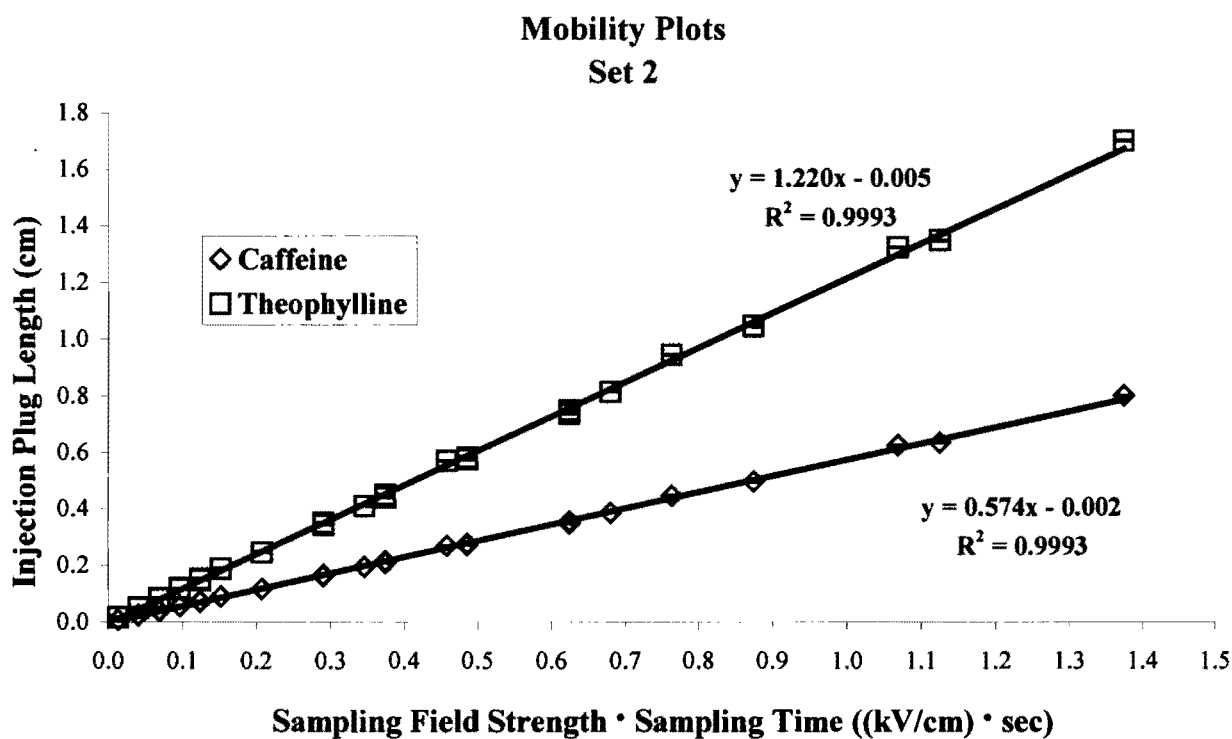
Figure 3-29: Graphical mobility analysis of caffeine and theophylline, set 2 data. Slope of line equals the total mobility (μ_{tot}).

Table 3-6: Total Mobility Summary

Caffeine	Migration Time (minutes)	Concentration (mg/mL)	μ_{slope}	%RSD	$\mu_{average}$	%RSD
Set 1	2.94 (2.15%)	0.248	0.687	0.15%	0.679	2.15%
Set 2	3.52 (1.79%)	0.113	0.574	0.23%	0.568	1.80%

Theophylline	Migration Time (minutes)	Concentration (mg/mL)	μ_{slope}	%RSD	$\mu_{average}$	%RSD
Set 1	3.12 (2.30%)	0.155	0.404	0.15%	0.641	2.29%
Set 2	3.79 (1.86%)	0.258	1.220	0.22%	0.527	1.88%

3-30 illustrates the results for caffeine. The point of intersection still corresponds to the 24 kV·sec described earlier. The only difference is this value is now divided by the column length (72 cm) in order to plot it as the field strength (E_s) along the x-axis. Theophylline received the same treatment and those results are noted in Figure 3-31. If these two graphs are overlaid, it is seen that the Otsuka/ Terabe model predicts both lines to have relatively the same slope and y-intersection, regardless of analyte mobility. It may be concluded that the maximum injection plug lengths predicted by the model need to be extended to incorporate mobility. The standard electrokinetic equations have already accounted for this.

Conclusions

In this chapter, electrokinetic sampling has been evaluated as it affects peak area and injection plug length reproducibility. It has likewise been concluded that longer sampling times and higher sampling voltages (field strengths) would result in better reproducibility values. However, these values do appear to have limitations with the formation of a concentration gradient in the diffuse layer surrounding the capillary-electrode assembly. In the future, the addition of sample vortexing to the CZE hardware may alleviate the gradient effect. Mathematical methods developed for predicting the plug length maximum need to be extended to incorporate analyte mobility. Graphical mobility analysis offers a new and unique method for determining the total mobility values for each of the analytes with greater precision.

Caffeine Mobility
Theoretical Limit vs. Experimental
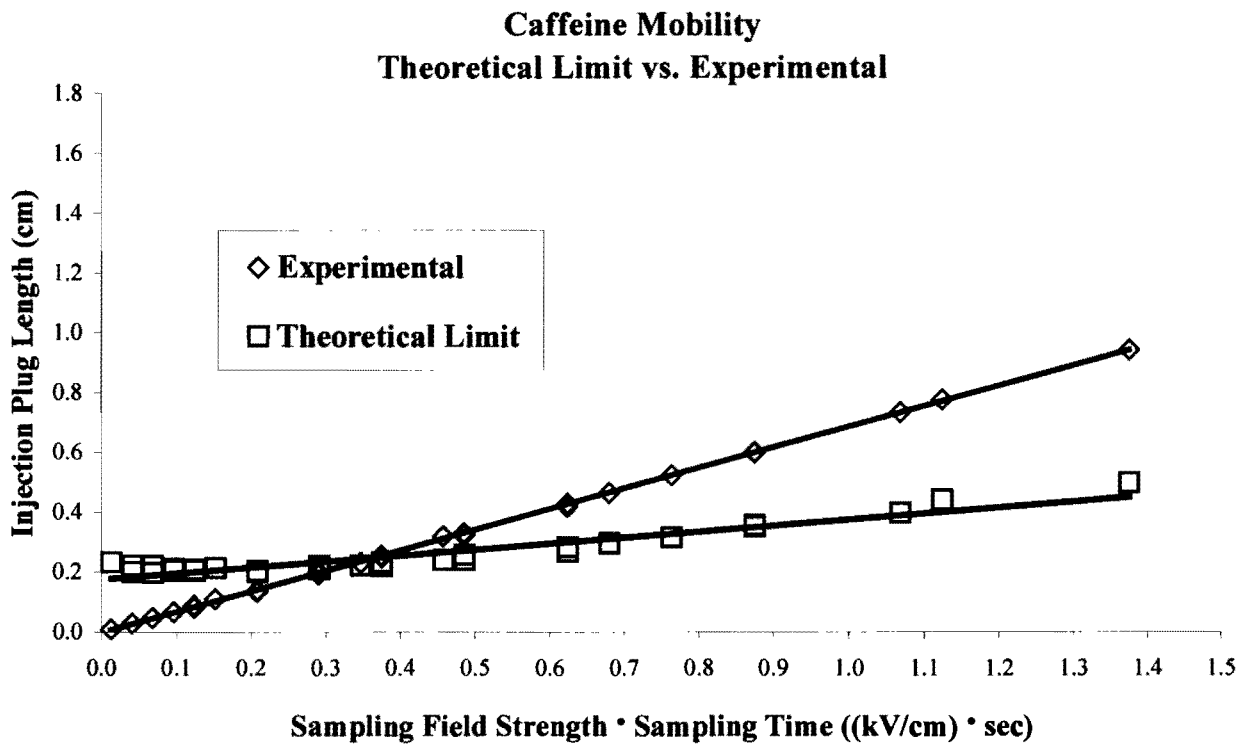
Figure 3-30: Graphical mobility analysis of caffeine, set 1 data, for theoretical limit and experimental plug lengths.
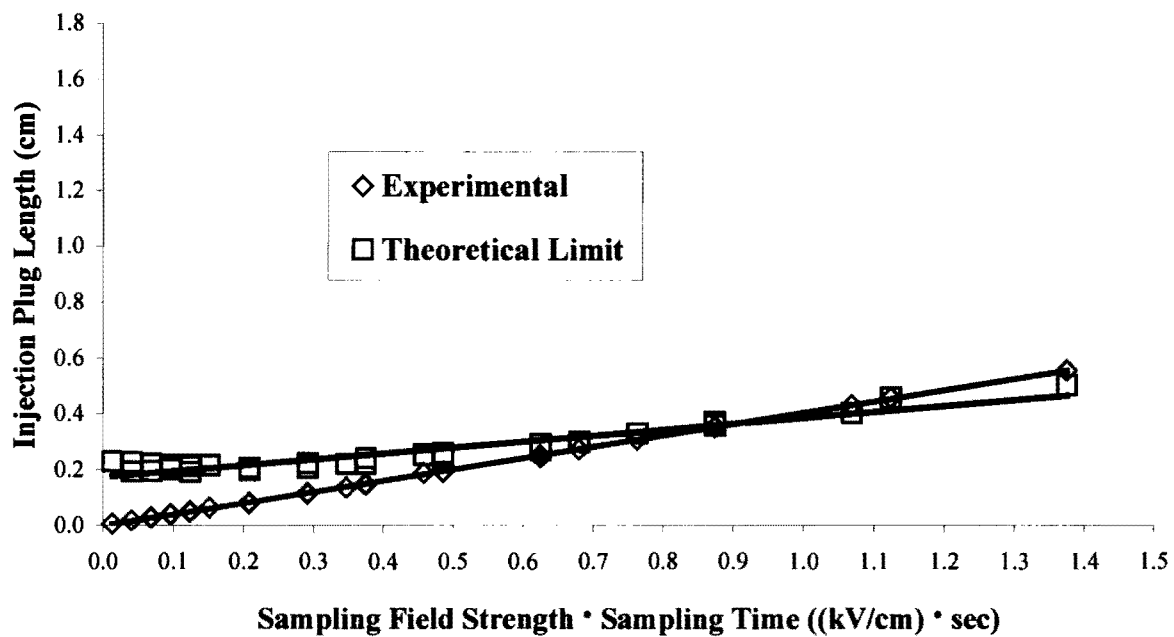
Figure 3-31: Graphical mobility analysis of theophylline, set 1 data, for theoretical limit and experimental plug lengths.

Chapter IV

Assessment of Buffering Systems by Graphical Mobility Analysis

SUMMARY

Traditionally, electrophoretic mobility plots are constructed during the method development process for capillary zone electrophoresis (CZE) in order to select the operational pH. The migration times are read directly from the electropherograms and used to solve for total analyte mobility by dividing the analytes total velocity by the applied field strength. The electrophoretic mobility is calculated by subtracting the total mobility of a neutral marker from each of the analytes being separated. The operating pH is chosen where the analytes experience different electrophoretic mobilities and minimal effects due to their pKa values using the plot. Care is usually taken not to select an operating pH outside the effective range of the buffer system.

In an effort to better understand the effect of buffer pH on separations in CE, graphical mobility analysis (GMA) has been implemented and contrasted to the traditional method described above. GMA has lead to better assessment of the buffering system as illustrated in the electrophoretic mobility plots described in this chapter. GMA monitoring of electrophoretic mobility emphasizes the need for proper functioning buffers at the requisite pH values by illustrating the regions where the buffering system proves inadequate. It may

be concluded that the use of GMA for mobility determinations demonstrates buffer inadequacies more predominantly than traditional methods.

INTRODUCTION

In capillary zone electrophoresis, a buffer solution may provide the ions required to carry the current and detection is done directly on the capillary.[1,2,34-36] When a current passes through an ionic solution, anions migrate toward the anode while cations migrate toward the cathode.[2] The types of buffer solutions used to aid in this transportation are very dependent on the application; however, the buffer must maintain the requisite pH. As mentioned in previous chapters, inside the capillary there is a force due to voltage and a force due to viscous drag. Both of these forces compose the electrophoretic flow velocity (v_{el}):[1,2,34-36]

$$v_{el} = \frac{zeE}{6\pi\eta r_h} \qquad (4\text{-}1)$$

where charge, z, and hydrodynamic radius, r_h, are variable. The charge of an electron (e), the field strength (E), and the viscosity (η) are constants in the above expression. Selectivity is based on the ratio of the charge to the hydrodynamic radius.[1,2,36]

Electroosmotic flow constitutes the bulk flow within the capillary. Under typical conditions, the silica capillary has a charged surface that attracts counter ions into the adjacent layers of liquid, forming a double layer. When there is an electric field component parallel to the capillary wall, that field will pull the counter ions along the surface, dragging

the solution with it and inducing flow.[1] Removing the charged surface would minimize this type of flow. Under the influence of positive separation potentials and when electrophoretic and electroosmotic flow are in the same direction, overall transport will be towards the cathode. This allows both anions and cations to be detected. This will occur if the electroosmotic flow component outruns the electrophoretic component of an anionic compound. The overall movement generated within the bulk solution is dependent upon buffer concentration, pH, and the addition of organic modifiers.[2] All of these play a role in modifying the variables composing the electroosmotic flow (v_{eo}) as defined by the Smoluchoski equation.[2,34]

$$v_{eo} = \frac{\varepsilon \xi E}{\eta} \qquad (4\text{-}2)$$

where ε is the dielectric constant, ξ is the zeta potential of the liquid-solid interface, E is the field strength, and η is the viscosity of the buffer.

The total mobility of an analyte (μ_{tot}), sometimes referred to as the apparent mobility, is comprised of the combination of electrophoretic, μ_{el}, and electroosmotic, μ_{eo}, mobilities.[2]

$$\mu_{tot} = \mu_{el} + \mu_{eo} \qquad (4\text{-}3)$$

Experimentally, the total mobility may be calculated using the following equation:[2]

$$\mu_{tot} = \frac{(L_d / t_m)}{(V / L_t)} \qquad (4\text{-}4)$$

where L_d is the length of the capillary from the inlet to the detector window, t_m is the migration time, V is the separation voltage, and L_t is the total length of the capillary. All analytes in solution will be affected by the electroosmotic flow. Therefore, in order to obtain separation, proper control of the parameters governing electrophoretic mobility is essential. The electrophoretic mobility is commonly found by manipulating Equations 4-3 and 4-4 above to obtain the following expression:[38-42]

$$\mu_{ep} = \frac{L_d L_t}{V} \left(1/t_m - 1/t_o \right) \qquad (4\text{-}5)$$

In this equation t_o is the migration time of the neutral marker. It is used to measure the extent of electroosmotic flow. Examples of typical electroosmotic markers include thiourea and acetone. As described earlier in Equation 4-1, differences in the charge to hydrodynamic radius ratio will correlate directly to the separation of ions in solution because of the differences in the calculated μ_{ep}. Therefore, the role of buffer pH is critical in the selection of separation parameters.

Typically, electrophoretic mobility plots are constructed as a tool in the method development process.[2,38] This is simply a map of analyte electrophoretic mobility as a function of pH. Ideally, the pH is chosen where ions are experiencing different mobilities and are not experiencing any type of equilibria associated with their pKa values. In

accordance with the theory presented above, neutral molecules will exhibit no electrophoretic mobility and will serve only to measure the movement of the electroosmotic forces composing the flow of the bulk solution.

In an electropherogram, migration time (total mobility) plays a key role in analyte identification. The straight-forward application of Equations 4-4 and 4-5 above is commonly employed for these purposes.[38-42] Other simulations of electrophoretic mobilities have been developed with commercial computer software systems in order to monitor the impacts of ionic strength on electroosmotic flow or to predict the separation of peptides as a result of pH and ionic strength of the run buffer.[91,92] However, some of these software systems require input of the ion's electrophoretic mobility, a value which can not always be found in the literature.[92]

Analyte migration time reproducibility also affects the total mobility values obtained using Equation 4-4. Recently, Altria, *et. al.*, have made significant steps in accounting for such variables by modifying the method validation protocols, commonly employed in HPLC method development, for CZE techniques.[45] Internal standards have proven to drastically increase experimental precision of migration time values. Of course, this correlates directly with the improvement of the mobility values ascertained. The use of mobility ratios in order to obtain lower relative standard deviation (RSD) values and provide more reliable experimental measurements has been discussed in earlier contributions to CZE literature as well.[93-95] Other attempts have also been made to accommodate the same variations which internal standards appear to correct. Examples of these attempts include mobility

determinations that have been derived using two or more system marker compounds.[38,96]

Valko, *et.al.* used marker compounds of known electrophoretic mobility to elucidate the physicochemical parameters governing a separation during an electrophoretic run.[38] In their paper, they state that poor repeatability of the electroosmotic flow velocity acts as the major contributor of the resulting variations seen as migration times.[38] Their theory predicts reproducible mobility values using Equation 4-6 below and provides the experimental data legitimizing their claim.[38]

$$\mu_{ep(x)} = \frac{t_1 t_2 (\mu_{ep1} - \mu_{ep2}) - t_x(\mu_{ep1}t_1 - \mu_{ep2}t_2)}{t_x(t_2 - t_1)} \quad (4\text{-}6)$$

The subscripts 1 and 2 refer to the chosen markers and x refers to the analyte.

Graphical Mobility Analysis (GMA)

In this chapter, an application of a new graphical method of mobility analysis is presented. Previous work, described in detail in chapter 3, has already proven the use of GMA as a more precise measurement of total analyte mobility.[97] In that study, experimental total mobility data were calculated using Equation 4-4 above and averaged for 150 individual data points for each of two analytes. These data points reflected the total mobilities based on the migration times of caffeine and theophylline during a study of electrokinetic sampling conditions. GMA was also used on this data. GMA improved total mobility reproducibility calculations by a factor of at least 8 with all relative standard deviation values falling below 0.23%.[97]

As developed in the previous chapter, the principle of GMA is based upon equations governing electrokinetic injection. The equation below is used to calculate the amount of material introduced to the column (Q) when an electrokinetic injection is performed.[2]

$$Q = (\mu_{ep} + \mu_{eo})\pi r^2 E_s C t_s \qquad (4\text{-}7)$$

μ_{ep} = electrophoretic mobility E_s = field strength during sampling

μ_{eo} = electroosmotic mobility t_s = injection time

r = capillary radius   C = concentration of solute

This equation corrects for sampling discrimination caused by varying degrees of electrophoretic mobility experienced by each of the solutes.[2,36] Assuming minimal solute-wall effects, the injected volume, V_{inj}, of each solute can be calculated from the original analyte concentration.[97]

$$C = Q/V_{inj} \qquad (4\text{-}8)$$

The injection plug length (l_{inj}) can be determined by manipulating the known expression for cylindrical volume.

$$l_{inj} = V_{inj}/\pi r^2 \qquad (4\text{-}9)$$

By substituting Equation 4-8 into Equation 4-9, the length of the injection plug becomes

$$l_{inj} = (Q/C) / \pi r^2 \qquad\qquad (4\text{-}10)$$

Since Q, the quantity injected, is defined by Equation 4-7; it may be substituted into Equation 4-10. Most of the factors will cancel and the total mobility, μ_{tot}, can be exchanged for the sum of μ_{ep} and μ_{eo}. (Equation 4-3) Now the length of the injection plug is defined by the equation below:[90,97,98]

$$l_{inj} = \mu_{tot}E_s t_s \qquad\qquad (4\text{-}11)$$

In accordance with Equation 4-11, if the calculated length of the injection plug is plotted versus the sampling field strength (E_s) as multiplied by the sampling time (t_s), the line generated has a slope equal to total analyte mobility, μ_{tot}. This is the definition of graphical mobility analysis. It is recommended to use at least three different electrokinetic sampling conditions in order to have at least three points to define the line. Table 4-1 lists a possible set of electrokinetic sampling conditions and the resulting x-axis values that would be attained for GMA using the experimental parameters defined later in this chapter. The electrophoretic mobility used in the construction of an electrophoretic mobility plot can then be calculated by subtracting the total mobility of a neutral marker from the total mobility of the analyte. This is a simple rearrangement of Equation 4-3 or 4-5 above.[2]

$$\mu_{el} = \mu_{tot} - \mu_{eo} \qquad\qquad (4\text{-}12)$$

Table 4-1: Electrokinetic Sampling Voltages and Times

Voltage (kV)	Time (seconds)	$E_s \cdot t_s$ [(kV·sec)/cm]
3	5	0.21
5	5	0.35
7	5	0.49

*n = 3, column length used to calculate field strength at time of sampling is L_t = 72 cm.

As mentioned previously, neutral markers do not experience electrophoretic flow.

In order to demonstrate the applicability of graphical mobility analysis, capillary electrophoresis was implemented in the separation of caffeine and theophylline over a pH range of 6 to 11. An electrophoretic mobility plot of the two analytes was constructed using the mobilities as ascertained from Equation 4-4 above for the representative electropherogram reflecting each pH level. This plot was compared with the plot constructed from the mobility values attained using GMA. Both of these methods of determining analyte mobility were the subjected to Equation 4-12 in order to determine the electrophoretic mobility. It is important to note that Equations 4-5 and 4-12 presented earlier are technically the same, just rearranged algebraically.

EXPERIMENTAL SECTION

Chemicals. Standard samples of caffeine and theophylline, whose structures are shown in Figure 4-1, were obtained from Aldrich Chemical Co. (Milwaukee, WI) and used without further purification. Sodium hydroxide was purchased from Aldrich. Sodium phosphate monobasic, dibasic, and tribasic were received from Fisher Scientific (Fair Lawn, NJ) and prepared at concentrations of 0.01 M each using de-ionized water. Buffer solutions for each pH level between 6 and 9.2 were prepared by mixing monobasic and dibasic phosphate solutions until the proper pH was measured. The dibasic and tribasic phosphate solutions were combined in the preparation of buffers ranging from 9.2 to 11. Mixing the two salt solutions minimized variations that may have interfered due to differing ionic strengths if
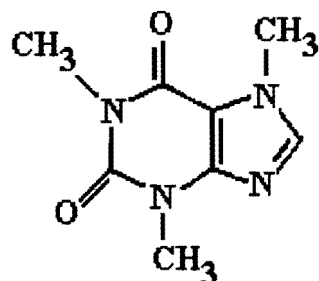
Caffeine (Neutral)
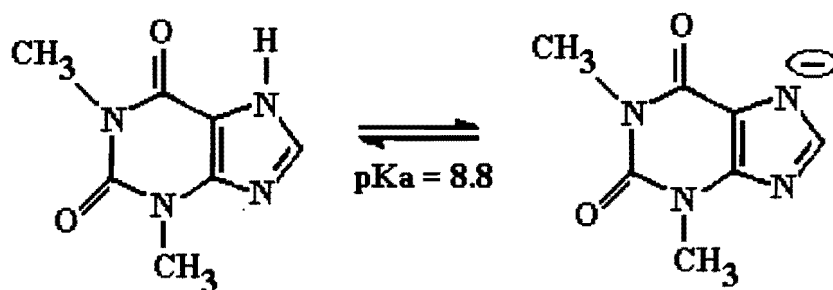
Theophylline

Figure 4-1: Caffeine and theophylline. The two molecules differ in placement of a methyl group on the seventh position nitrogen.

strong acids or bases were utilized for pH adjustment. A list of the pH's used in this study is summarized in Table 4-2. Buffer solution preparation was followed by vacuum filtration using a 0.45 μm disk filter. Caffeine and theophylline were prepared at concentrations of 0.25 mg/mL and 0.10 mg/mL. Both compounds were diluted with the buffer solution prepared at each pH level.

Instrumentation. An ABI 270A CE instrument (PerkinElmer, Norwalk, CT) was used. This system was upgraded to the software level of an ABI 270A-HT model to allow controlled sampling at various voltages. Sampling voltages and times are the same as those outlined in Table 4-1. The average injection plug length was calculated for each injection set and the slope was determined using Microsoft® Excel 2000 software. Table 4-1 provided the values for the x-axis. A PerkinElmer fused silica capillary was used (72 cm x 50 μm i.d.) for the separation. The length to the detection window was 50 cm. Turbochrom (PerkinElmer, Norwalk, CT) provided the data output.

Electrophoretic Conditions. The method used in this study is similar to a method found in the literature used to evaluate system suitability.[34] A new capillary was cleaned using the following hydrodynamic wash routine at 20 psi: 15 minutes 1.0 N NaOH, 15 minutes de-ionized water, 15 minutes 0.1 N NaOH, 15 minutes run buffer. Samples were run consecutively. Overall column temperature was held at 30°C. The following steps were taken to complete the separation at each new pH level. The buffer was flushed through the column for 30 minutes. After equilibrating the column to the new pH, each injection was made following additional flushing of the column for two minutes with buffer. Sampling

Table 4-2: List of pH values implemented.

pH
6.0
7.0
8.0
8.5
8.8
9.0
9.2
9.5
10.0
11.0

was completed at each of the conditions described in Table 4-1. Finally, separation was performed at 30 kV with a run time of 5 minutes for each injection. Analysis was repeated three times at each set of electrokinetic sampling conditions. The ultraviolet adsorption detector was set to 220 nm.

RESULTS AND DISCUSSION

Figure 4-1 displays the expected ionic states of caffeine and theophylline within the pH range being studied (Table 4-2). Caffeine served as the neutral marker and therefore, had a total mobility equivalent to that of the electroosmotic flow. Theophylline has a pKa of 8.8, and will experience equilibrium, as illustrated in Figure 4-1, within ±2 pH units of the pKa value. Experimental conditions were selected to monitor equilibrium behavior closely within this range. Caffeine elutes before theophylline in each of the electropherograms presented in Figure 4-1 with the exception of pH 6.0. As theophylline experiences more electrophoretic behavior due to its ionization, its mobility will change and its separation from caffeine will increase.

Figure 4-2 illustrates the separation of caffeine and theophylline. Here the electropherograms are presented at each pH level. At a pH of 6, caffeine and theophylline co-elute. Both of these compounds are neutral at this pH as shown in Figure 4-1. Regular CZE is not capable of separating neutral compounds of such similar structures for reasons described in earlier chapters. As the pH increases, theophylline becomes more and more
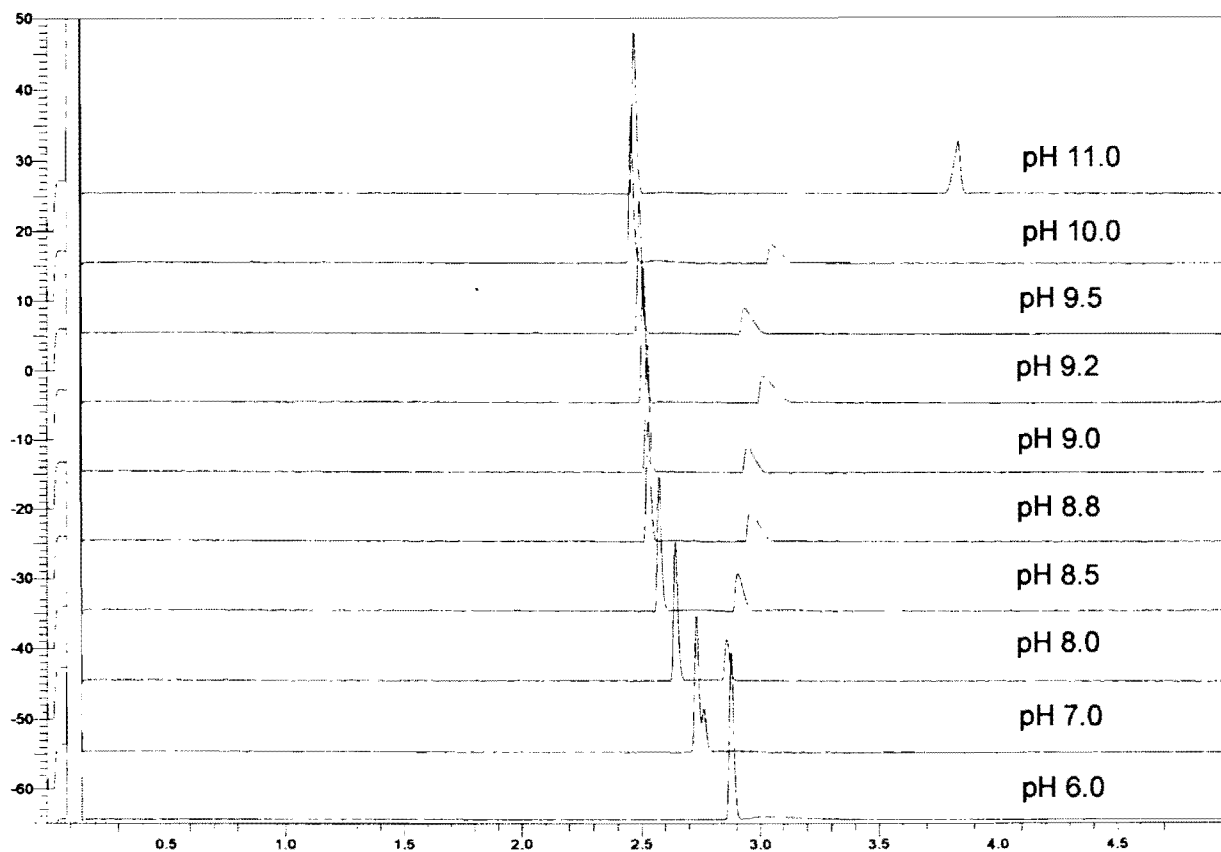
Figure 4-2: Electropherograms representing pH effects on analyte mobility. Caffeine elutes before theophylline except at pH 6.0. Here the two analytes co-elute because they are neutral.

negatively charged. As mentioned previously, the addition of this electrophoretic mobility due to the charged ion will contribute to the separation of the two peaks. At a pH of 7, this effect is barely noticed and at pH 8, the two analytes are baseline resolved. Caffeine experiences a shift to shorter migration times throughout the pH range studied. This occurs because higher pH solutions contribute to a charge intensive double layer along the capillary walls.[2] As discussed earlier, the movement of this charge toward the cathode comprises the electroosmotic flow. Therefore, if more charge is present, faster flow rates can be expected for neutral compounds. Theophylline also experiences changes in migration time. Peak shape is compromised in the region dominated by equilibrium behavior. At a pH of 10.8, theophylline should be completely negatively charged. The results at pH 11 show a symmetrical peak, reflecting that result.

Figure 4-3 shows an electrophoretic mobility plot that was constructed using Equations 4-4 and 4-5 and the migration times of caffeine and theophylline resulting from the electropherograms presented in Figure 4-2. Because caffeine is a neutral marker, its electrophoretic mobility is zero, as seen in Figure 4-3. Theophylline became more negatively charged as it moved through the pH range dominated by its pKa. When analytes are not experiencing any charge fluctuation, their slope reflecting electrophoretic mobility will equal zero. Theophylline has a plateau at pH's of less than 6.8 because it is neutral like caffeine in that region. At pH's higher than 10.8, another plateau would be seen at approximately -0.28 $cm^2/kV \cdot sec$. The data presented in Figure 4-3 does not illustrate this region because the range of pH studied did not allow proper measurement of the electrophoretic mobility values.
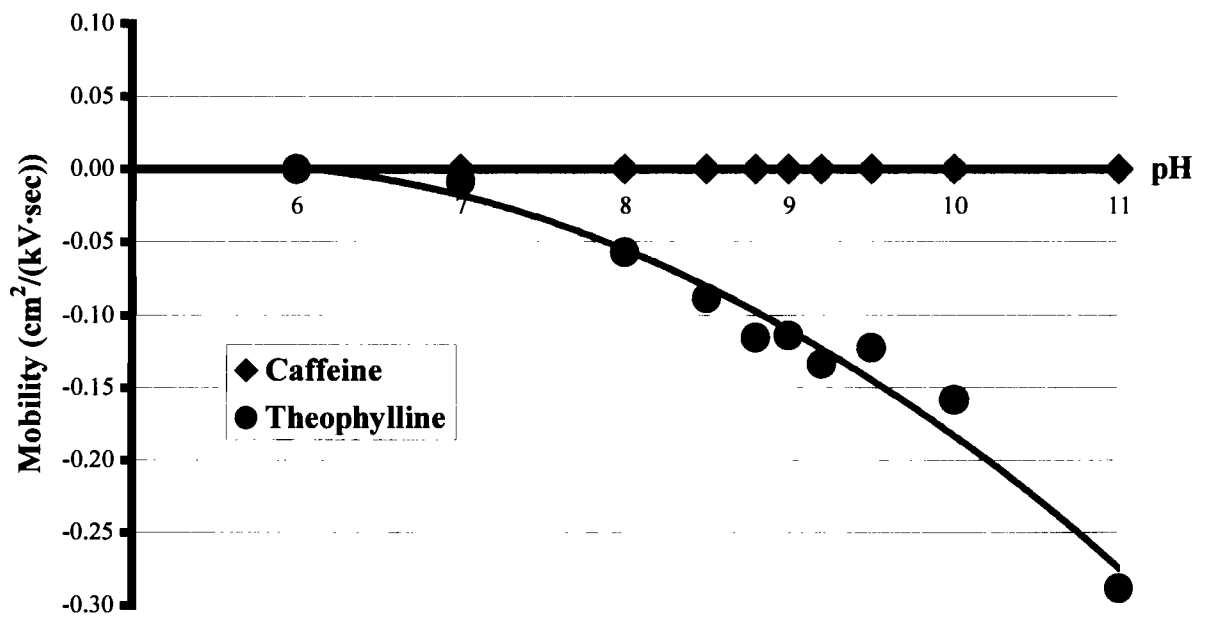
Figure 4-3: Typical electrophoretic mobility analysis using the data acquired in Figure 4-2 and Equations 4-4 and 4-5.

Graphical mobility analysis (Equation 4-11) was also used to assess the total mobility of caffeine and theophylline. The resulting electrophoretic mobility plot is illustrated in Figure 4-4 where the electrophoretic mobilities determined by GMA and Equation 4-12 are plotted as a function of pH. The same trend exists for pH 6 to 8 as shown earlier in Figure 4-3. However, from pH 8.5 to 10 there is a deviation from the anticipated results. The phosphate buffer systems implemented in this study have pKa values at 7.2 and 12.7.[2,3,38] The useful ranges for the phosphate buffer are therefore between 6.2 to 8.2 and 11.7 to 13.7.[38] The combination of this information and the equilibria associated within the measured pH range of 8.5 to 10 reflect a region not buffered properly using phosphate regardless of the separations obtained and illustrated in Figure 4-2. If the data attained in this region were eliminated, the expected curve illustrated in Figure 4-3 would result. This claim is clearly indicated in Figure 4-5. The point at pH 11 has been left in Figure 4-5 although it is also outside of the upper buffering range because theophylline was completely ionized. One may notice that because of the lacking buffering capacity this value is slightly higher than the one obtained in Figure 4-3 using Equations 4-4 and 4-5. As mentioned previously, if this pH region were to be studied more intensively, more conclusive information would confirm the usage of the GMA technique and have identified the other plateau.

Conclusions

Overall, GMA has lead to better assessment of the buffering system as illustrated in the electrophoretic mobility plots described in this chapter. Although the traditional methods of plot construction using Equations 4-4 and 4-5 give results reflective of the changes in pKa,

Electrophoretic Mobility Plot
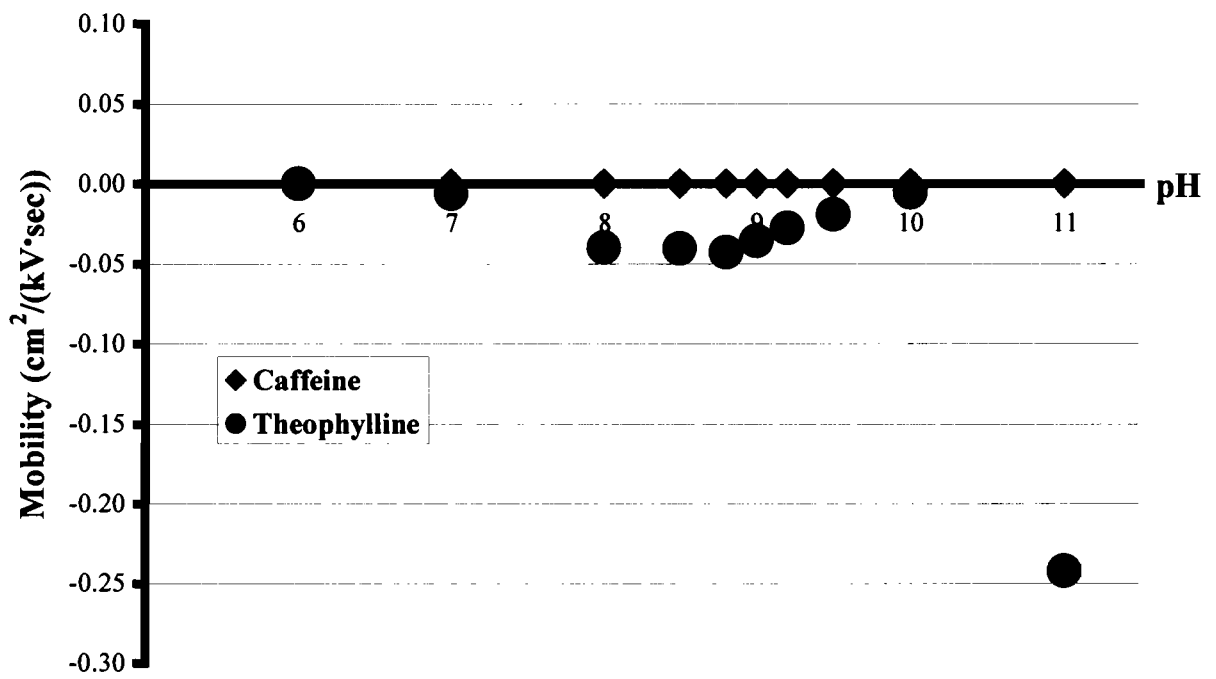
Figure 4-4: Results of graphical mobility analysis and Equation 4-12.

Electrophoretic Mobility Plot
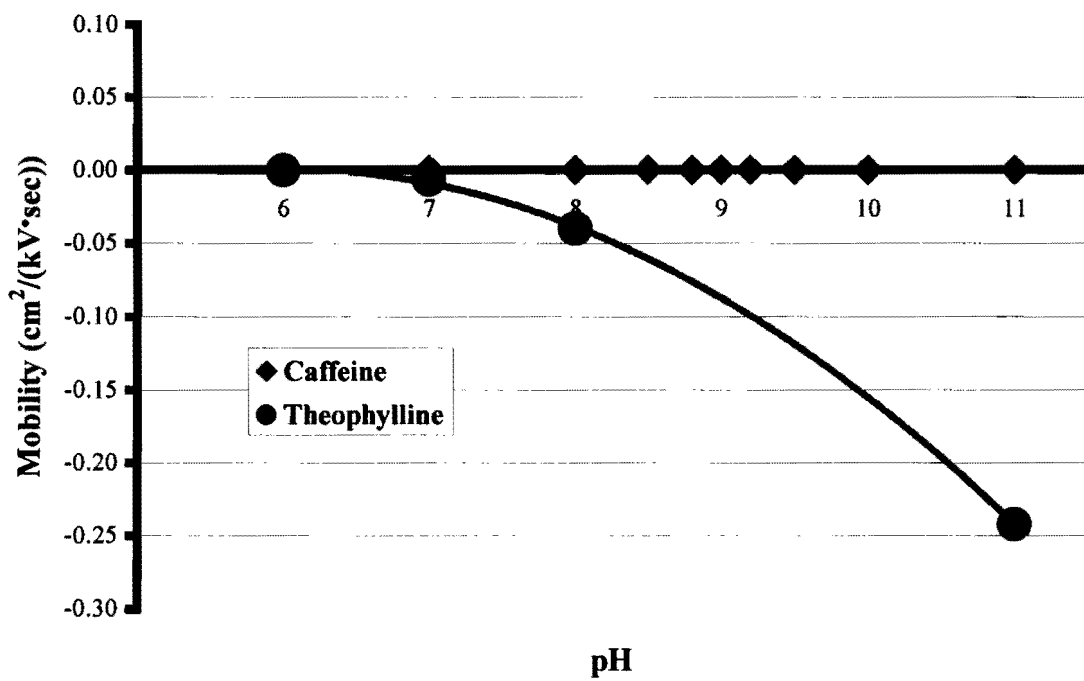
Figure 4-5: Results of graphical mobility analysis and Equation 4-12 without results attained outside of phosphate buffering capabilities.

they cannot be concluded as reproducible electrophoretically outside the buffering

capabilities of the system. Long term usage at pH ranges not adequately maintained by

buffering may shift separation variables such as migration times due to lack of pH control.

The short-term separations shown were still good in these regions, as was illustrated in

Figure 4-2, with the exception alterations in peak shape due to the approach of analyte

equilibria conditions. GMA monitoring of electrophoretic mobility emphasizes the need for

proper functioning buffers at the requisite pH values by illustrating the regions where the

buffering system proved inadequate. During method development processes, and as

discussed elsewhere in this chapter, proper selection of the buffer is critical in maintaining

reproducible migration times, *i.e.* mobility values. Therefore, it may be concluded that the

use of GMA followed by Equation 4-5 illustrates buffer inadequacies more predominantly

than traditional methods. (Equations 4-4 and 4-5)

Chapter V

Evaluation of Sodium Hydroxide Wash Steps in Capillary Zone Electrophoresis with Electrokinetic Sampling

SUMMARY

Much of the literature corresponding to method development in capillary zone

electrophoresis describes sodium hydroxide rinse cycles as important steps in the preparation

for injection and analysis. In this chapter, five different pre-injection conditions and four

different quantitation techniques are evaluated as they affect the overall separation of

caffeine and theophylline using capillary zone electrophoresis with electrokinetic injection.

When quantitation methods such as internal standardization or internal area normalization are

used, pre-injection rinsing conditions are irrelevant. When using external standardization

and corrected peak areas, better results may be obtained by omitting the NaOH wash step if

at all possible. It is suggested that in cases where compounds adhere to the column walls,

making such a wash step necessary, longer buffer rinsing cycles following a sodium

hydroxide rinse may improve the consistency of separation parameters including migration

time and peak area reproducibility.

INTRODUCTION

One of the most common difficulties in the use of capillary zone electrophoresis (CZE) in

research laboratories today is the struggle to validate analytical methods using similar

methodology to gas and liquid chromatography.[43,45] Recently, several efforts have focused

on developing more representative validation procedures for CZE methods.[44,45] This is

necessary, because although capillary electrophoresis produces results similar to those seen

in chromatography, it remains an electrophoretic technique, with different governing

parameters applied to evaluate system performance. Altria, *et.al.* outline these validation

procedures, which include the necessity of evaluating capillary pre-injection rinsing

techniques as well as capillary variation, reagent source, electrolyte stability, long term

injection precision, operator training, and additional robustness parameters.[45] The goal of

this chapter is to evaluate the effect of different NaOH rinse procedures on the precision of

migration times and peak areas for a simple two-component separation.

When a separation is performed using CZE, common preparations includes conditioning

the capillary for 15 minutes with 1 N NaOH, 15 minutes with de-ionized H_2O, and 15

minutes with 0.1 N NaOH.[2,34] Finally, the run buffer is circulated through the column and

the capillary is considered ready for use. A typical separation sequence consists of two pre-

sampling steps. The capillary is first washed with 0.1 N NaOH and then the separation buffer

is cycled through the column. Injection and timed separation cycles follow immediately.

Using a strong base such as NaOH ionizes free silanol groups and may cleave any epoxide

linkages within the capillary wall.[2] On occasions where analytes adhere to the capillary wall,

a strong base wash step will help in their removal prior to subsequent separations, thus rejuvenating capillary performance. Performance is regained because each time 0.1 N NaOH is passed through the column, there is a redistribution of the zeta potential along the capillary wall. Sometimes, however, alterations in the electrical double layer distribution are difficult to restore to the exact original conditions. A change in migration time and peak area can likewise be observed. This is especially true when electroosmotic flow modifiers or buffer additives are used.[43,46,94,99,100] Buffer additives (not used in this study) may necessitate more extensive cleaning requirements to help restore expected results.[101]

Repeated rinses using sodium hydroxide between injections may also give rise to variations in migration time as the strong base strips the inner surfaces of the capillary. This may alter the internal diameter of the capillary in a non-uniform fashion, an effect that will compromise the contributing variables to electroosmotic flow. In order to evaluate the effects of the NaOH rinsing procedure, the following experimental design is employed in a separation of caffeine and theophylline. Five sets (A-E) of pre-injection rinse procedures (or wash steps) are presented in Table 5-1. Each of the pre-injection wash step sets was evaluated as it affects quantitative precision of migration time and peak area. In much of the chemical industry, method development criteria require peak area relative standard deviation (RSD) values to be less than 2%.[45] Further requirements are imposed by regulating bodies regarding inter-laboratory transference of analytical methods.[102,103] Our data were evaluated using four methods of quantitation, as they permit the satisfaction of these precision guidelines. These include: external standard,[104] internal standard,[46,51,82] corrected peak area,[43,46,52,102,105] and internal area normalization[54] techniques.

Table 5-1: Pre-injection rinse cycles

Sample Set	0.1*N* NaOH Wash (minutes)	BGE (minutes)
A	0	2
B	2	2
C	2	5
D	2	10
E	5	5

External and internal standardization are two techniques commonly implemented in chromatography. When using external standardization, solutions are prepared at known concentrations and peak heights and/or areas are obtained directly from the integration system. Usually, this is done for a series of solutions and the results are plotted against concentration in order to obtain an external calibration curve.[35] The equation representing this curve graphically may then be used to calculate the concentration of an unknown. Internal standardization is very similar to external standardization except it avoids any uncertainties introduced by sample injection by observing the ratio of analyte to internal standard peak heights and/or areas. When choosing an internal standard it is important that the peak is well resolved and elutes close to the analyte peak.[35]

Corrected peak area is achieved by dividing the peak area obtained by the migration time.[2]

$$CPA = PA\ /\ MT \hspace{3cm} (5\text{-}1)$$

Where CPA is the corrected peak area, PA is the peak area and MT is the migration time. Much of the newer software systems developed for CZE analysis are equipped with this capability.[43] However, in cases where electrokinetic injection is utilized, the correction may not be necessary or useful.[44,52,54]

Internal area normalization requires the following operation:[35]

$$NA = PA_i\ /\ \Sigma PA \hspace{3cm} (5\text{-}2)$$

Where the normalized area (NA) is equal to the peak area of the analyte of interest divided by the sum of all peak areas obtained per electropherogram.[35] This method also avoids uncertainties resulting from sample injection.

EXPERIMENTAL SECTION

Chemicals. Standard samples of caffeine and theophylline were obtained from Aldrich Chemical Co. (Milwaukee, WI) and used without further purification. Sodium hydroxide was purchased from Aldrich. Sodium phosphate monobasic and sodium phosphate dibasic were received from Fisher Scientific (Fair Lawn, NJ) and prepared at concentrations of 0.01 *M* each using de-ionized water. The pH 7.5 buffer solution was prepared by mixing monobasic and dibasic phosphate solutions until the proper pH was measured. This was followed by vacuum filtration using a 0.45 μm disk filter. Caffeine and theophylline were prepared at concentrations of 0.2 mg/ml and 0.1 mg/ml. Both ions were diluted with the buffer solution.

Instrumentation. An ABI 270A CE instrument (PerkinElmer, Norwalk, CT) was used. This system was upgraded to the software level of an ABI 270A-HT model to allow controlled sampling at various voltages. A PerkinElmer fused silica capillary was used (72 cm x 50 um i.d.). The length to the detection window was 50 cm. The Dionex SP4270 integrator (San Jose, CA) provided the data output.

Electrophoretic Conditions. The method used in this study is similar to a method found

in the literature used to evaluate system suitability.[34] This experiment was performed

manually in a three day time period. At the beginning of the first day the capillary was

cleaned using the following wash routine: 15 minutes 1.0 N NaOH, 15 minutes de-ionized

water, 15 minutes 0.1 N NaOH, 15 minutes buffer. Pre-sampling steps are listed in the Table

5-1. Each rinse procedure was accomplished by flushing the capillary for the times given by

creating a pressure difference of 20 psi between the buffer reservoirs. Each sample set was

followed by a 5 kV electrokinetic injection of the sample for 5 seconds. The separation took

approximately 4.5 minutes at a separation voltage of 30 kV. The ultraviolet adsorption

detector was set to 220 nm. Overall column temperature was held at 30°C. Samples were

run consecutively and the column was rinsed for 5 minutes with 0.1 N NaOH and 5 minutes

with the buffer in-between sample sets. Sample sets consisted of 25 injections each.

RESULTS AND DISCUSSION

External vs. Internal Standard Evaluation

A typical electropherogram illustrating the separation of caffeine and theophylline is

depicted in Figure 5-1. Caffeine and theophylline are baseline resolved with migration times

of 2.52 minutes and 2.60 minutes, respectively. Figures 5-2 through 5-5 represent the

external standard response results regarding migration time and peak area for 25 injections of

each of the pre-injection rinse cycles outlined in Table 5-1. Figures 5-2 and 5-3 reflect the

migration time reproducibility. The relative standard deviation of migration time is

improved when the sodium hydroxide wash step is omitted from the experimental procedure
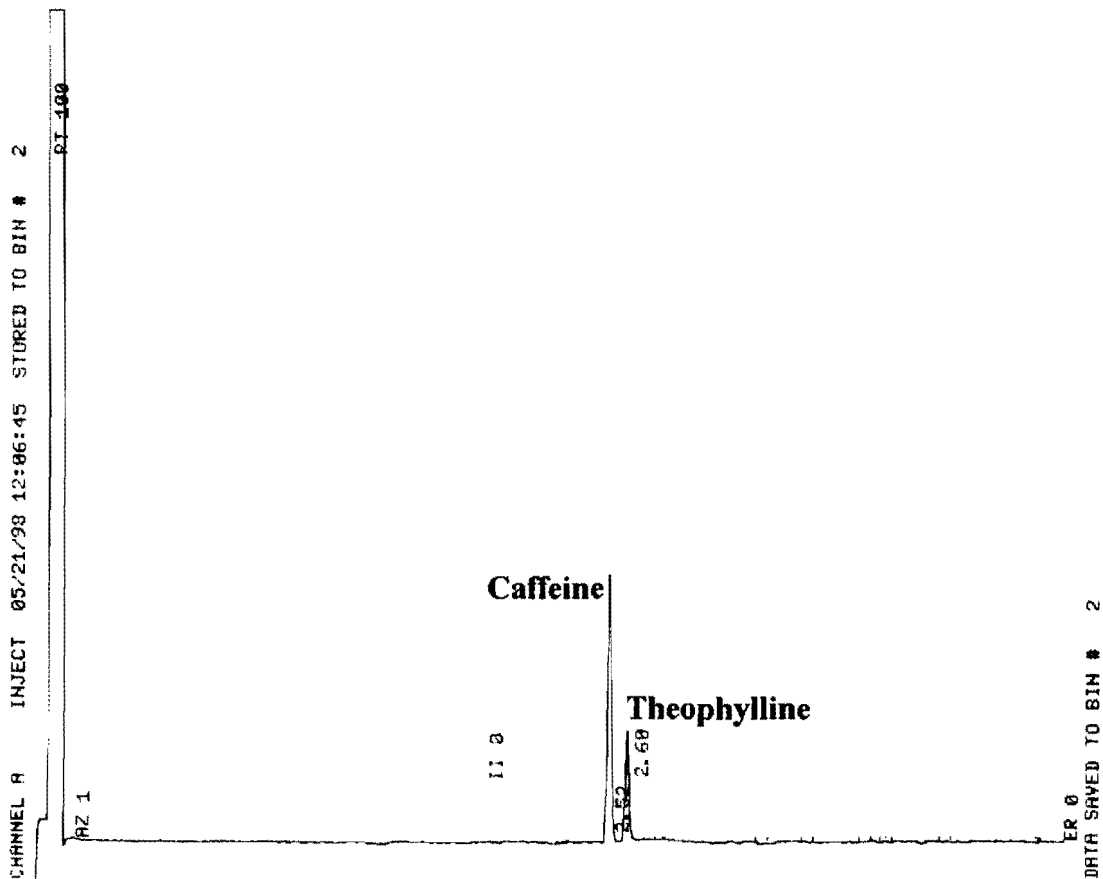
Figure 5-1: Typical separation of caffeine and theophylline. The BGE was a pH 7.5 phosphate buffer. The electrokinetic injection was made at 5 kV, 5 sec and the separation voltage was 30 kV. Detection at 220 nm.

Caffeine
Migration Time
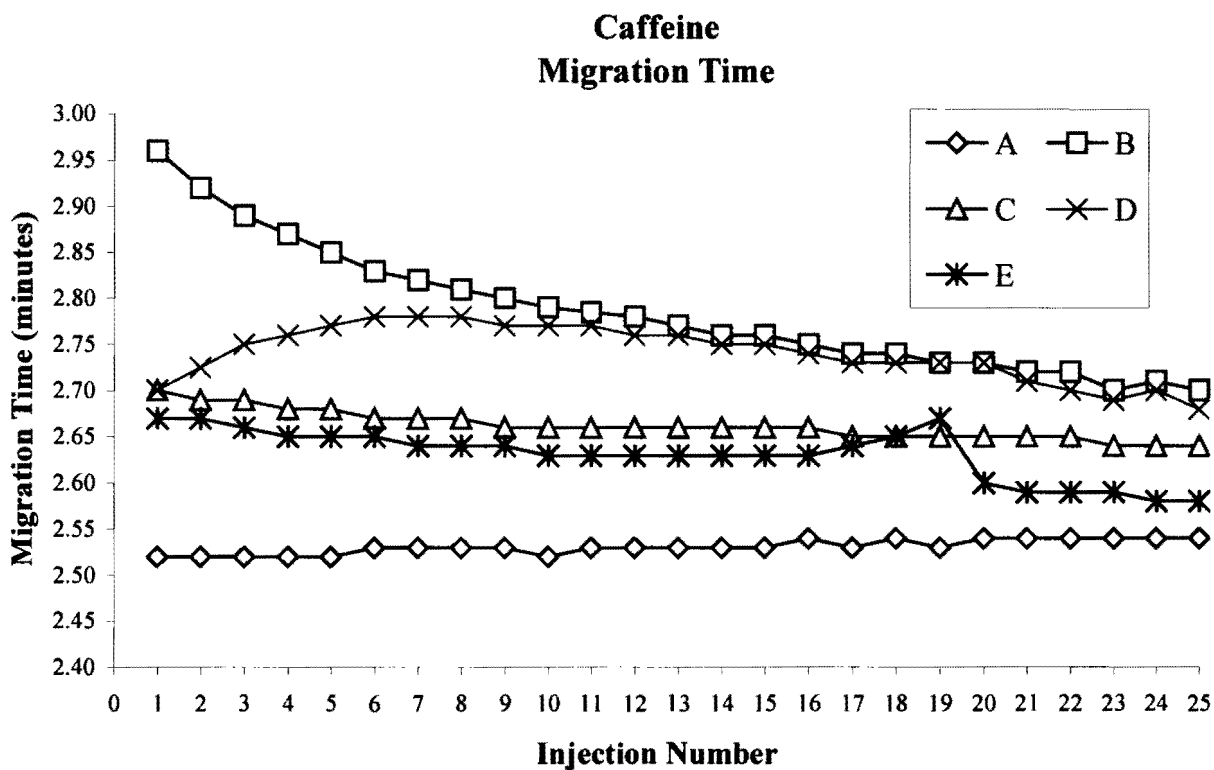
Figure 5-2: Migration time of caffeine for each of the pre-rinse cycles listed in Table 5-1 using external standardization. Relative standard deviation values are as low as 0.30% for system A. System B has the highest amount of variation (2.50%RSD).

Theophylline Migration Time

Figure 5-3: Migration time of theophylline for each of the pre-rinse cycles listed in Table 5-1 using external standardization. Relative standard deviation values are as low as 0.11% for system A. System B has the highest amount of variation (2.85%RSD).

Caffeine
Peak Area
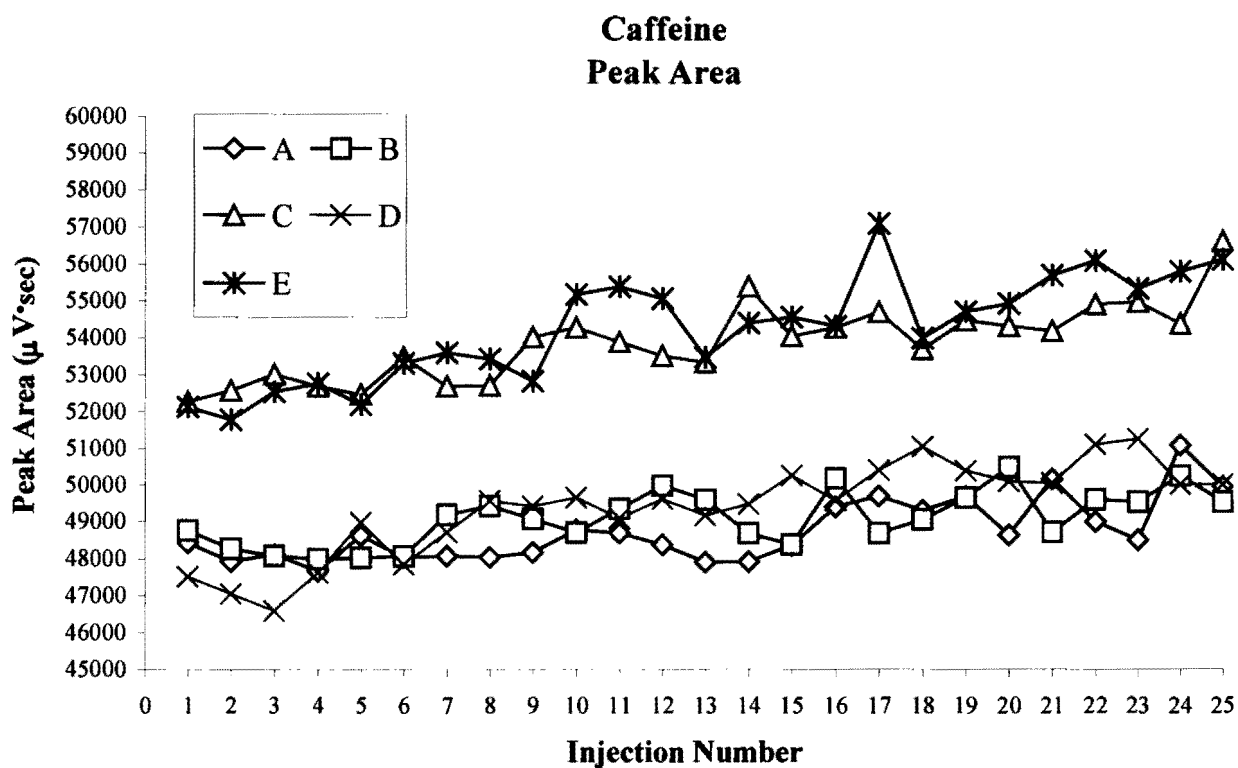
Figure 5-4: Peak area of the neutral marker for each of the pre-rinse cycles listed in Table 5-1 using external standardization. Systems A, B, and D appear to reflect a different sample population than systems C and E.

Theophylline
Peak Area
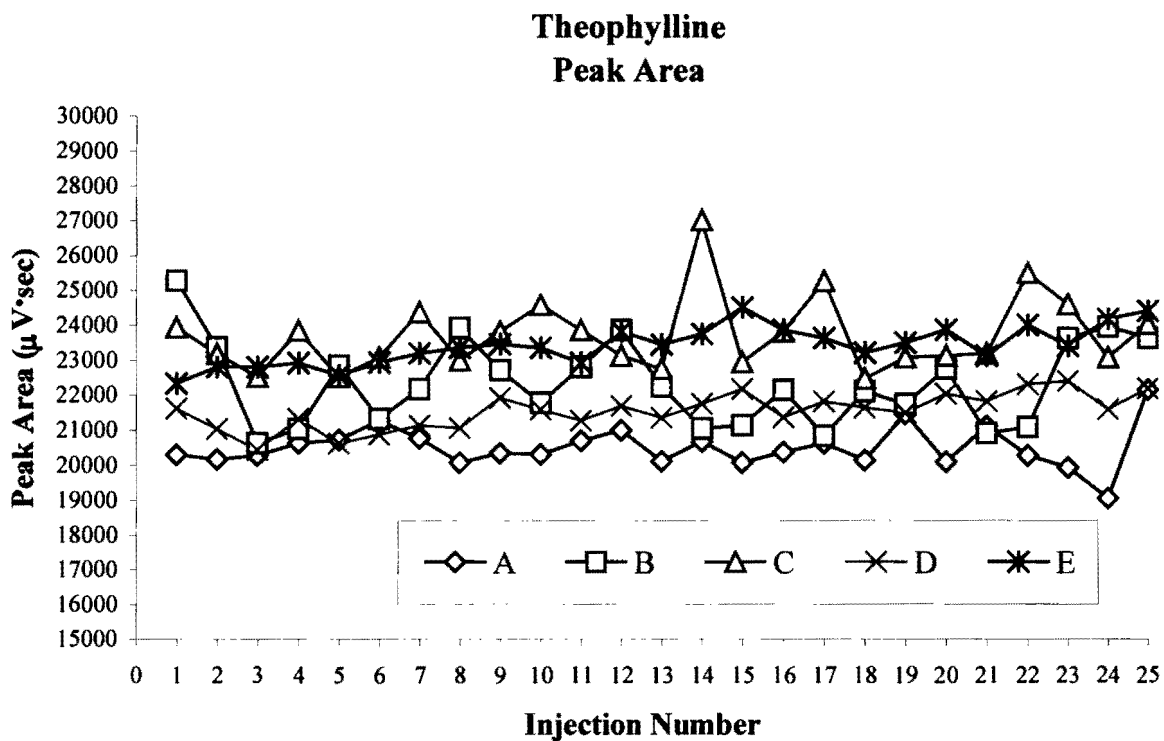
Figure 5-5: Peak area of theophylline for each of the pre-rinse cycles listed in Table 5-1 using external standardization. Sample sets overlap over a rather large range of peak area values.

as illustrated in set A of Figures 5-2 and 5-3. For both caffeine and theophylline, data set A reflects a different reported migration time than sets C and E. Sets C and E reflect similar migration times. After 10 injections, data sets B and D also converge upon similar migration times but report a value different than those obtained for sets A, C, and E. It is hypothesized that each time the 0.1 N NaOH is passed through the column there is a redistribution of the zeta potential along the capillary wall. Wall potential variations would definitely alter the times at which analytes elute because of their contribution to electroosmotic flow. It is also possible that the inner diameter of the capillary is increasing in a non-uniform fashion as the strong base strips the inner surfaces. External migration time relative standard deviation values decrease from 2.50% (Table 5-2, set B) to 0.30% (Table 5-2, set A) for caffeine when the base wash step is eliminated. Theophylline reproducibility values also improved from 2.85% to 0.11% RSD (Table 5-2, sets A and B).

In situations where compounds do not adhere to the capillary wall, it may be concluded that the omission of the wash step drastically improves migration time reproducibility. However, in cases where the wash step is needed, such as when analytes are clinging to the wall surfaces, better reproducibility may be achieved by simply cycling the buffer through the column for longer intervals after the sodium hydroxide wash step is used. Figures 5-2 and 5-3 illustrate the results summarized in Table 5-2 in terms of migration time reproducibility. Table 5-2 (and Figures 5-2 and 5-3) shows that reproducibility values of less than 2% can be obtained provided that the buffer cycling times are increased and external standardization is employed.

Table 5-2: Summary of Averages and Percent Relative Standard Deviations using External Standardization

	External Standardization							
	Caffeine				Theophylline			
Set	MT	%RSD	PA	%RSD	MT	%RSD	Average	%RSD
A	2.53	0.30	48742	1.74	2.60	0.11	20507	2.93
B	2.79	2.50	49097	1.49	2.89	2.85	22360	5.53
C	2.66	0.60	53877	1.93	2.75	0.87	23709	4.54
D	2.74	1.11	49379	2.51	2.85	1.12	21545	2.35
E	2.63	1.05	54280	2.64	2.74	1.09	23415	2.38

Figure 5-6 incorporates the use of caffeine as an internal standard in the evaluation of migration time reproducibility of our five sets of pre-injection conditions. Dividing the migration time attained for theophylline by the migration time of caffeine performs this computation. Internal standardization drastically improves the reproducibility of theophylline migration time values. This is clearly concluded due to the narrow range of y-axis values displayed in Figure 5-6. The migration values for each set average approximately to 1.04 regardless of the pre-injection conditions implemented (Table 5-3). Therefore, it may be concluded that CZE migration time quantitation is independent of the pre-injection rinse requirements as long as internal standards are employed.

Precision obtained by migration time values did not repeat itself in the external evaluation of peak areas illustrated in Figures 5-4 and 5-5. For caffeine, sets A, B, and D appear to reflect a different sample population than systems C and E. All data sets appear to increase with the injection number. The average peak area given in Table 5-2 for set A is 0.43 standard deviations away from the average reported for set B. Therefore, there is only a 33.2% confidence interval suggesting both means are representative of the same statistical population. This confidence interval was determined by first pooling the standard deviations of both populations and then using the z-test to perform the calculation.[88,89] Reproducibility does not appear to be influenced by extended buffering cycles following the sodium hydroxide wash.

Theophylline is approximately half the concentration of caffeine in these solutions. Peak area results for theophylline for pre-injection rinse conditions A-E are shown in Figure 5-5.

**Migration Time of Theophylline
with Caffeine as Internal Standard**
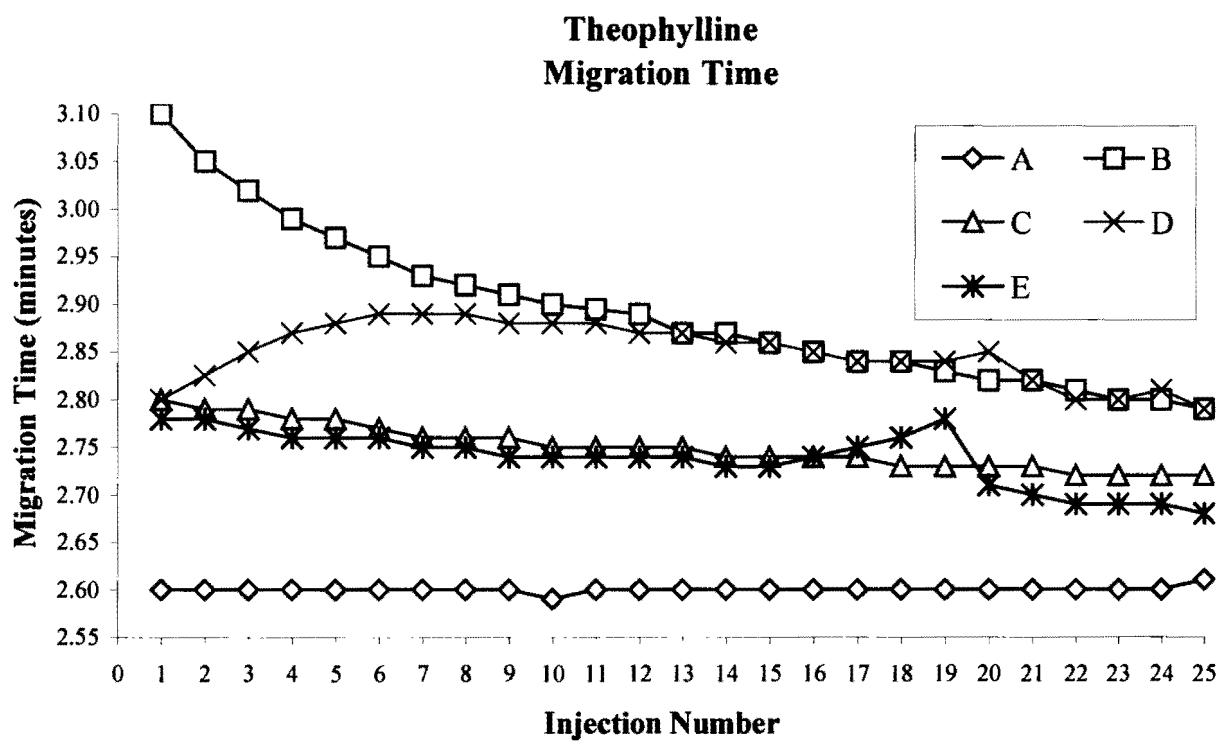
Figure 5-6: Migration time of theophylline for each of the pre-rinse cycles listed in Table 5-1 using caffeine as the internal standard. Relative standard deviation values are all less the 0.40%.

Table 5-3: Summary of Averages and Percent Relative Standard Deviations using Internal Standardization

Set	Internal Standardization of Theophylline			
	MT	%RSD	PA	%RSD
A	1.03	0.28	0.42	3.27
B	1.04	0.37	0.46	5.11
C	1.03	0.32	0.44	3.91
D	1.04	0.15	0.44	1.77
E	1.04	0.15	0.43	2.03

*Caffeine was used as the internal standard.

Sample sets overlap over a rather large range of peak area values. The confidence interval

could not be calculated for sets A and B of theophylline because the standard deviations of

the two means given were not homogenous. Relative standard deviation values increased

from 2.93% to 5.53% (Table 2, sets A and B) with the addition of the wash step using the

external standardization technique. It can be deduced from Table 5-2 and Figure 5-5 that

there is a decrease in %RSD in regards to peak area when longer buffering cycles are used

after the 0.1 N NaOH wash step (Figure 5-5, set C and D data). However, this cannot be

assumed a conclusive observation because the same trend was not seen for caffeine using this

method of quantitation (Table 5-2, Figure 5-4).

Figure 5-7 incorporates the use of caffeine as an internal standard in the evaluation of

peak area reproducibility of our five sets of pre-injection conditions outlined in Table 5-1.

As seen previously with respect to the results provided for migration time, the internal

standardization technique provides a narrow range of y-axis values in which the area ratios

overlap consistently. In each set the average area ratio obtained approximates 0.44. The

ratio is calculated by dividing the peak area obtained for theophylline by the area of caffeine.

Therefore, it can once again be concluded that the use of internal standardization allows CZE

peak area quantitation to be independent of the pre-injection rinse requirements. However,

even when internal standardization of peak areas was utilized, relative standard deviations

did not remain less than 2%. This possibility is noted in previous discussions of this

quantitation method.[46,82] Results are exemplified in Table 5-3.
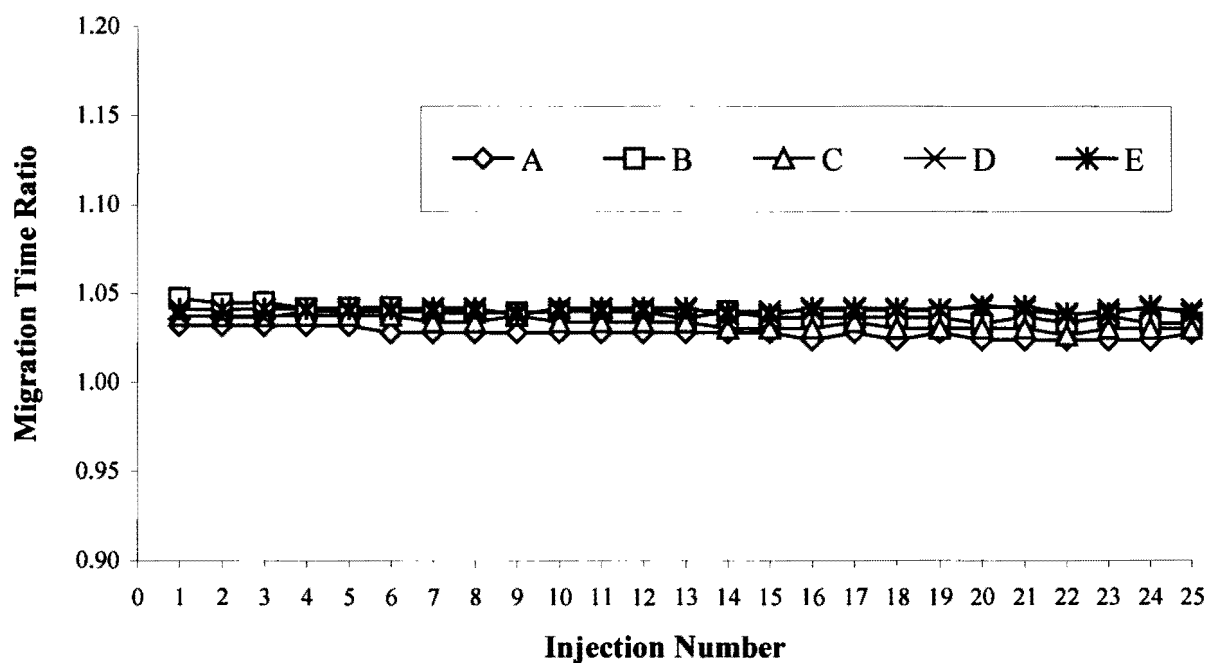
**Theophylline Area
with Caffeine as Internal Standard**

Figure 5-7: Peak area of theophylline for each of the pre-rinse cycles listed in Table 5-1 using caffeine as the internal standard. Average value of each set approximates 0.44 while relative standard deviation values range from 1.77% (set D) to 5.11% (set B).

Evaluation of Corrected Peak Area

The use of corrected peak area as defined by Equation 5-1 is graphically represented in

Figures 5-8 and 5-9 for caffeine and theophylline for pre-injection conditions A-E. The use

of this quantitation technique does not show significant improvement in comparison to

external standardization (Figures 5-4 and 5-5). In Figure 5-8, data sets B and D appear to

reflect a different sample population than sets C and E. The same is true of set A. In Figure

5-9, sample sets are also shown to overlap a wide range of values along the y-axis. Also,

relative standard deviation values regarding peak area reproducibility have increased for

most sample sets. This is illustrated in a comparison between external and corrected peak

areas (Tables 5-2 and 5-4). Percent relative standard deviation values for sets B-E using

external standardization are lower than values obtained using corrected peak area for both

caffeine and theophylline. The only time corrected peak area appeared to increase measured

precision is in data set A and, as seen in Figure 5-2, this is the data set with the most

consistent migration time values recorded per separation. Therefore, it may be concluded

that corrected peak area has produced relatively no significant improvement in comparison to

external standardization. This may be due to the fact that electrokinetic injection was

implemented in this study. Corrected peak areas are normally used to adjust for mobility

biases obtained during the CZE separation. However, it is believed that the biases imposed

by using electrokinetic injection cancel those exhibited due to migration speeds as the

analytes pass the detector window.[54] It may also be included that the use of a sodium

hydroxide wash step adds variability in the peak area/ migration time results obtained.

Caffeine
Corrected Peak Area
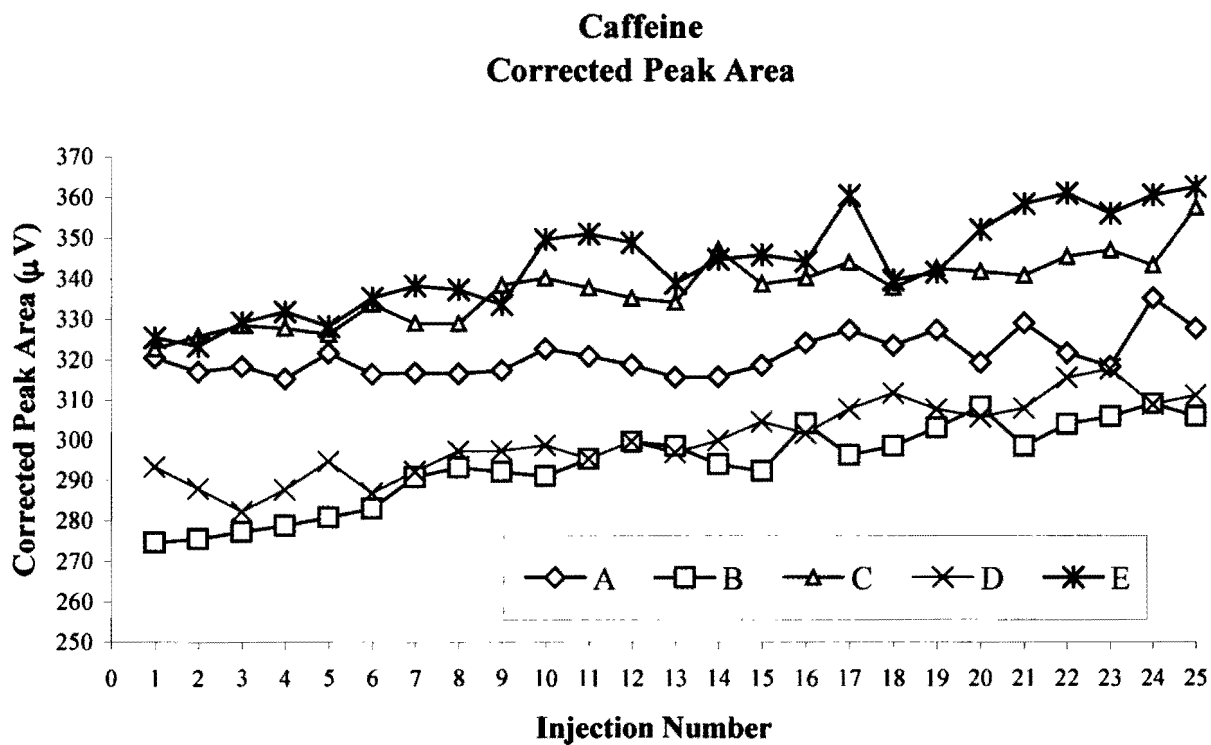
Figure 5-8: Corrected peak area of caffeine for each of the pre-rinse cycles listed in Table 5-1 using corrected peak area values. Sets B and D appear to reflect a different sample population than sets C and E. The same is true of set A.
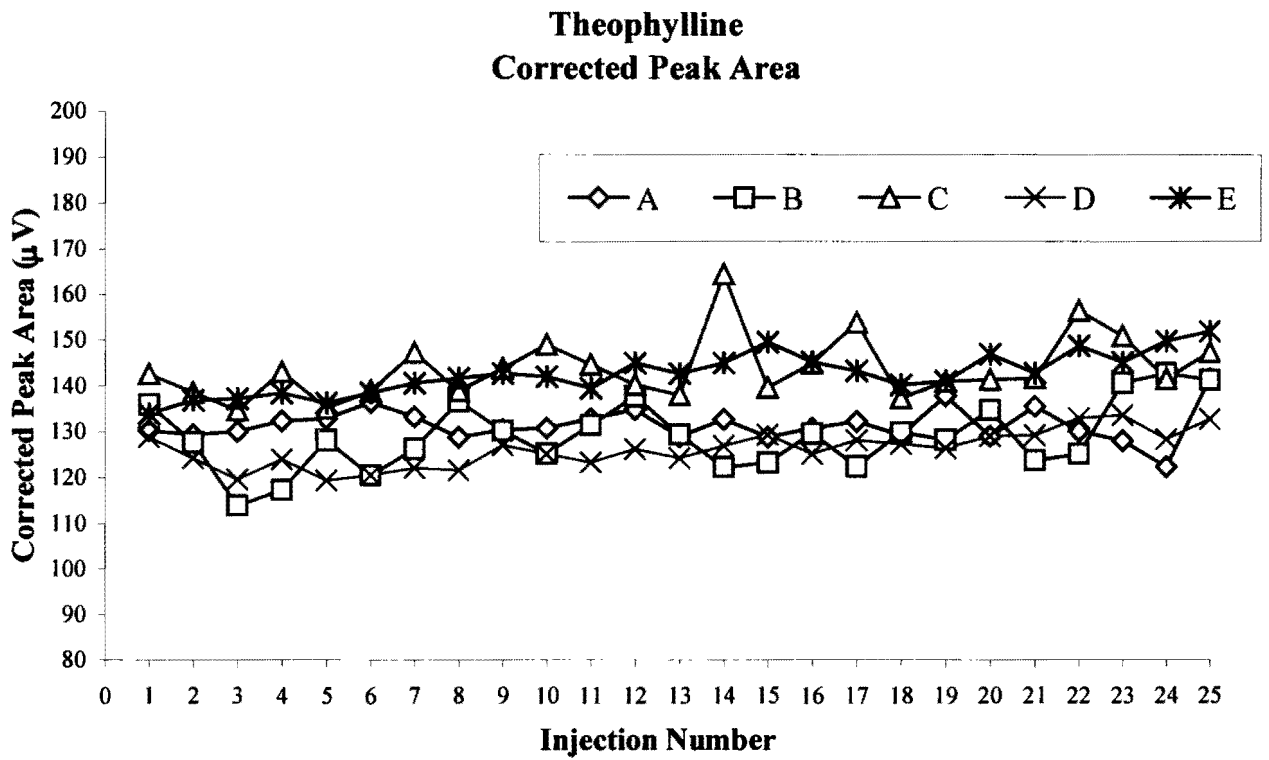
Figure 5-9: Peak area of theophylline for each of the pre-rinse cycles listed in Table 5-1 using corrected peak area values. Sample sets overlap over a large range of peak area values.

Table 5-4: Summary of Averages and Percent Relative Standard Deviations using Corrected Peak Areas

	Corrected Peak Area			
	Caffeine		Theophylline	
Set	Average	%RSD	Average	%RSD
A	321	1.59	131	2.87
B	294	3.56	129	5.76
C	337	2.45	144	4.84
D	300	3.10	126	3.10
E	344	3.47	143	3.22

Evaluation of Internal Area Normalization

Of all the quantitation methods implemented in this study, internal area normalization has

given the best results in terms of ascertaining the mean value of the statistical population

regardless of pre-injection rinse conditions for both caffeine and theophylline. In order to

obtain these results, peak areas were subjected to the calculation outlined in Equation 5-2.

The narrow range of y-axis results confirming this observation is illustrated in both Figures

5-10 and 5-11 for both caffeine and theophylline. In each of these graphs, the average values

for both caffeine and theophylline approximate 0.70 and 0.30 consistently and regardless of

pre-injection column conditioning. Table 5-5 represents the summary of average and relative

standard deviation values of the five data sets. The guideline proposed by Altria suggests

reproducibility values of less than 2% RSD as acceptable in terms of CZE quantitation.[45]

Internal area normalization allows the approach of such measurements with the exception of

data sets A-C for theophylline. The slight increases in these %RSD values are unexplained,

however it is possibly an artifact of using a data system originally designed for HPLC for

CZE. The same may have been true for the results regarding internal standardization.

Conclusions

As a result of this study we conclude that for our samples, pre-injection rinsing conditions

are irrelevant when internal standardization or internal area normalization are utilized. If

these methods are not implemented, better results may be obtained by omitting the NaOH

wash step if at all possible. In cases where compounds adhere to the column walls making

such a wash step necessary, longer buffer rinsing cycles following the basic rinse may

146

Caffeine
Internal Area Normalization
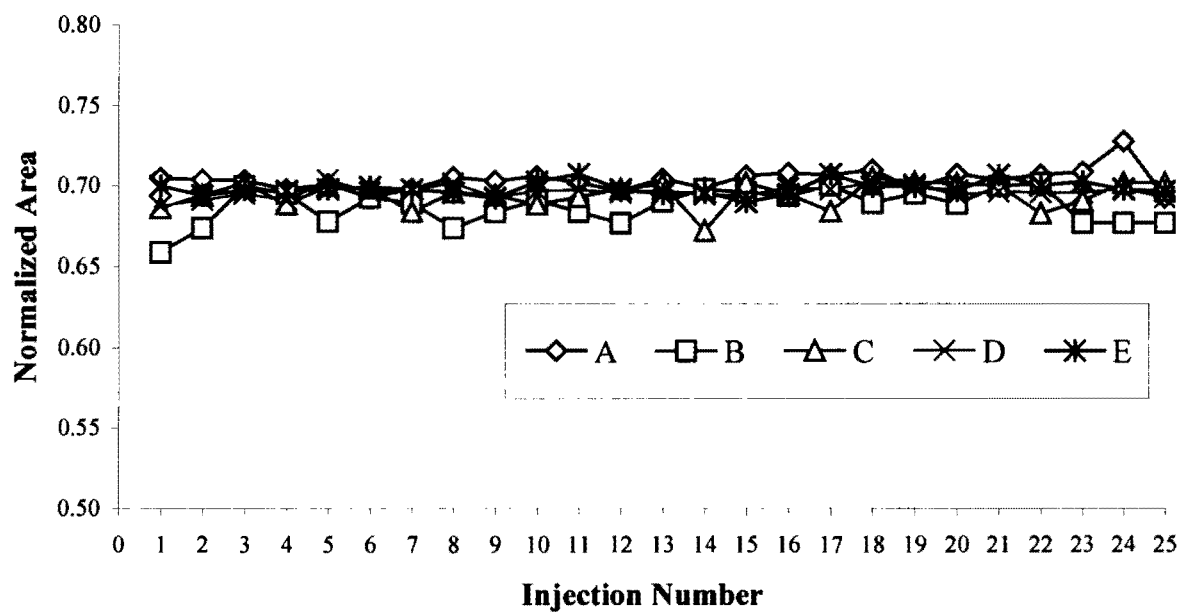
Figure 5-10: Peak area of caffeine for each of the pre-rinse cycles listed in Table 5-1 using internally normalized areas. Average value of each set approximates 0.70 while RSD's range from 0.54% (set D) to 1.58% (set B).
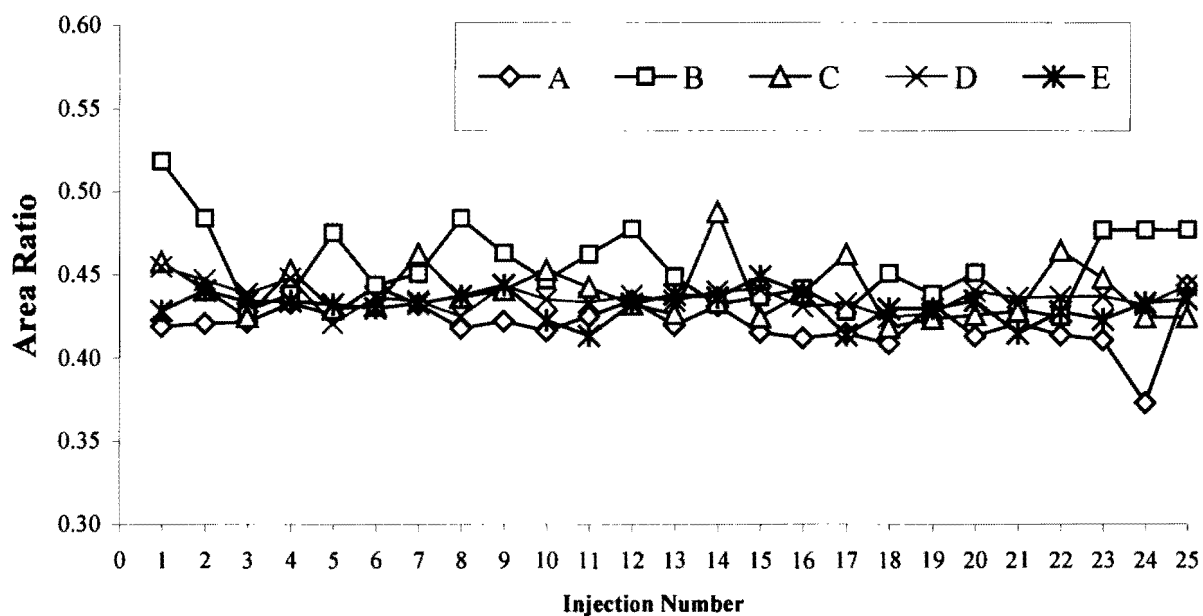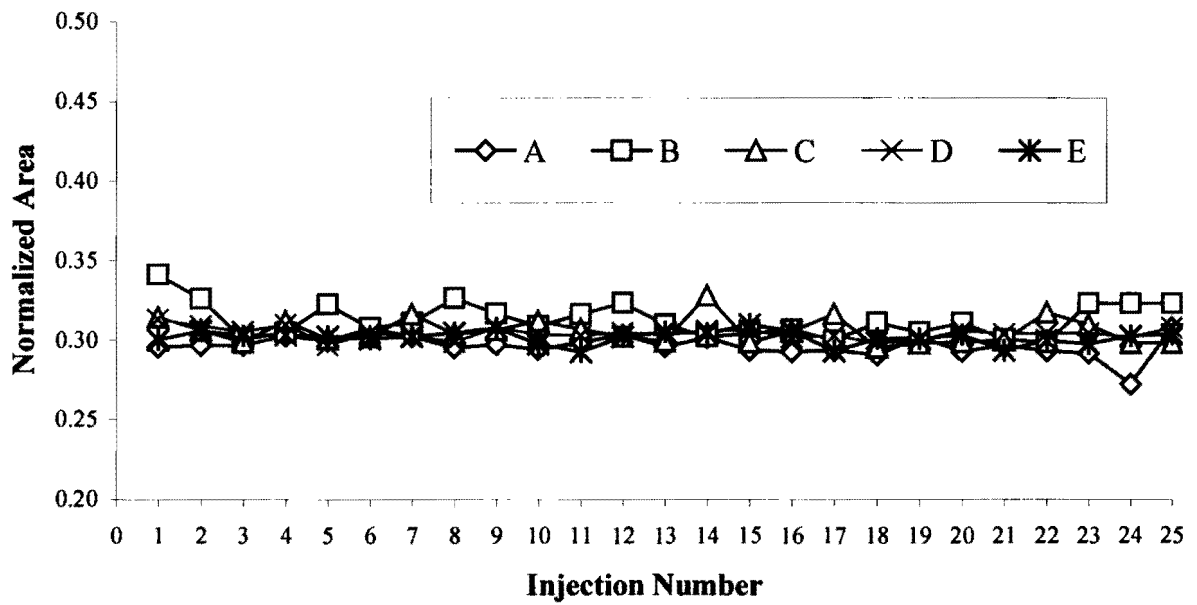
Figure 5-11: Peak area of theophylline for each of the pre-rinse cycles listed in Table 5-1 using internally normalized areas. Average value of each set approximates 0.30 while RSD's range from 1.23% (set D) to 3.48% (set B).

Table 5-5: Summary of Averages and Percent Relative Standard Deviations using Internal Area Normalization

| Set | Internal Area Normalization | | | |
| | Caffeine | | Theophylline | |
	Average	%RSD	Average	%RSD
A	0.70	0.98	0.30	2.33
B	0.69	1.58	0.31	3.48
C	0.69	1.18	0.31	2.68
D	0.70	0.54	0.30	1.23
E	0.70	0.61	0.30	1.42

improve the consistency of separation parameters including migration time and peak area

reproducibility.

Chapter VI

Separation of Bimetallic Ruthenium Complex Isomers

SUMMARY

Capillary zone electrophoresis (CZE) has been employed for the first time in the

separation of bimetallic isomers. Polymetallic complexes are of current interest in the

literature due to their complexity and wide range of potential applicability. The first isomeric

compound to be studied is [Ru(tpy)Cl]$_2$(bpm)$^{2+}$ (tpy = 2,2':6',2"-terpyridine) (bpm = 2,2'-

bipyrimidine). The synthesis and isolation of the isomers were monitored using

electrochemical analysis. Peaks at 1.1 V and 1.4 V confirmed the presence of the bimetallic

complex in both cyclic voltammetry and square wave voltammetry. A shift in the MLCT

band from 618 nm to 610 nm using UV spectroscopy also supported the presence of the *cis*-

[Ru(tpy)Cl]$_2$(bpm)$^{2+}$ and *trans*-[Ru(tpy)Cl]$_2$(bpm)$^{2+}$ configurations. The isomers were then

separated in approximately 4 minutes in a fused-silica capillary column with phosphate

buffer of pH 7.5 at an applied voltage of 20 kV followed by direct UV detection. An

electrophoretic concentration step (stacking) was utilized in order to improve peak shape.

The corresponding *cis* and *trans* isomers of this complex exhibit migration times of 3.45 and

3.94 minutes, respectively.

INTRODUCTION

The separation of transition metal ions by CZE as complexes has proven to be more sensitive than cation determination with indirect UV detection.[106] One of the most common uses of ruthenium in capillary electrophoresis has not only been as a component in a sample matrix but also as a systematic component in on-column detection.[107,108] In past transition metal analyses, much work has been done using complexing agents such as EDTA, polyaminocarboxylate (Quin 2), and hydroxyquinoline-5-sulphonic acid chelating systems in order to increase ion sensitivity.[106,109] Sometimes complexation has even been employed directly on-column as a buffer additive coupled with bi-directional injection techniques.[106,110] Recent studies, however, employ CZE as a powerful technique in the study of isomeric polymetallic complexes. These structures have been of great interest because of their uses as photosynthetic mimics, supramolecular compounds, and chiral and isomeric arrangements.[106] Bimetallic compounds are of interest due to their binding affinity to DNA. The nature of this interest comes from the photochemical processes that these compounds may exhibit when included within the DNA architecture.[106] Over the past twenty years much work has been done in the design of synthetic molecular configurations in order to incorporate suitable components that will yield functional assemblies capable of performing operations such as energy, electron or ion transfer, information storage, or signal transduction.[111-117] The design of such molecules cascades from the overall concept of supramolecular chemistry as it pertains to photochemical processes.

In the design of the ruthenium bimetallic complex, 2,2'-bipyrimidine (bpm) serves as the binding ligand. In 1977, Hunziker and Ludi presented a paper illustrating a series of complexes which could be synthesized using 2,2'-bipyrimidine.[113] The four ligating sites of this molecule (Figure 6-1) lead to ligand bridged compounds of various complexity and various degrees of electron interaction of metal centers.[113] The terminal ligand chosen for this synthesis is 2,2':6',2"-terpyridine (tpy). The tridentate nature of this molecule will form three covalent bonds with each of the ruthenium (II) metal centers. The position of these bonds will give rise to *cis* and *trans* isomers of the bimetallic complex noted by the positioning of the remaining chloride atoms. Although these isomers are of identical charge to mass ratios, separation using CZE is still possible because of the differences in dipole moment. The stronger dipole moment for the *cis* configuration influences the electrical double layer surrounding the ion and the resulting hydrodynamic volume differently from the *trans* isomer. This slight difference is the basis for the separation. Improved separation peak shape is achieved through the use of on-column sample stacking.[2,68,69,118] In this technique the sample is prepared in the same buffer composition as the run buffer but with the buffer components at a slightly lower concentration. The sample ions will migrate very rapidly within the sample plug due to the greater conductivity within the injection zone. Differences in conductivity at the boundary will slow the sample ion movement and allow for on-column concentration. This helps to alleviate peak variance due to detection.

EXPERIMENTAL SECTION

Chemicals. Ru(tpy)Cl$_3$ was previously prepared in the laboratory.[116] 2,2'-Bipymidine was
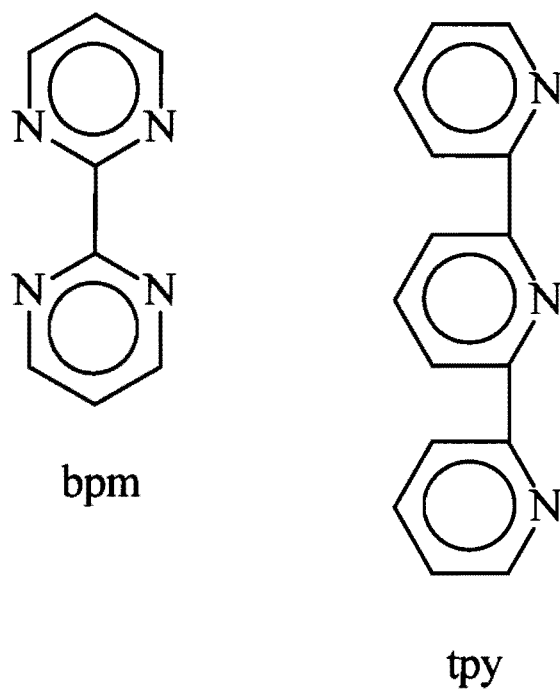
Figure 6-1: 2,2'-Bipyrimidine (bpm) has four ligating sites capable of binding the two ruthenium centers. 2,2': 6',2"-Terpyridine (tpy) was the chosen terminal ligand.

purchased from Lancaster Synthesis. (Windham, NH) Triethylamine was purchased from

Aldrich Chemical Co. (Milwaukee, WI) and Fisher Scientific (Fair Lawn, NJ) supplied the

lithium chloride. Both sodium phosphate monobasic and sodium phosphate dibasic were

received from Fisher Scientific and prepared at concentrations of 0.01 M each using de-

ionized water. The pH 7.5 buffer solution was prepared by mixing monobasic and dibasic

phosphate solutions until the proper pH was measured. This was followed by vacuum

filtration using a 0.45 μm filter. Tetrabutyl ammonium chloride and ammonium

hexafluorophosphate were purchased from Fisher. Tetrabutyl ammonium

hexafluorophosphate was purchased from Lancaster Synthesis and dried in a vacuum oven

for 8 hours. This was stored in a desiccator prior to use as the supporting electrolyte in cyclic

voltammetry. Burdick and Jackson (Muskegon, MI) provided solvents utilized for

electrochemical analysis. These solvents were dried using 4 Å molecular sieves purchased

from Aldrich and activated via standard protocols immediately before use.[116] All other

solvents were of reagent grade or better and purchased from Aldrich. In preparation for UV

and electrochemical analysis, small amounts of sample were diluted in approximately 3 mL

of acetonitrile. The samples used for CZE were prepared at a concentration of 0.21 mg/mL

in the 0.010 M buffer after undergoing a metathesis reaction with tetrabutyl ammonium

chloride.

Instrumentation. Voltammetry data was collected using a BAS CV-50W

Electrochemical Analyzer. The Hewlett-Packard 8452A Diode Array Spectrophotometer

(Agilent, Palo Alto, CA) was used to obtain absorption data. The electrophoresis results

were obtained from an ABI 270A Capillary Electrophoresis (PerkinElmer, Norwalk, CT)

instrument. The separation was performed in a PerkinElmer fused silica capillary (72 cm x 50 μm i.d.) with a detection window length of 50 cm. The Dionex SP4270 integrator (San Jose, CA) provided the data output. Hyperchem version 5.0 software provides a three-dimensional model of the two isomers of the $[Ru(tpy)Cl]_2(bpm)^{2+}$ complex.

Synthesis: A mixture of $Ru(tpy)Cl_3$ (0.410 g, 1.11 mmol), 2,2'-bipyrimidine (bpm) (0.061 g, 0.386 mmol), LiCl (0.020 g, 0.465 mmol), and triethylamine (1 mL) in 4:1 95% ethanol: water (25 mL) was refluxed for 8 hours. The reaction mixture was cooled to room temperature, concentrated to a volume of approximately 5 mL, and filtered. To the filtrate, 4 mL of saturated aqueous NH_4PF_6 was added. The solution was re-filtered and the precipitate was collected. This black precipitate was re-dissolved in acetonitrile (ACN) (3 mL) and re-precipitated by addition to 500 mL of dry diethyl ether. The precipitate was collected using vacuum filtration. The crude yield was 0.427 g. The resulting precipitate (0.012 g) was re-dissolved in a minimum amount of 1:1 ACN: H_2O and the solution was chromatographed using gravity feed flash chromatography. The column was slurry packed with lipophilic Sephadex LH-20 size exclusion resin prepared by the manufacturer's instructions. Elution with 1:1 ACN: H_2O gave a leading grass-green fraction which was collected and dried. The later eluting red fraction, the monometallic complex, was not collected. Cyclic and square wave voltammetry confirmed the presence of the bimetallic ruthenium complex. A small portion of the green fraction collected after separation on the SEC column described above was rotovapped to dryness and re-dissolved in acetone. Three milliliters of saturated tetrabutyl ammonium chloride was added to precipitate the chloride salt. The resulting metathesis reaction permitted the precipitated complex to dissolve in the

0.010 M phosphate buffer solution for capillary electrophoresis. The remaining portion of the collected green band was submitted to further purification. The two isomers were obtained by dissolving the green bimetallic complex in the smallest amount of 1:1 ACN: CH_3OH solution. This solution was chromatographed on an alumina column using 1:1 ACN: CH_3OH. Small fractions of the broad green band were collected. An orange impurity eluted in the region between the two isomers. Each fraction was monitored using visible spectroscopy. The fractions contaminated with the orange band were discarded. Voltammetry and UV spectroscopy were performed on the front (isomer A) and back (isomer B) ends of the elution band.

Electrophoretic Conditions. The capillary was cleaned using the following hydrodynamic wash routine at 20 psi: 15 minutes 1.0N NaOH, 15 minutes de-ionized water, 15 minutes 0.1N NaOH, 15 minutes buffer.[2] Sample was injected electrokinetically at 10 kV for 5 seconds. The separation took approximately 4.0 minutes at a separation voltage of 20 kV. Absorbance was measured at 308 nm. Overall column temperature was held at 30°C.

RESULTS AND DISCUSSION

The reaction scheme describing the synthesis of $[Ru(tpy)Cl]_2(bpm)^{2+}$ is illustrated in Figure 6-2. Ruthenium (III) terpyridine trichloride was combined in a 4:1 ratio with 2,2'-bipyrimidine in 4:1 ethanol: water. The ratios and solvent were chosen to encourage formation of the bimetallic complex. Triethylamine was added to reduce Ru^{3+} to Ru^{2+}. The ruthenium (II) ion is more labile and will allow the rapid substitution of the chloride ligands.

$Ru(tpy)Cl_3 + bpm \quad [Ru(tpy)Cl](bpm)^+$ (red monometallic complex)

$[Ru(tpy)Cl](bpm)^+ + Ru(tpy)Cl_3 \quad [Ru(tpy)Cl]_2(bpm)^{2+}$
(green bimetallic
complex)

Figure 6-2: Reaction scheme for the bimetallic ruthenium complex.

Excess lithium chloride was added in order to prohibit replacement of the remaining chlorides with aqua groups, avoiding the complex acid/ base equilibria of the coordinated aqua ligands.

Cyclic voltammetry was performed on aliquots of the reaction mixture throughout the synthesis in order to monitor the reaction. Figures 6-3a and 6-3b confirm the formation of the bimetallic complex. Peaks occurring at 1.1 V and 1.4 V represent each ruthenium atom reversibly oxidizing from a +2 to a +3 ion, respectively. The Osteryoung square wave voltammetry shown in Figure 6-3b has three peaks. In square wave voltammetry the current is measured at different parts of the square wave to give the effect of taking the first derivative of what you would expect to see in a linear sweep voltammogram.[119] The first peak at 1.1 V is the first ruthenium ion oxidizing from a +2 to a +3 oxidative state. The second ruthenium transition will occur at a higher potential due to inductive effects of the first oxidation. This transition at 1.4 V is seen as a doublet. The *cis* and *trans* positioning of the remaining chloride groups slightly alter the potential of the second transition. This indicates that there is more than one isomer in the bimetallic complex. Isomer purification of the heterogeneous green band was performed using a 1:1 mixture of methanol and acetonitrile on an alumina column.

Square wave voltammetry (Figures 6-4a and 6-4b) confirmed the isolation of the *cis* and *trans* isomers as illustrated by small shifts in the recorded Ep values. Additional peaks included in Figure 6-4b are attributed to sample contamination. The likely contaminant is $[Ru(tpy)_2]^{2+}$ since it has the same charge type and oxidizes in this potential region. Small

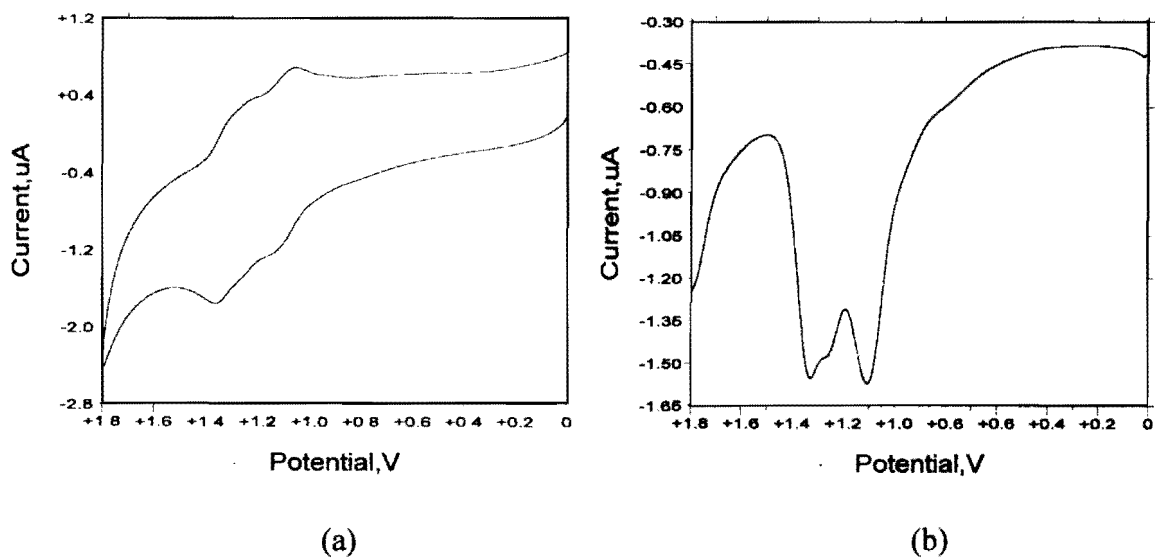**Figure 6-3:** (a) Cyclic voltammetry of the bimetallic complex before isomer purification. (b) Square wave voltammetry presents a clearer representation of the oxidation described.
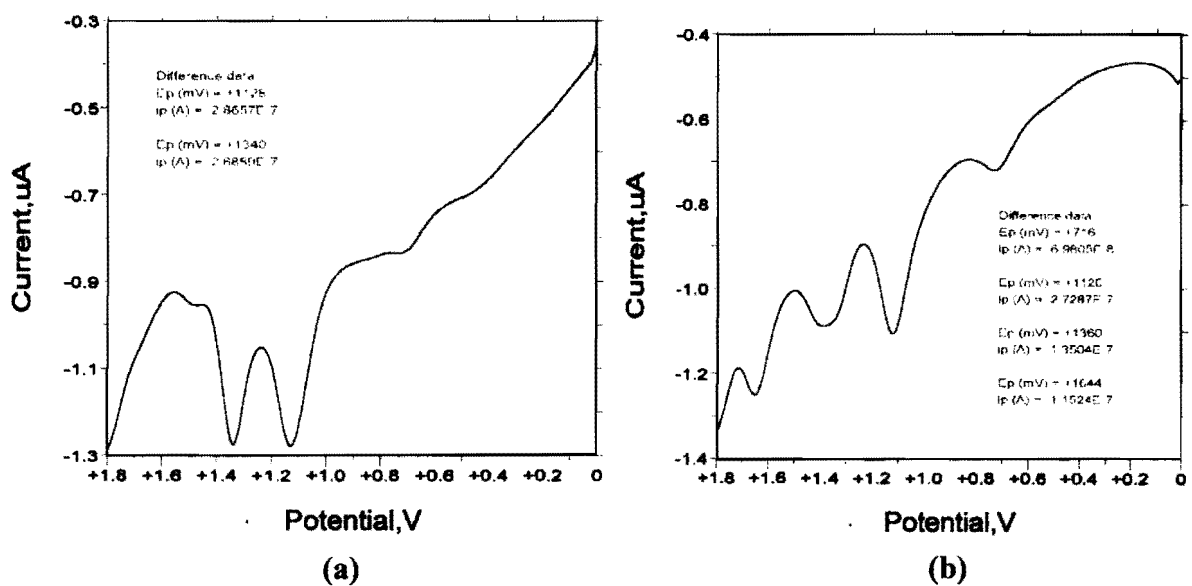
Figure 6-4: Square wave voltammetry of the (a) front and (b) back ends of the broad green elution band from the alumina column after removal of orange contaminates. The solvent consisted of a 1:1 CH₃OH: ACN mixture.

differences at approximately 1.4 V in peak shape and potential are due to the differences in polarity between the *cis*-[Ru(tpy)Cl] $_2$(bpm)$^{2+}$ and *trans*-[Ru(tpy)Cl] $_2$(bpm)$^{2+}$ configurations.

UV spectroscopy was used to confirm the presence of the two isomers, as seen by the slight shift in the MLCT band from 618 nm to 610 nm, as illustrated in Figure 6-5. Again, this shift is due to the two different arrangements of the isomers. The *cis* conformation contributes a net dipole to the overall structure. More work is needed to confirm the *cis/ trans* identities of isomers A and B. Geometrically optimized space-filling models of the *cis*-[Ru(tpy)Cl]$_2$(bpm)$^{2+}$ and *trans*-[Ru(tpy)Cl]$_2$(bpm)$^{2+}$ complexes are depicted in Figure 6-6.

Another method of isolating the isomers in the heterogeneous green band invoked the use of CZE. CZE typically separates compounds on the basis of differences in the ratio of charge to hydrodynamic volume. In the case of the ruthenium isomers this ratio is a constant value. However, the differences maintained by bond polarity are adequate to obtain a separation. Hypothetically, the additional polarity experienced by the *cis*-[Ru(tpy)Cl] $_2$(bpm)$^{2+}$ should allow it to reach the detector before the *trans*-[Ru(tpy)Cl] $_2$(bpm)$^{2+}$ configuration. (Figure 6-7) Further work needs to be completed in an effort to confirm the proposed elution order. Peak shape was maintained by preparing the sample in a buffer that was slightly less concentrated than that of the run buffer. Differences in conductivity over the injection plug would allow on-column concentration of the analyte due to sample stacking.
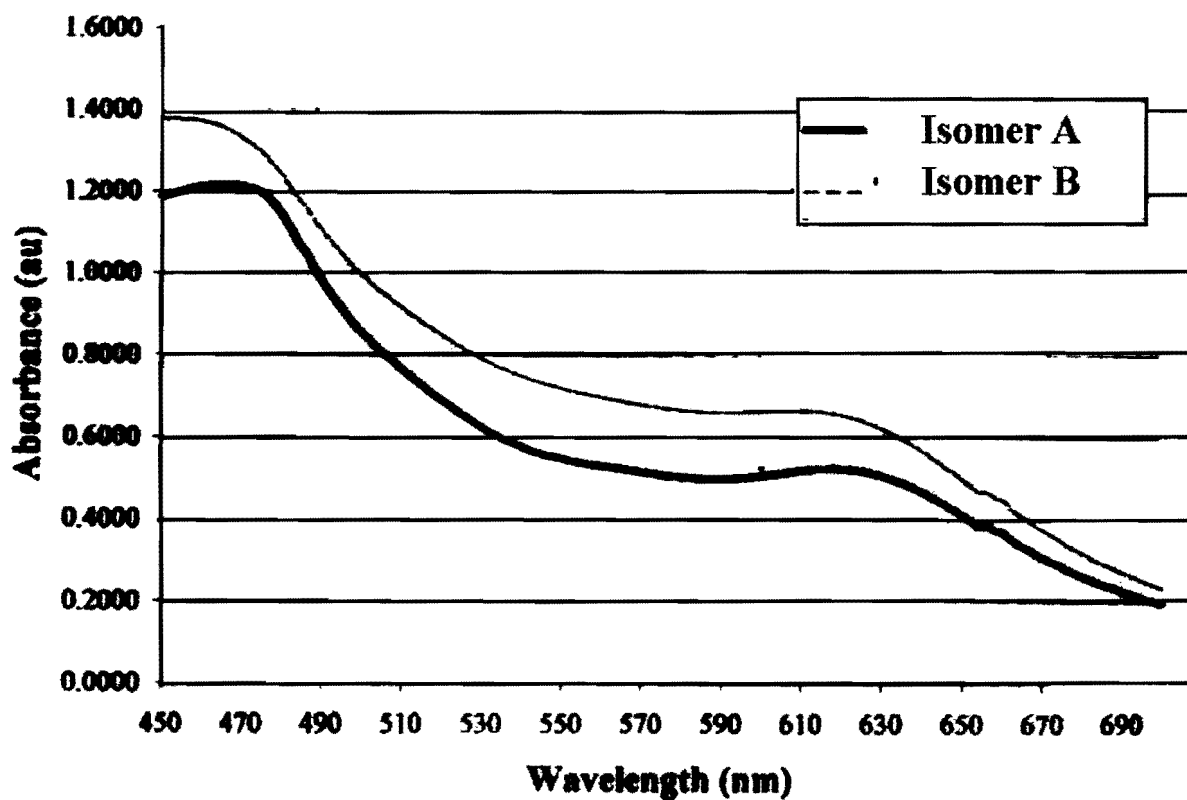
Figure 6-5: UV confirmation of the presence of the two isomers is seen by the small shift in the MLCT band from 618 nm to 610 nm.
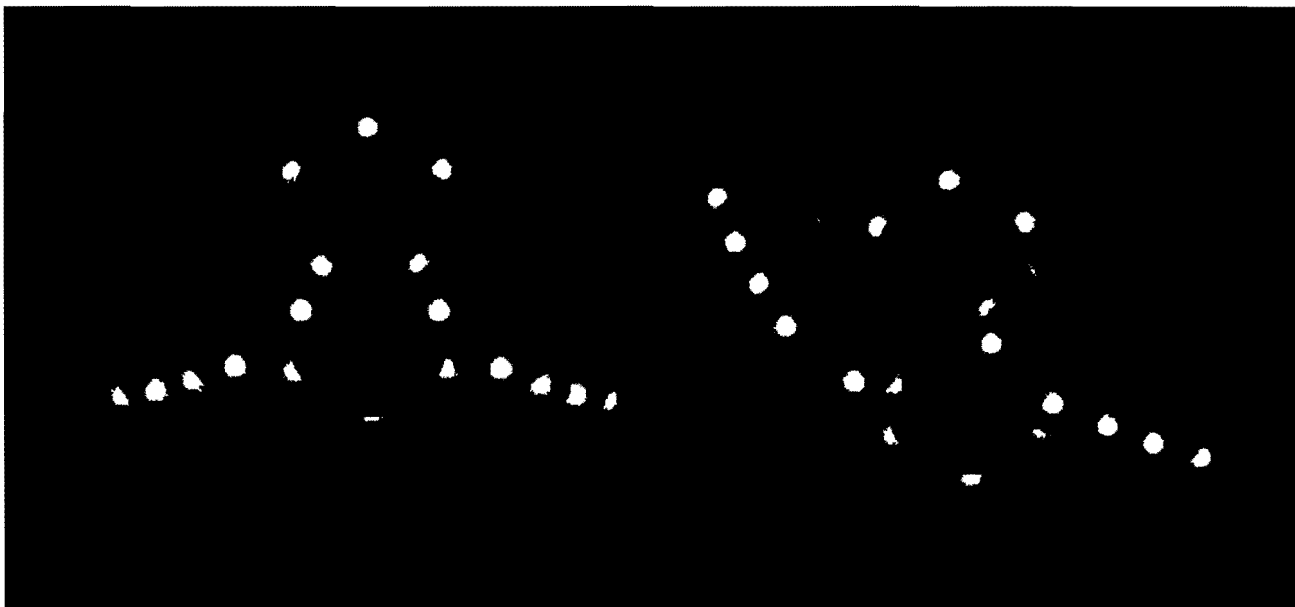
Figure 6-6: Three-dimensional model of the *cis* and *trans* isomers of the Ru(tpy)Cl]$_2$(bpm)$^{2+}$ complex.
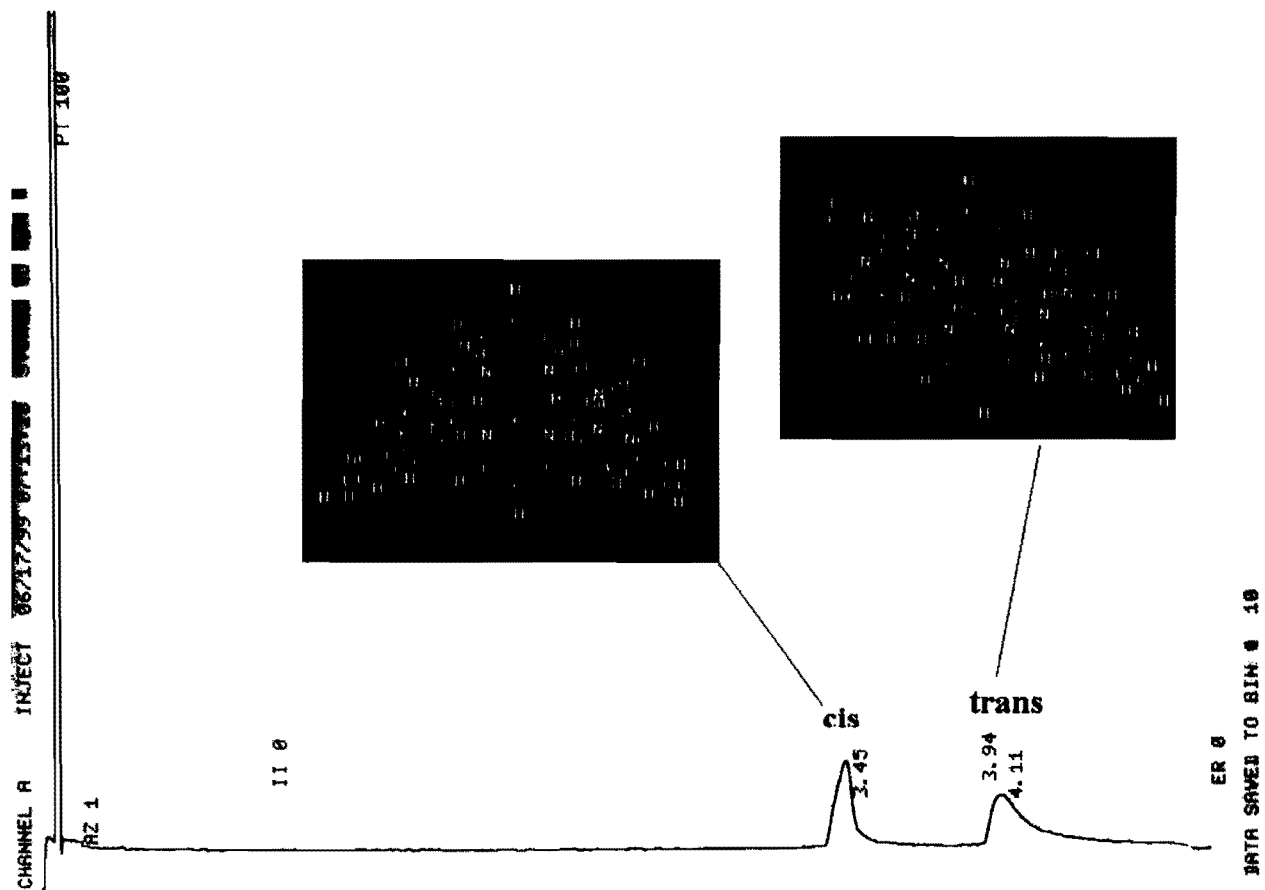
Figure 6-7: Capillary electropherogram of bimetallic ruthenium complex isomer mixture. More work need to be done to confirm the assigned peaks.

165

Conclusions

Capillary electrophoresis has been proven to be a powerful technique in the analysis of isomeric polymetallic complexes. In instances where differences in polarity exist, capillary electrophoresis may be used as a means of analyte identification and separation. Strong chromophores such as those present in 2,2':6'2''-terpyridine will enhance on-column detector sensitivity especially when used in conjunction with sample stacking. The use of this type of ligand increases the number of possible products which may be synthesized using 2,2'-bipyrimidine as the binding ligand. Future work will include incorporating these structures within the DNA double helix. Perhaps then capillary electrophoresis may be employed in the determination of DNA binding constants.[120]

Chapter VII

Overall Conclusions

Electrokinetic sampling has been evaluated as it pertains to method validation protocol using capillary zone electrophoresis. Factors affecting reproducibility of injection plug lengths, migration times, and peak areas for caffeine and theophylline have been studied. Longer sampling times and higher sampling voltages result in better reproducibility values. However, the extent to which these values can be increased is limited by concentration gradient formation in the diffuse layer surrounding the capillary-electrode-solution interface. Mathematical models, such as that developed by Otsuka and Terabe for predicting maximum injection plug lengths were extended in order to incorporate analyte mobility.

A new method of determining analyte mobility has also been developed. Graphical mobility analysis (GMA) offers a new and unique approach of calculating analyte mobility values with greater precision. GMA has also lead to better assessment of buffering systems using electrophoretic mobility plots during the method development process. Here, the need for proper functioning buffers at the requisite pH values was emphasized.

Further experimentation was done regarding migration time and peak area reproducibility as influenced by electrokinetic sampling for differing sodium hydroxide pre-injection procedures. Much of the literature corresponding to method development in capillary zone electrophoresis describes sodium hydroxide rinse cycles as important steps in preparation for injection and analysis. Five different pre-injection conditions and four different quantitation

techniques have been evaluated as they affect the overall separation performance of caffeine and theophylline using capillary zone electrophoresis with electrokinetic injection. When quantitation methods such as internal standardization or internal area normalization are used, pre-injection rinsing conditions are irrelevant. With external standardization and corrected peak areas, better results may be obtained by omitting the sodium hydroxide wash step if at all possible. It is suggested that in cases where compounds adhere to the column walls making such a wash step necessary, longer buffer rinsing cycles following a sodium hydroxide rinse may improve the consistency of separation parameters including migration time and peak area reproducibility.

With a better understanding of electrokinetic injection, theories were tested as capillary zone electrophoresis was employed for the first time in the separation of bimetallic isomers. Polymetallic complexes are of current interest in the literature due to their complexity and wide range of potential applicability. The first isomeric compound to be studied is $[Ru(tpy)Cl]_2(bpm)^{2+}$ (tpy = 2,2':6',2"-terpyridine) (bpm = 2,2'-bipyrimidine). The synthesis and isolation of the isomers were monitored using electrochemical analysis. Peaks at 1.1 V and 1.4 V confirmed the presence of the bimetallic complex in both cyclic voltammetry and square wave voltammetry. A shift in the MLCT band from 618 nm to 610 nm using UV spectroscopy also supported the presence of the cis-$[Ru(tpy)Cl]_2(bpm)^{2+}$ and $trans$-$[Ru(tpy)Cl]_2(bpm)^{2+}$ configurations. The isomers were separated using a fused-silica capillary column with phosphate buffer of pH 7.5 at an applied voltage of 20 kV followed by direct UV detection. An electrophoretic concentration step (stacking) was utilized in order to improve peak shape. The corresponding cis and $trans$ isomers of this complex exhibit

migration times of 3.45 and 3.94 minutes. Further work needs to be completed in an effort to confirm the proposed elution order.

The applicability of capillary zone electrophoresis covers a wide range of separation possibilities. It is our hope that the work presented here regarding the fundamental aspects of electrokinetic sampling will provide further motivation for the use of CZE in an ever-increasing number of validated methods for industrial and pharmaceutical analysis. In the future, the same methodology defined by the scope of this dissertation, can be used to improve reproducibility in areas where electrokinetic sampling is the preferred method of injection. This would include applications involving capillary gel electrophoresis (CGE). Projects exploring the integrity of graphical mobility analysis are also warranted. Separations of compounds with multiple pKa values or different buffering systems would test the ruggedness of the GMA assessment of total mobility. Finally, it was stated that more work is needed to identify the elution order of the bimetallic compounds. Perhaps, in the future, CZE will become a routine method of determining mobility constants for these new structural isomers.

Literature Cited

1. Giddings, J.C. *Unified Separation Science;* Wiley and Sons, Inc.: New York, 1991.

2. Weinberger, R. *Practical Capillary Electrophoresis*; Academic Press, Inc.: New York, 1993.

3. Mathews, C.K. and van Holde, K.E. *Biochemistry, 2nd ed.*; Benjamin/ Cummings Publishing Company, Inc.: New York, 1996.

4. Bockris, J. O'M. and Reddy, A.K.N. *Modern Electrochemistry · 1*; Plenum Publishing Corporation: New York, 1970.

5. Mikkers, F.E.P.; Everaerts, F.M.; Verheggen, Th. P.E.M., *J. Chromatogr.* **1979**, *169*, 11.

6. Lee, M.L.; Yang, F.J.; Bartle, K.D. *Open Tubular Column Gas Chromatography: Theory and Practice*: Wiley and Sons, Inc.: New York, 1984.

7. Jorgenson, J. and Lukacs, K.D. *Anal. Chem.* **1981**, *53*, 1298.

8. Hjertén, S. *J. Chromatogr.* **1983**, *270*, 1.

9. Hjertén. S. and Zhu, M.-D. *J. Chromatogr.* **1985**, *346*, 265.

10. Terabe, S.; Otsuka, K.; Ichikawa, K.; Tsuchiya, A.; and Ando, T. *Anal. Chem.* **1987**, *59*, 1230.

11. Terabe, S.;Miyashita, Y.; Shibata, O.; Barnhart, E.R.; Alexander, L.R.; Patterson, D.G.; Karger, B.L.; Hosoya, K.; Tanaka, N. *J. Chromatogr.* **1990**, *516*, 23.

12. Cole, R.O.; Sepaniak, M.J.; Hinze, W.L.; Gorse, J.; Oldiges, K. *J. Chromatogr.* **1991**, *557*, 113.

13. Yik, Y.F.; Ong, C.P.; Khoo, S.B.; Lee, H.K.; Li, S.F.Y. *J. Chromatogr.* **1992**, *589*, 333.

14. Yik, Y.F.; Ong, C.P.; Khoo, S.B.; Lee, H.K.; Li, S.F.Y. *Environ. Monit. Assess.* **1991**, *19*, 73.

15. Nishi, H.; Fukuyama, T.; Matsue, M.; Terabe, S. *J. Chromatogr.* **1990**, *513*, 279.

16. Nishi, H. and Matsuo, M. *J. Liq. Chromatogr.* **1991**, *14*, 973.

17. Saltoh, T.; Hoshino, H.; Yotsuyanagi, T. *J. Chromatogr.* **1989**, *469*, 175.

18. Saltoh, T,; Kiyohara, C.; Suzuki, N. *HRC & CC* **1991**, *14*, 245.

19. Saltoh, T.; Hoshino, H.; Yotsuyanagi, T. *Anal. Sciences* **1991**, *7*, 494.

20. Saltoh, T,; Kiyohara, C.; Suzuki, N. *J. High Res. Chromatogr.* **1991**, *14*, 245.

21. Nishi, N.; Tsumagari, N.; Kakimoto, T.; Terabe, S. *J. Chromatogr.* **1989**, *465*, 331.

22. Ong, C.P.; Ng, C.L.; Lee, H.K.; Li, S.F.Y. *J. Chromatogr.* **1991**, *559*, 537.

23. Burton, D.E.; Sepaniak, M.J.; Maskarined, M.P. *J. Chromatogr. Sci.* **1986**, *24*, 347.

24. Fujiwara, S.; Iwase, S.; Honda, S. *J. Chromatogr.* **1988**, *447*, 133.

25. Ong, C.P.; Ng, C.L.; Chong, N.C.; Lee, H.K.; Li, S.F.Y. *J. Chromatogr.* **1991**, *547*, 419.

26. Weinberger, R.; Sapp, E.; Moring, S. *J. Chromatogr.* **1990**, *516*, 271.

27. Gassman, E.; Kuo, J.E.; Zare, R.N. *Science*, **1985**, *346*, 263.

28. Olivares, J.A.; Nguyen, N.T.; Yonker, C.R.; Smith, R.D. *Anal Chem.* **1987**, *59*, 1230.

29. Wallingford, R.A. and Ewing, A.G. *Anal. Chem.* **1987**, *59*, 1762.

30. Kuhr, W.G. and Yeung, E.S. *Anal. Chem.* **1988**, *60*, 1832.

31. Beale, S.C. *Anal. Chem.* **1998**, *70*, 279R.

32. Masterson, W.L. and Hurley, C.N. *Chemistry Principles and Reactions*; Saunders Publishing Company, Inc.: New York, 1989.

33. Bard, A.J. and Faulkner, L.R. *Electrochemical Methods: Fundamentals and Applications*; John Wiley and Sons, Inc.: New York, 1980.

34. Rasmussen, H.T. *Electrokinetic Separations in Fused Silica Capillaries;* Virginia Polytechnic Institute and State University: Blacksburg, 1990.

35. Skoog, D.A.; Leary, J.J. *Principles of Instrumental Analysis, 4th ed.;* Saunders: Fort Worth, TX, 1992.

36. Weinberger, R. *Practical Capillary Electrophoresis;* CE Technologies: New York, 1997.

37. Heiger, D. *High Performance Capillary Electrophoreseis, 2nd ed.*; Hewlett-Packard Company: France, 1992.

38. Valkó, I.E.; Sirén, H.; Riekola, M.L.; Jumppanen, J.H. *J. Microcolumn Separations*, **1996**, *8*, 421.

39. Lin, C.E.; Chang, C.C.; Lin, W.C. *J. Chromatogr. A* **1997**, *768*, 105.

40. Cross, R.F. and Cao, J. *J. Chromatogr. A* **1998**, *809*, 159.

41. Li, D.; Fu, S.; Lucy, C.A. *Anal Chem.* **1999**, *71*, 687.

42. Lin, C.E.; Lin, W.C.; Chiou, W.C.; Lin, E.C., Chang, C.C. *J. Chromatogr. A* **1996**, *755*, 261.

43. Faller, T. and Engelhardt, H. *J. Chromatogr. A* **1999**, *853*, 83.

44. Kunkel, A.; Degenhardt, M.; Schirm, B.; Wätzig, J.; *J. Chromatogr. A* **1997**, *768*, 17.

45. Altria, K.D. and Rudd, D.R. *Chromatographia* **1995**, *41*, 325.

46. Altria, K.D. and Fabre, H. *Chromatographia* **1995**, *40*, 313.

47. Evans, C.E. *Anal. Chem.* **1997**, 69, 2952.

48. Fishman, H.A.; Amudi, N.M.; Lee, T.T.; Scheller, R.H.; Zare, R.N. *Anal. Chem.* **1994**, *66*, 2318.

49. Knox, J.H. and McCormack, K.A. *Chromatographia* **1994**, *38*, 279.

50. Ostuka, K.; Terabe, S. *J. Chromatogr.* **1989**, 480, 91.

51. Shihbabi, Z.K. and Hinsdale, M.E. *Electrophoresis*, **1995**, *16*, 2159.

52. Watzig, H. and Dette, C. *J. Chromatogr.* **1993**, *636*, 31.

53. Rose, D.J. and Jorgenson, J.W. *Anal. Chem.* **1982**, *60*, 642.

54. Qi, S.; Huang, A.; Sun, Y. *Anal. Chem.* **1996**, *68*, 1342.

55. Lee, T.L. and Yeung, E.S. *Anal. Chem.* **1992**, *64*, 1226.

56. Tsuda, T. and Zare, R.N. *J. Chromatogr.* **1991**, *559*, 103.

57. Tsuda, T.; Mizuno, T.; Akiyama, J. *Anal. Chem.* **1987**, *59*, 799.

58. Wallingford, R.A. and Ewing, A.G. *Anal. Chem.* **1987**, *59*, 678.

59. Sziele, D.; Bruggman, O.; Doring, M.; Freitag, R.; Schugerl, K. *J. Chromatogr.* **1994**, *669*, 254.

60. Linahares, M.C. and Kissinger, P.T. *Anal. Chem.* **1991**, *63*, 2076.

61. Pu, Q.S. and Fang, Z.L. *Analytica Chimica Acta*, **1999**, *398*, 65.

62. Bao, L. and Dasgupta, P.K. *Anal. Chem.* **1992**, *64*, 991.

63. Zhou, S.Y.; Zuo, H.; Stobaugh, J.F., Lunte. C.E., Lunte, S.M. *Anal. Chem.* **1995**, *67*, 594.

64. Hogan, B.L.; Lunte, S.M.; Stobaugh, J.F.; Lunte, C.E. *Anal. Chem.* **1994**, *66*, 596.

65. Effenhauser, C.S.; Manz, A. and Widmer, H.M. *Anal. Chem.* **1995**, *67*, 2284.

66. Fang, Q.F.; Wang, F.R.; Wang, S.L.; Liu, S.S.; Xu, S.K.; Fang, Z.L. *Analytica, Chimica, Acta* **1999**, *390*, 27.

67. Dose, E.R. and Guiochon, G.A. *Anal. Chem.* **1991**, *63*, 1154.

68. Burgi, D.S. and Chien, R.L. *Anal. Chem.* **1991**, *63*, 2042.

69. Chien, R.L. and Burgi, D.S. *Anal. Chem.* **1992**, *64*, 1046.

70. Aebersold, R. and Morrison, H.D. *J. Chromatogr.* **1990**, *516*, 79.

71. Wolf, S.M. and Vouros, P. *Anal. Chem.* **1995**, *67*, 891.

72. Albert, M.; Debusschere, L.; Demesmay, C.; Rocca, J.L. *J. Chromatogr. A* **1997**, *757*, 281.

73. Chien, R.L. and Burgi, D.S. *J. Chromatogr.* **1991**, *559*, 141.

74. Zhang, C.X. and Thormann, W. *Anal. Chem.* **1996**, *68*, 2523.

75. Foret, F.; Szoko, E.; Karger, B.L. *J. Chromatogr.* **1992**, *608*, 3.

76. Stegehuis, D.S.; Tjaden, U.R.; van der Greef, J. *J. Chromatogr.* **1992**, *591*, 341.

77. Stegehuis, D.S.; Irth, H.; Tjaden, U.R.; van der Greef, J. *J. Chromatogr.* **1991**, *538*, 393.

78. Kaniansky, D. and Marak, J. *J. Chromatogr.* **1990**, *498*, 191.

79. Reinhoud, N.J.; Tjaden, U.R.; van der Greef, J. *J. Chromatogr.* **1993**, *641*, 155.

80. Křivánková, L.; Gebauer, P.; Boček, P. *J. Chromatogr. A* **1995**, *716*, 35.

81. Dose, E.V. and Guiochon, G.A. *Anal. Chem.* **1991**, *63*, 1063.

82. Altria, K.D.; Clayton, N.G.; Harden, R.C.; Hart, M.; Hevizi, J.; Hailey, P.A.; Makwana, J.V.; Portsmouth, M.J. *Chromatographia* **1994**, *39*, 180.

83. Jorgenson, J. W.; Rose, D. J. *Anal. Chem.* **1988**, *60*, 642-648.

84. Dose, E.R. and Guiochon, G.A. *Anal. Chem.* **1991**, *63*, 1154.

85. Wätzig, H. and Dette, C. *Fresenius J. Anal. Chem.* **1993**, *345*, 403.

86. Wätzig, H. and Dette, C. *J. Chromatogr.* **1996**, 636, 31.

87. Dose, E.R. and Guiochon, G.A. *Anal. Chem.* **1992**, *64*, 123.

88. Graham, R.C. *Data Analysis for the Chemical Sciences, A Guide to Statistical Techniques*; VCH Publishers, Inc.: New York, 1993.

89. Gonick, L. and Smith, W. *The Cartoon Guide to Statistics*; HarperCollins Publishers, Inc.: New York, 1993.

90. Khaledi, M.G. *High Performance Capillary Electrophoresis Theory, Techniques, and Applications*; John Wiley & Sons, Inc.: New York, 1998.

91. Thormann, W.; Zhang, C.X.; Caslavska, J.; Gebauer, P.; Mosher, R.A. *Anal. Chem.* **1998**, *70*, 549.

92. Cifuentes, A. and Poppe, H. *Electrophoresis* **1995**, *16*, 516.

93. Rasmussen, H.T. and McNair, H.M. *J. Chromatogr.* **1990**, *516*, 223.

94. Palmer, C.P. and Vandeginste, B.G.M. *J. Chromatogr. A* **1995**, *718*, 153.

95. Yang, J.; Bose, S.; Hage, D.S. *J. Chromatogr. A* **1996**, *735*, 209.

96. Vespalec, R.; Gobauer, P.; Boček, P. *Electrophoresis* **1992**, *13*, 677.

97. Blake, C. A. and Snow, N.H. *unpublished results*.

98. Huang, X.; Gordon, M.J.; Zare, R.N. *Anal. Chem.* **1988**, *60*, 377.

99. Ehmann, T.; Bachman, K.; Fabry, L.; Rufer, H.; Serwe, M.; Ross, G.; Pahlke, S.; Kotz, L. *J. Chromatogr. A* **1998**, *816*, 261.

100. Chen, N.; Wang, L.; Zhang, Y. *J. Liq. Chromatogr.* **1993**, *16*, 3609

101. Coufal, P.; Stulik, K.; Claessens, H. A.; Cramers, C.A. *J. High Res. Chromatogr.* **1994**, *17*, 325.

175

102. Altria, K.D.; Harden, R.C.; Hart, M.; Hevizi, J.; Hailey, P.A.; Makwana, J.V.; Portsmouth, M.J. *J. Chromatogr.* **1993**, *641*, 147.

103. Horwitz, W. *Anal. Chem.* **1982**, *54*, 67A.

104. Cohen, N. and Grushka, E. *J. Chromatogr. A* **1994**, *678*, 167.

105. Nielen, M.W.F. *J. Chromatogr.* **1991**, *588*, 321.

106. Krokin, O.V.; Xu, W.; Hoshino, H.; Shpigun, O.A.; and Yorsuyanagi, T. *Chem. Lett.* **1996**, *1095*, 1095.

107. Zhao, J.; O'Shea, T.J.; and Lance, S.M. *J. Chromatogr.* **1994**, *680*, 271.

108. Barnett, N.W.; Hindson, B.J.; Lewis, S.W.; and Purcell, S.D. *Anal. Commun.* **1998**, *35*, 321.

109. Timerbaev, A.R.; Buchberger, W.; Semenova, O.P.; and Bonn, G.K. *J. Chromatogr.* **1993**, *630*, 379.

110. Haumann, I. And Bachmann, K. *J. Chromatogr.* **1995**, *652*, 539.

111. Lehn, J.M. *Angew. Chem., Int. Ed. Engl.* **1988**, *27*, 89.

112. Denti, G.; Campagna, S.; Sabatino, L.; Serroni, S.; Ciano, M.; and Balzani, V. *Inorg. Chem.* **1990**, *29*, 4750.

113. Hunziker, M.; Ludi, A. *J. Amer. Chem. Soc.*, **1977**, *22*, 1370.

114. Denti, G.; Campagna, S.; Ricevuto, V.; Serroni, S.; Ciano, M.; and Balzani, V. *Inorg. Chim. Acta.* **1991**, *182*, 127.

115. Pellizetti, E. and Schiavello, M. eds. *Photochemical Conversion and Storage of Solar Energy*; Kluwer Academic Publishers: Netherlands, 1991; 27-45.

116. Mongelli, Matthew. *Laboratory notebook.* 1999.

117. Wallace, A.W. and Murphy, W.R. *Inorganica Chimica Acta.* **1989**, *166*, 47.

118. Burgi, D.S. *Anal.Chem.* **1993**, *65*, 3726.

119. Kissinger, P.T. and Heineman, W.R. *Laboratory Techniques in Analytical Chemistry, 2nd. Ed.*; Marcel Dekker, Inc.: New York, 1996; Chapter 5.

120. Li,C. and Martin, L.M. *Anal. Biochem.* **1998**, *263*, 72.